AN INTEGRATED MULTI - DISCIPLINARY GEOPHYSICAL APPROACH TO GROUNDWATER EXPLORATION IN THE NEBO GRANITE, NORTHERN PROVINCE

WJ Botha • M Combrinck • FS Botha • JL van Rooy

WRC Report No. 862/1/01

Water Research Commission

AN INTEGRATED MULTI-DISCIPLINARY GEOPHYSICAL APPROACH TO GROUNDWATER EXPLORATION IN THE NEBO GRANITE, NORTHERN PROVINCE

Report to the
WATER RESEARCH COMMISSION

by

W J Botha*, M Combrinck*, F S Botha** & J L van Rooy*

*University of Pretoria
**Department of Water Affairs and Forestry

WRC Project No 862/1/01
ISBN 1 86845 808 3

SEPTEMBER 2001

AN INTEGRATED MULTI-DISCIPLINARY GEOPHYSICAL APPROACH TO GROUNDWATER EXPLORATION IN THE NEBO GRANITE, NORTHERN PROVINCE.

Contributors

W.J. Botha*
M. Combrinck*
F.S. Botha**
J.L. van Rooy*

* University of Pretoria
** Department of Water Affairs and Forestry

Report to the

WATER RESEARCH COMMISSION

WRC PROJECT K5/862/0/1

ACKNOWLEDGEMENTS

The research described in this report resulted from a project funded by:

Water Research Commission
Council for Geoscience
Department of Water Affairs and Forestry
Geodass (Fugro) Pty Ltd

The Steering Committee responsible for this project consisted of the following persons:

Mr. A. G. Reynders	Water Research Commission
Mr. K. Pietersen	Water Research Commission
Mr. H. Maaren	Water Research Commission
Mrs. E. M. Lenyai	NRF
Ms. T. Cele	NRF
Prof F. Hodgsen	Institute for Groundwater Studies, Univ. of the Free State
Mr. W.H. du Toit	Department of Water Affairs and Forestry
Mr. C.J. Haupt	Water Systems Management
Mr. S. Marais	Department of Water Affairs and Forestry
Mr. R. Meyer	CSIR
Mr. K. Sami	Council for Geoscience
Dr. E.H. Stettler	Council for Geoscience
Dr. J.L. van Rooy	University of Pretoria
Prof. W.J. Botha	University of Pretoria
Ms. M. Combrinck	University of Pretoria

The financing of the project and the contributions of the members of the Steering Committee are gratefully acknowledged.

EXECUTIVE SUMMARY

INTRODUCTION

During the preceding ten years, a very large number of boreholes were drilled on the Nebo granite as part of an Emergency Drought Relief Program. For various reasons, a very low success rate was obtained. Out of a hundred boreholes on the Nebo granite, 51 were dry, 42 had yields between 0,1 and 1,0 l/s and 7 had yields between 1,0 and 3,0 l/s. Based on these and similar results, the area was declared unsuited for groundwater development.

The use of geophysical techniques for the location of suitable targets for water supply boreholes is well understood. It is however in the application of these techniques, in traditionally poor groundwater potential areas such as the Lebowa Granite Suite of the Northern Province, National Groundwater Information System (NGIS), that the correct interpretation of the geophysical data become crucial in planning and developing community water supplies. To this end an integrated multidisciplinary approach was researched whereby airborne geophysical techniques combined with ground geophysics, geology, orthophotos, topocadastral data and detailed structural geological mapping are used in the siting of boreholes for groundwater development.

OBJECTIVES

The objectives of the research programme were as follows:

- To identify the known aquifers within the study area on the Nebo granite, using existing data from the Department of Water Affairs and Forestry.

- To obtain as much of the geophysical data used in the siting of these boreholes as possible, and to incorporate this into a database accessible to a geographical information system (GIS).

- To develop an integrated (airborne geophysical techniques combined with ground geophysics) approach to the siting of boreholes for the development of groundwater.

- To develop an extensive geophysical database to be incorporated into the National Groundwater Information system being compiled by the Department of Water Affairs and Forestry.

METHODOLOGY

Two areas of 10km X 10km were selected on the Nebo Granite. The two areas were separated by approximately 10km. The first area is characterized by having a large amount of outcrops, while the second area is characterized by very few outcrops. The major part of the study effort was spent on the first area. Optimum survey parameters from this area were then used on the second area.

In area 1 all available information on existing boreholes was entered into a GIS database. Where available, the geophysical data that were used to site the various boreholes were obtained, checked for accuracy, entered into the GIS database and evaluated as to the applicability of the various techniques. Where the geophysical data could not be found, ground geophysics were done by the research team. The GIS database was then used to assist in the identification of the various possible aquifers on the Nebo granite.

Airborne electromagnetic, magnetic and gamma-ray radiometric surveys as well as detailed structural mapping, were completed on area 1. These data sets were interpreted with special emphasis to identify zones of deep weathering, geological contacts, dykes, sills and structural information. The data were also processed to obtain the optimum parameters and minimum cost for an airborne survey of area 2. From this data, combined with the other data sets already mentioned, target areas were selected for ground geophysical surveys and possible borehole sites. The ground geophysical surveys consisted of magnetic and electromagnetic profiles. A number of boreholes were then drilled by the Department of Water Affairs and Forestry. Pump tests were also done on a number of successful boreholes.

RESULTS

Major structures were identified from the airborne geophysical data. These consisted of dolerite/granite contacts, dolerite dykes and fault/fractures. Drilling results proved that the dolerite/granite contacts, whether associated with dolerite sills or dykes, did not yield any significant groundwater. Faults/fractures did however yield groundwater far in excess of the yield that was traditionally associated with the Nebo granite. A number of the holes drilled on fractures/faults were pump tested and some were finally developed for local use.

The geophysical approach used in this project introduced two innovations relative to the traditional approach for groundwater exploration used on the Nebo granites. In the first instance the area was investigated on a regional scale rather than the very localized scale used in the past. In the second instance, airborne geophysical data was used as an aid in identifying and mapping structures of regional extent.

In the first test area airborne data included magnetic, radiometric and electromagnetic values. Interpretation of these results indicated that airborne magnetic data should be sufficient to allow for the mapping of major structures. Downward continuation of this data significantly reduced the amount of ground follow-up that was needed to locate the target in the field.

The electromagnetic technique then proved to work exceptionally well in determining whether there were weathering associated with the target structure and in locating an optimum borehole position.

In the second test area the airborne data were limited to magnetic and radiometric information. Since only four targets, all with the same strike orientation, were drilled in this area, it is difficult to evaluate the geophysical results for this area, except that the interpreted structures were intersected in the drilled boreholes.

CONCLUSIONS AND RECOMMENDATIONS

Based on the results obtained, it is concluded that a regional approach to groundwater exploration is essential before any area can be classified as unsuitable for groundwater development. In a regional approach the use of airborne magnetic data has long been proven by the mineral industry to be a cost effective and essential aid in regional structural mapping, especially where a scarcity of outcrops occur. A line spacing of 100m for an airborne survey for groundwater development is recommended. It is not recommended that the airborne data alone should be used for borehole siting, but that interpreted structures should be pin pointed in the field, using ground geophysics.

Where faults and fracture sones are the primary targets, it is recommended that the electromagnetic technique be used. This technique is more sensitive to these kinds of targets, yields more information and is more cost effective than the traditional DC resistivity techniques.

Page

LIST OF CONTENTS

Chapter 9: Summary, conclusions and recommendations

List of figures and tables

CHAPTER 1

INTRODUCTION

1.1 GENERAL

During the preceding ten years, a very large number of boreholes were drilled on the Nebo granite as part of an Emergency Drought Relief Program. For various reasons, a very low success rate was obtained. Out of a hundred boreholes on the Nebo granite, 51 were dry, 42 had yields between 0,1 and 1,0 l/s and 7 had yields between 1,0 and 3,0 l/s. Based on these results, the area was declared unsuited for groundwater development.

The use of geophysical techniques for the location of suitable targets for water supply boreholes is well understood. It is however in the application of these techniques in traditionally poor groundwater potential areas such as the Lebowa Granite Suite of the Northern Province, National Groundwater Information System (NGIS), that the correct interpretation of the geophysical data become crucial in planning and developing community water supplies. To this end an integrated multidisciplinary approach was researched whereby airborne geophysical techniques combined with ground geophysics, geology, orthophotos, topocadastral data and detailed structural geological mapping in one area are used in the siting of boreholes for groundwater development.

Two 10x10km target areas, separated by approximately 15km, situated in the southern district of the Northern Province, figure 1, were chosen for the study. The area has one of the lowest water/capita/day ratios in the country (Environmental Potential Atlas [ENPAT], version 1, 1994).

The relative positions of the two study areas is shown in figure 2.

1.2 OBJECTIVES

The objectives of the research programme are as follows:

- To identify the known aquifers on the Nebo granite, using existing data from the Department of Water Affairs and Forestry.

- To obtain as much of the geophysical data used in the siting of these boreholes as possible, and to incorporate this into a database accessible to a geographical information system (GIS).

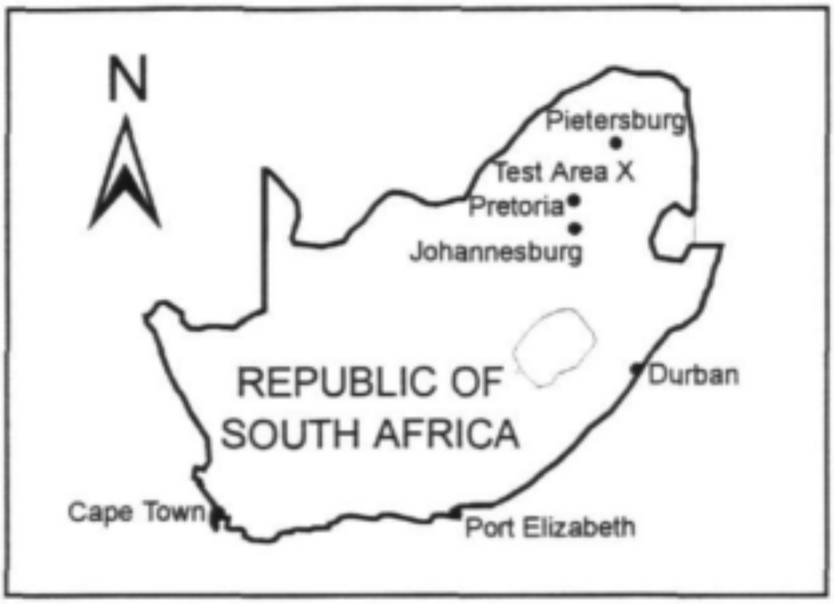

Figure 1: Locality map of study area

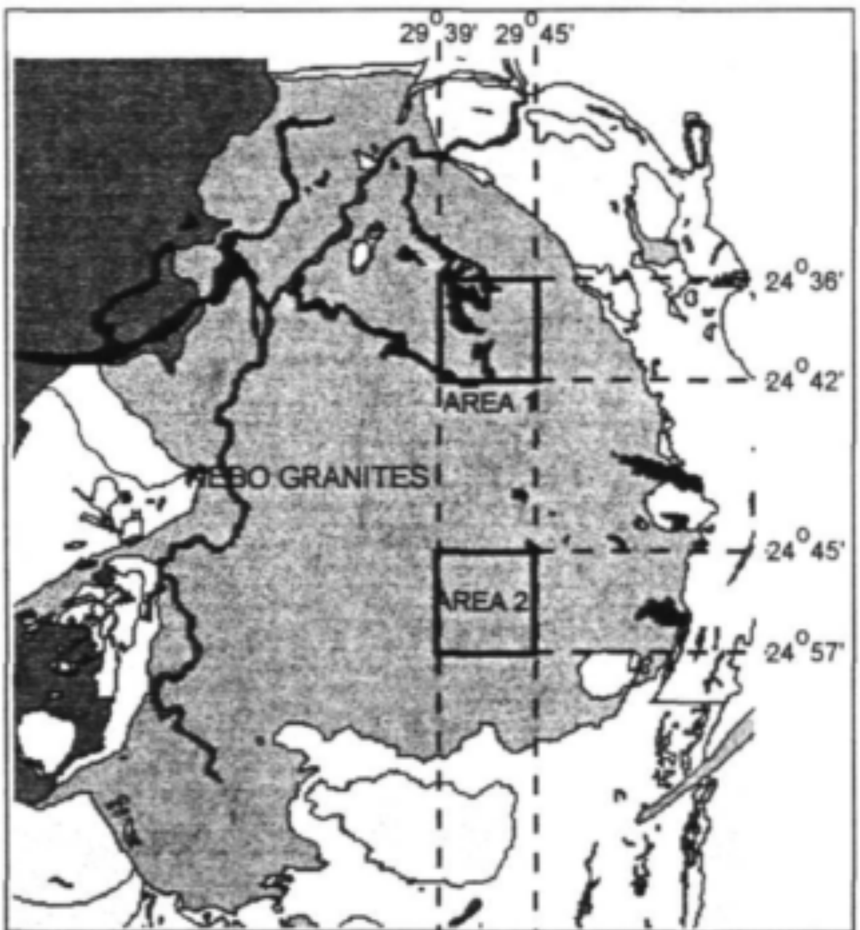

Figure 2: Map showing Nebo Granites, dolerite dykes and sills (black) and two research areas

- To develop an integrated (airborne geophysical techniques combined with ground geophysics and detailed structural mapping of the northern test area) approach to the siting of boreholes for the development of groundwater.

- To develop an extensive geophysical database to be incorporated into the National Groundwater Information system being compiled by the Department of Water Affairs and Forestry.

These objectives can be summarized as presented in figure 3:

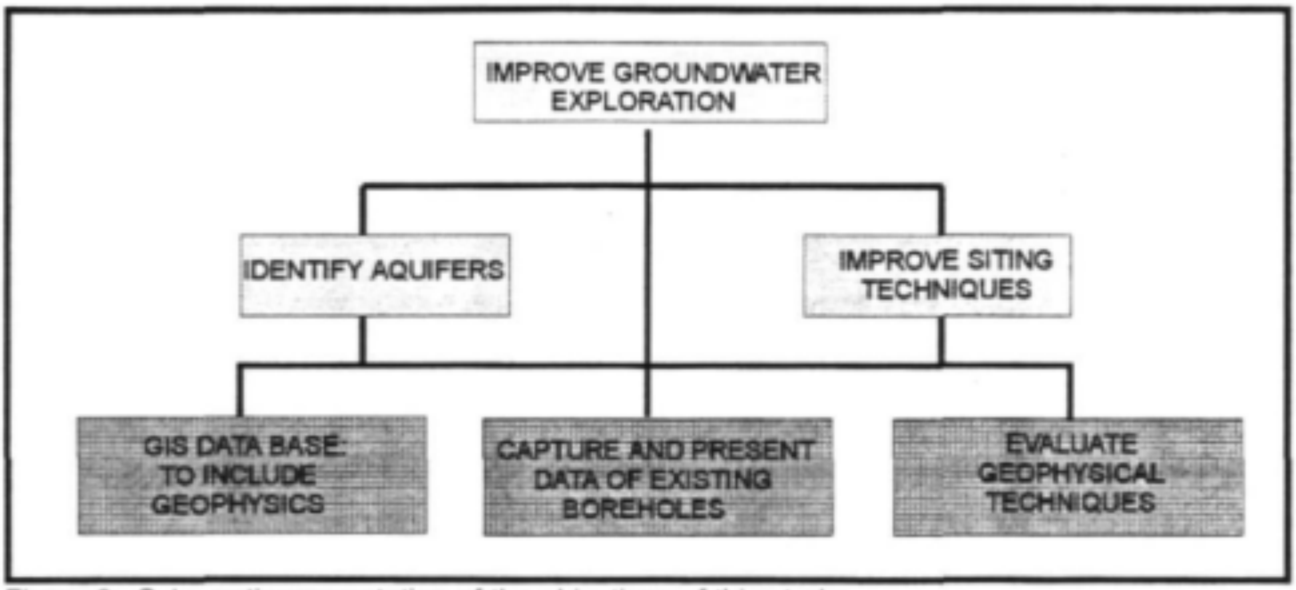

Figure 3: Schematic presentation of the objectives of this study.

The degree to which these objectives has been met, is summarised in the conclusion.

Identification of aquifers

This can only be done if the location of boreholes can be accurately placed on maps and the geophysical interpretation used to site the boreholes can be evaluated for its correctness. The most efficient way of undertaking this, was through the use of a GIS, incorporating all relevant data.

Evaluation of different geophysical techniques

Airborne magnetics, frequency domain EM and spectrometric gamma-ray techniques were applied in the study area and targets on the ground were followed up with magnetic and EM surveys. Ample data therefore exist to determine which data sets play the leading role in improving the selection of groundwater yielding boreholes.

1.3 GEOLOGY AND GEOHYDROLOGY

1.3.1 Geology

The study area is underlain by the Lebowa Granite Suite of the Bushveld Igneous Complex, figure 2.

The most important lithological unit in the area is the Nebo Granite, a sill-like granitic intrusion, (Kent, 1980). It dips to the west and varies in the study area in thickness from 420m in the south to 2,4km in the north. Its age is determined as 1920±40Ma (Tankard, 1982). The granite exhibits a crude stratiform layering with a coarse-grained gray granite at the base, grading up through medium-grained gray and red, then through red granophyric granite, and finally granophyre, although this sequence is not always complete at one location. The most important minerals are quartz, feldspar and minor but variable amounts of hornblende or biotite. Mafic minerals are more abundant in the coarser grained varieties. Accessory minerals are zircon, fluorite (which affect the drinking quality of the water), apatite, sphene, epidote and magnetite. Alteration of the primary minerals yields biotite, chlorite, saussurite, epidote, hematite and fine aggregates of clay minerals, (Tankard, 1982).

1.3.2 Structural Geology

Discontinuities (joints, shear zones and faults) in the Nebo Granite are prominent in the outcrop areas, where orientations of such structures can be measured. Prominent discontinuities can be followed for several kilometers using field mapping, aerial photographs and satellite images (Botha, 2000). A total of 761 measurements of different discontinuities were taken in area 1, recording the dip and strike orientations (Hoffman, 1997), figure 4. This was plotted on stereo nets from which Rose diagrams were derived. Botha (2000) concluded that genetically different fractures occur in the Nebo Granite, namely, cooling fractures, shear zone fractures (faulting) and quartz-rich fractures due to hydrothermal activity (intrusion). Furthermore the shear zones and fractures have a more broken appearance at the surface than the surrounding granite (evident from outcrops). Fine grained dolerite intrusions show some of the same geological fractures, some having the same orientation as in the granite. This implies that fracturing took place before, during and after Karoo times, (Botha, 2000).

On the basis of the structural orientation measurements in area 1, it is evident that three different geological settings exist. The geological settings can be divided into the granite north of the dolerite intrusion, the dolerite intrusion and the granite south of the dolerite intrusion. Some strike orientations occur in all three geological settings while others concentrate in the area above, below or within the dolerite intrusions, (Botha, 2000). The most prominent strike orientations that were mapped, were 40-50^0 and 140-150^0 (Hoffman, 1997). The structures mapped in this area correspond to the strike direction of known regional structures occurring on the sub-continent. This implies that the stresses active in the study area originated on a regional scale (Botha, 2000).

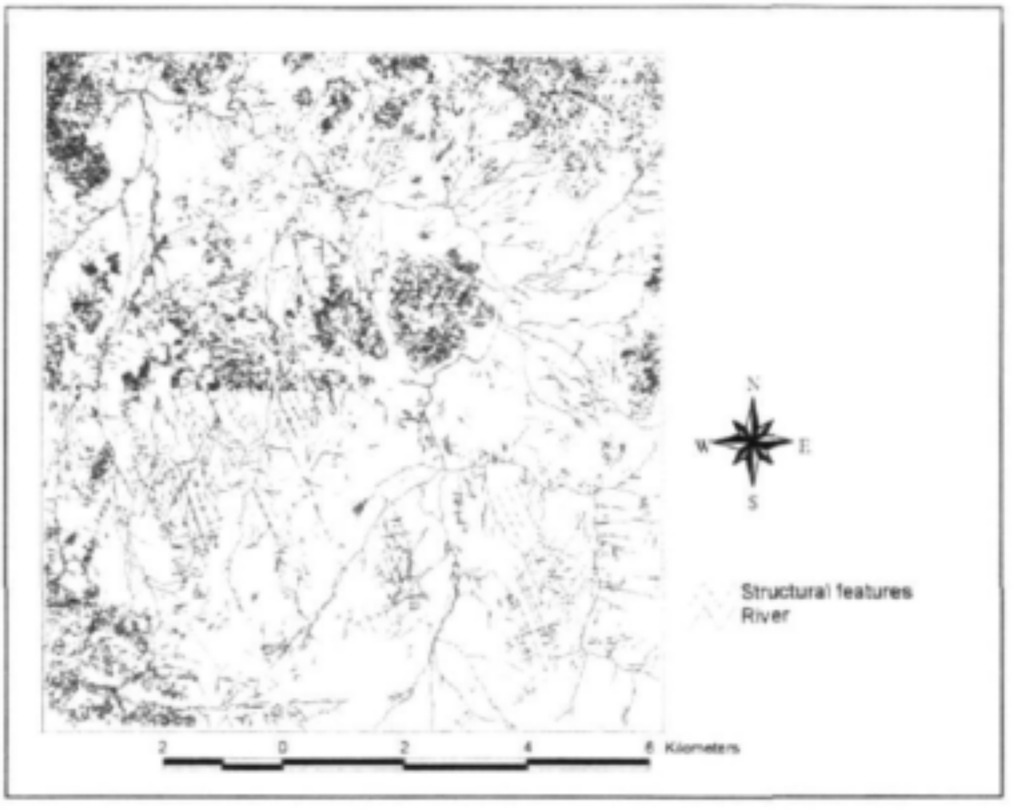

Figure 4: Map indicating measured structural features in area 1, (Hoffman, 1997)

1.3.3 Surface water, recharge and rainfall

The availability of surface water in the area is restricted to non-perennial streams and fountains, most of which are severely contaminated, (Botha, 2000). There are very few dams, reservoirs or any other form of water infrastructure and individuals have to walk up to 15km per day in order to fetch water for their most basic needs.

The building of dams have been proposed, but a feasibility study has shown that for this specific area it is not a viable solution due to the rate of silting, (Haupt, 1997). The alternatives to surface water as source are either long distance pipelines from other areas or the efficient development and management of groundwater. Due to the fact that groundwater development is a more economic resource it is the first alternative that should be investigated and is therefore the subject of this study.

1.3.4 Groundwater aquifers, -level and -quality

The typical aquifers found in hard rock terrains such as covered by the study area are:

- basins in the granite caused by deep weathering, or
- weathered fractured zones associated with faults, dykes, shear zones or changes in lithology, (Project Panel, UNESCO, 1981).
- weathered contact zones along intrusive dykes

In this study emphasis was placed on the second type of target as basins in the area are very shallow and sensitive to droughts. Published groundwater levels vary between 5m and 30m depending on topography and recharge, (Vegter, 1995). Available results from this study has shown that contact zones along dykes do not yield water in the study area.

1.4 METHODOLOGY

A detailed study, as discussed below, was first done on test area 1. The results from this study were then used to determine the optimum parameters for a geophysical survey of area 2 and applied to this area as a test.

In area 1 all available information on existing boreholes was entered into a GIS database. Where available, the geophysical data that were used to site the various boreholes were obtained, checked for accuracy, entered into the GIS database and evaluated as to the applicability of the various techniques. Where the geophysical data could not be found, ground geophysics were done by the research team. The GIS database was then used to assist in the identification of the various possible aquifers on the Nebo granite.

Airborne electromagnetic, magnetic and gamma-ray radiometric surveys were completed on area 1. These data sets were interpreted with special emphasis to identify zones of deep weathering, geological contacts, dykes, sills and structural information. The data were also processed to obtain the optimum parameters and minimum cost for an airborne survey of area 2. From this data, combined with the other data sets already mentioned, target areas were selected for ground geophysical surveys and possible borehole sites. The ground geophysical surveys consisted of magnetic and electromagnetic profiles. A number of boreholes were then drilled by the Department of Water Affairs and Forestry to evaluate the effectiveness of the siting techniques and to investigate structures.

CHAPTER 2

THE DEVELOPMENT OF A GIS DATABASE

2.1 EXISTING BOREHOLE DATA

An intensive search was undertaken to locate all existing boreholes in area 1. A total of 38 boreholes were located. Since coordinates obtained from the Department of Water Affairs and Forestry (DWA&F) were inaccurate in the order of several hundreds of meters, accurate coordinates were obtained using a differential GPS. In addition to the 38 boreholes in the study area, information on 100 boreholes sited on the rest of the Nebo area were obtained and used in the quoted statistics in this chapter.

In order to identify the aquifers, and evaluate the siting of existing boreholes, all available data on the boreholes were obtained. The data for each hole consist of some or all of the following attributes:

- borehole number
- coordinates
- borehole depth
- depth of static water level
- associated geology
- yield (usually blow test yield)
- method of siting
- equipment, such as handpumps, associated with holes
- geophysical data used in the siting of the hole, if any

Contributors to this information are the National Groundwater Information System (from the DWA&F) and several consulting companies which worked on contract for DWA&F. Unfortunately, this data proved to be insufficient for the purposes of the study due to the following reasons.

The geophysical data (which is considered one of the most important aspects for the evaluation of the siting techniques), could not be located for any of the boreholes in the study area. Furthermore, the coordinates (when given) were not accurate enough to distinguish between several holes in the same area in the field. This made it impossible to use the rest of the DWA&F information since the information could not be tied to a specific borehole. The borehole numbers, which uniquely identify each hole, were weathered away in many cases. A number of boreholes were found with no numbers and consequently no information.

The geophysical information associated with the siting of each borehole was considered essential for the evaluation of the aquifer. It was considered quite possible that a low yield borehole can be considered not viable due to an incorrect interpretation of the geophysical information rather than a lack of water in a lineament. Due to the lack of availability of this data, it was decided to do geophysical profiles at all the existing holes where cultural noise (fences, power lines, metal-containing pipe lines and buildings, etc.) allowed for such a survey. At each site two perpendicular profiles of 200m length were completed with one of the profiles as close as possible to being perpendicular to one of the main structural directions, to maximize the geophysical response of possible structures on which the holes were drilled.

Of the boreholes that were investigated, 6 had active pumps, 1 had a broken pump, 10 were dry and 4 were unknown as far as water yield is concerned. Of the 10 dry holes, 9 would not have been recommended on the strength of the geophysical results. Only one was drilled on a good geophysical anomaly. Of the 6 water-yielding holes plus the 4 unknown holes, 7 were drilled on good geophysical anomalies while 3 were not optimally drilled on geophysical anomalies. The locality maps and relevant geophysical profiles are included in the database.

2.2 BOREHOLE DATA REPRESENTATION (Arcview 3.1)

The study required a large number of multi-disciplinary data sets to be compared. The most efficient way to do this is by means of a Geographical Information System (GIS). The software chosen was Arcview 3.1 for the following reasons:

- it is PC based
- it is already widely in use in the geophysical and groundwater community
- it is compatible with other databases (e.g. dBase, Arc-Info)
- it can be customized to have a user friendly interface giving easy access to all data

Arcview 3.1 makes use of *views* and *themes* with specific *attributes* to graphically represent data. In order to evaluate and compare the different data sets, they all had to be converted to a format acceptable by Arcview 3.1.

The different borehole data attributes are entered in a spreadsheet format and can be entered and edited directly in Arcview 3.1 or be imported from Excel, QuatroPro, dBase or any equivalent spreadsheet program. It can in fact even be imported from an ordinary text file created in a DOS editor or Notepad. As soon as this table is created in Arcview 3.1, the data can be used to create themes, which can be graphically displayed in views.

For this database the coordinates of the boreholes are used as unique identifiers and each borehole is represented as a point on a map-like display (the view), using these coordinates.

By choosing the **information** button, and clicking on a borehole all the attributes, in table format, of that borehole can now immediately be viewed. This is illustrated in figure 5.

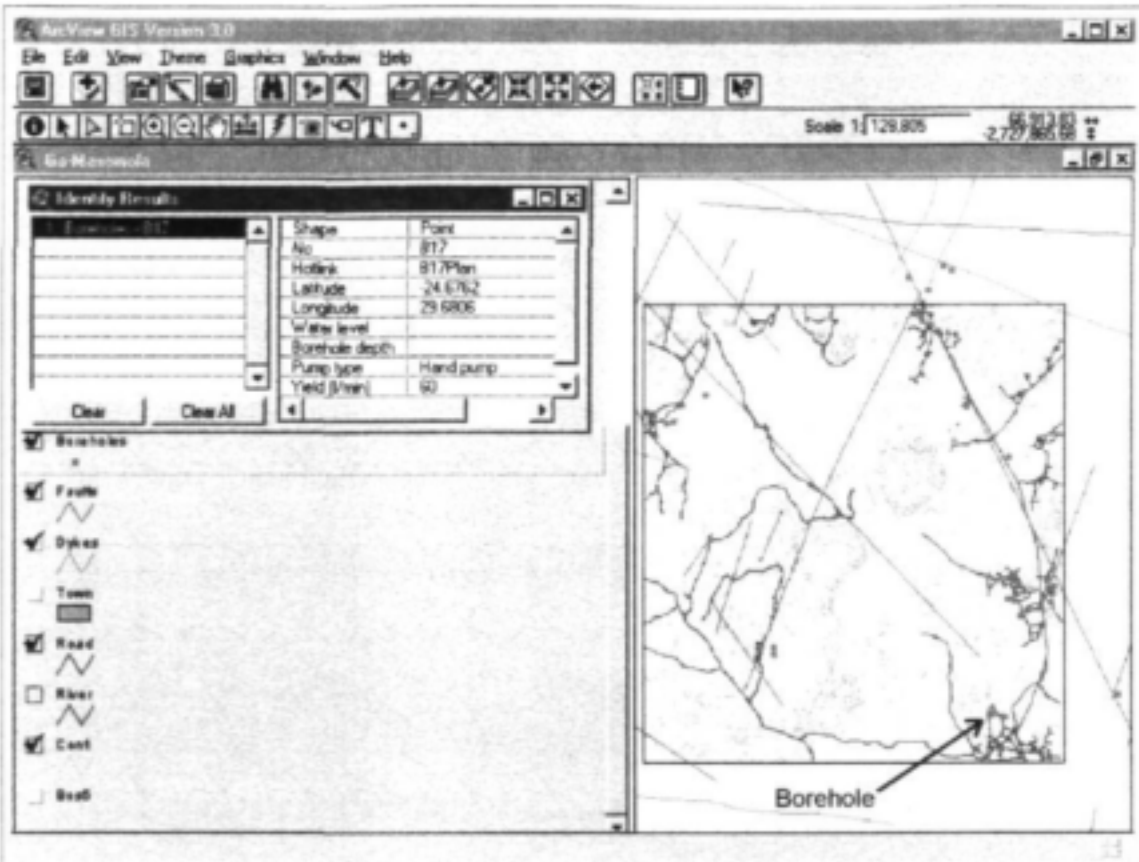

Figure 5: An ArcView screen image showing the boreholes overlain on topography and structure.

To have easy access the geophysical profiles at each borehole use was made of the **hotlink** function, which enables the user to recall any other view or image with a click of the mouse. For this specific study two views were created and "hotlinked" to each borehole. The first is a plan view showing the profiles relative to the borehole, the profile directions, the methods used and any significant landmarks or cultural noise sources. The next step is a view showing the geophysical profiles with borehole positions. (These were created in Corel Draw, and imported into Arcview 3.1 as TIFF files. Graphs can also be drawn in Arcview 3.1, but it was decided that the options were a bit limited for the information to be conveyed in a single view.) Figures 6 and 7 show the two data presentations that are hotlinked to Arcview.

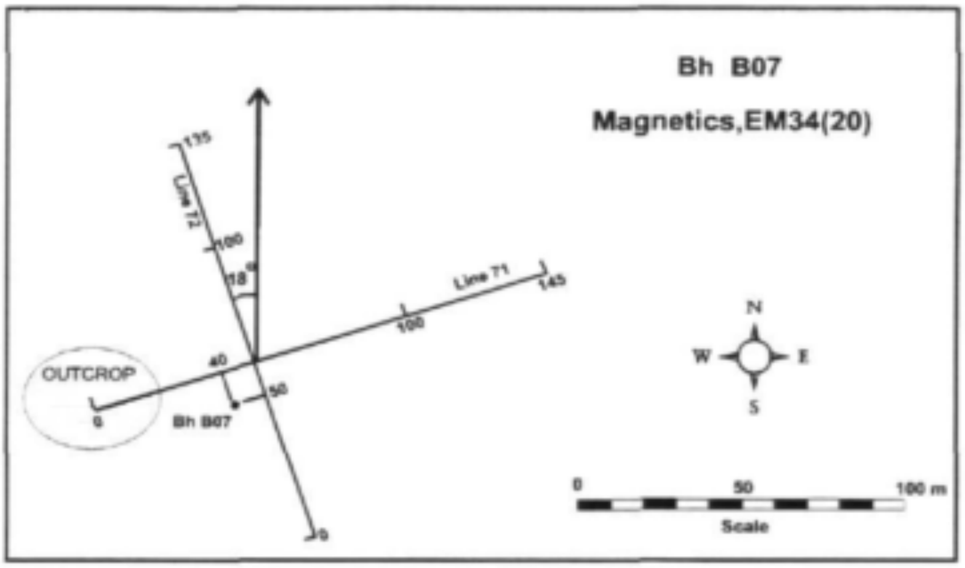

Figure 6: A map view of the profiles surveyed at a borehole

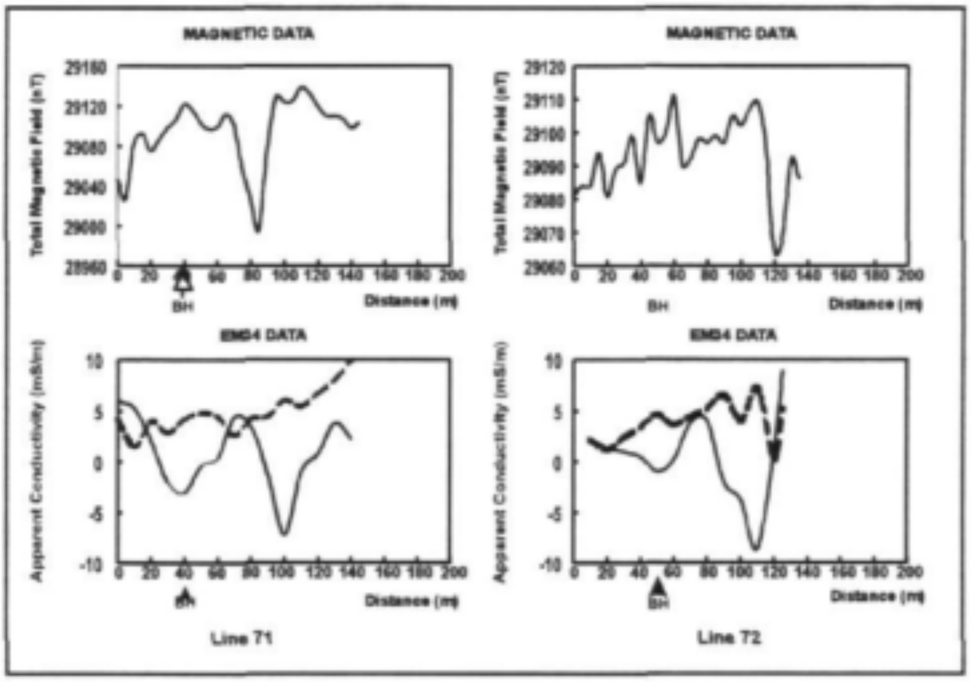

Figure 7: A view of the profiles surveyed at each borehole.

Once all the data are in the database it is very easy to use and extremely fast. It is now possible to simultaneously view all relevant information associated with a borehole, as shown in figure 8.

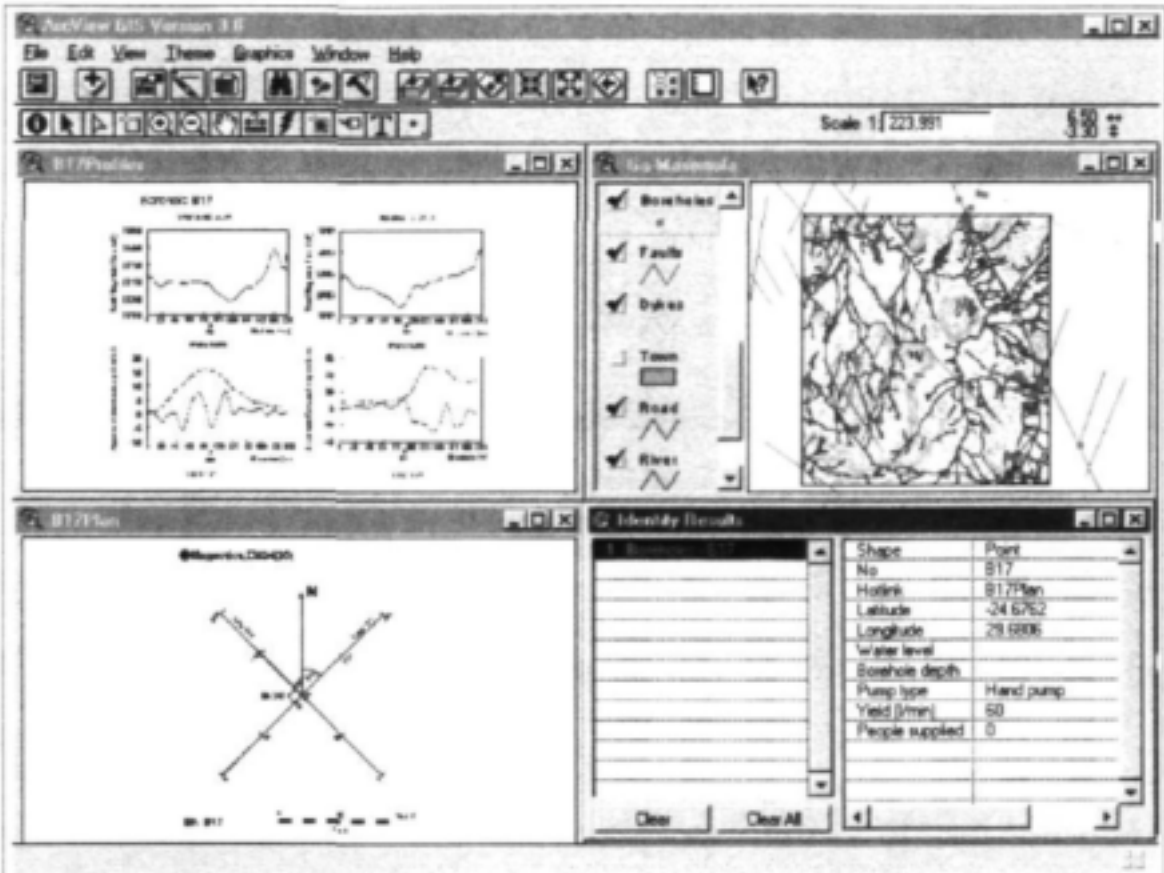

Figure 8: A screen view showing all relevant data associated with a borehole.

2.3 Remarks:

- Like all databases, it takes a considerable amount of time to do the physical data capturing, especially if the original formats are not compatible with Arcview 3.1.

- Queries and legends

  Some of Arcview 3.1's features that should be mentioned due to their special applicability for this study, are the **query** function and the **legend** editor. The legend editor enables the user to apply a variety of customized colour coded legends to a theme based on any of the attributes in the original data table. The query function enables the user to apply any kind of logical query (<, =, >, AND, OR, etc.) or combinations thereof to the data and will show all the boreholes for which the query is TRUE in yellow. An example of this is to find all boreholes that have been sited on magnetic anomalies AND have a yield higher than the average yield. This can then give an indication of the success of this specific method.

CHAPTER 3

GEOPHYSICAL TECHNIQUES TRADITIONALLY APPLIED TO BOREHOLE SITING

3.1 INTRODUCTION

This chapter contains a brief overview of geophysical techniques that are often routinely used in the siting of boreholes for groundwater development. One will often find that a specified technique is favoured in a certain area based on the field of expertise of the operator rather than on the physical properties of the target. When choosing a technique, it is essential to consider the physical properties of the target and the host rock and where possible, to use a combination of techniques.

3.2 DIRECT CURRENT RESISTIVITY SOUNDINGS AND PROFILING

These methods, also described as galvanic resistivity methods, are used to measure the earth's resistivity. Current is driven through one pair of electrodes (galvanic contacts) and the potential established in the earth by this current is measured with a second pair of electrodes (potential electrodes). This principle can be used to study variations in resistivity with depth (vertical sounding) or to study lateral resistivity variation (horizontal profiling).

The instrumentation used is usually relatively inexpensive, consisting basically of:

- a power source (DC or very low frequency alternating current)
- two or more current electrodes (usually made of steel)
- two or more potential electrodes (usually made of copper)
- lightweight cables
- multimeters for measuring current and voltage.

The method is based on Ohm's Law, the general form of which can be given as:

$$\mathbf{E} = \rho \mathbf{j} \tag{3.1}$$

where

E = electric field vector

j = current density vector

ρ = resistivity

For a three dimensional volume of material, as shown in figure 9, the resistance R, defined by Ohm's law as the ratio between potential difference and current, is proportional to the dimensions of the volume of material, that is :

$$R \propto \frac{L}{A} \tag{3.2}$$

where

A = area perpendicular to **j**
L = length in the direction of **j**
R = resistance (=$\Delta V/I$)
ΔV = potential difference over L
I = current

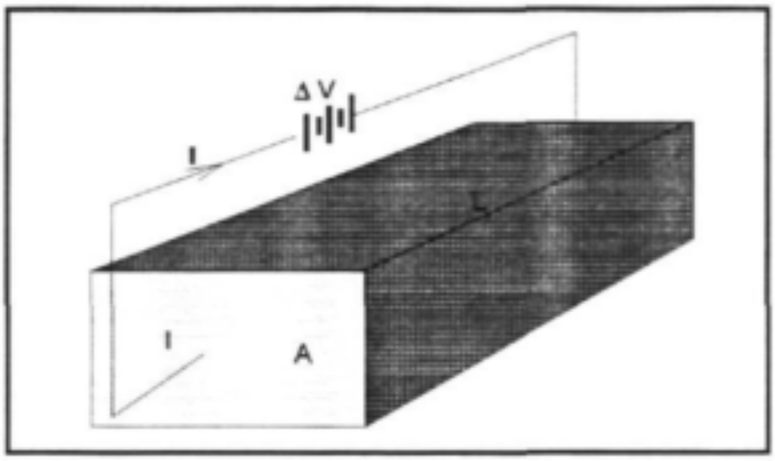

Figure 9: A volume of material defining the units used in equation 3.2

The proportionality constant is defined as the resistivity ρ with:

$$\rho = \frac{AR}{L} \tag{3.3}$$

From this, the resistivity is seen to have the dimensions of length and resistance, with SI units of Ωm (ohm.meter).

When doing resistivity measurements in the field, however, the medium being measured is often not a homogeneous, isotropic earth. In such a case a known current is passed through the earth and the resulting potential distribution caused by this, is observed using the potential difference (ΔV) measurements between two electrodes. This potential is then compared to the potential that would have been observed in a homogeneous, isotropic earth. The ratio of the measured potential to the theoretical potential, for the special case of the theoretical potential equal to unity, is called the *apparent resistivity* and is the fundamental parameter used in this technique, (Keller and Frischknecht, 1966).

The apparent resistivity values can be interpreted to give either a resistivity profile with depth or to map lateral variations in resistivity. The method can be applied to map:

- weathered basins (using depth soundings)
- vertical structures such as faults and lithological contacts (using profiling). The method is however not recommended for vertical structures since it is more sensitive to resistive targets and the profile generated by a vertical target can be relatively complex to interpret, (Botha, 1975).

A serious disadvantage of applying the resistivity technique is that good physical contact is needed between the current electrodes and the earth in order to force a large enough current into the earth. In the northern study area, the many outcrops rendered the technique inapplicable for most of the sites identified from the airborne data.

3.3 FREQUENCY DOMAIN ELECTROMAGNETIC TECHNIQUES (FDEM)

The FDEM induction techniques are best suited for detecting steeply dipping good conductors at shallow depths. This makes it ideal for detecting weathered structures such as faults and fractures, (Telford et al, 1990).

Electromagnetic systems are based on the principles that all electrical currents have magnetic fields associated with them and that all time varying magnetic fields will induce current in a conductor. A time varying magnetic field is generated by driving an alternating current through a wire loop or antenna. If any conductive material is present in the associated magnetic field, currents normal to the direction of the magnetic field will be induced in the conductor. These induced currents, in turn, create their own associated magnetic fields that, together with the primary field associated with the original transmitter, forms part of the total magnetic field. This resultant magnetic field is then measured in terms of the voltage induced in the receiver loop, (Keller and Frischknecht, 1966).

In the FDEM methods, measurements can be made of the in-phase and quad-phase (out of phase) components of the total magnetic field. The EM34, designed to operate at low induction numbers ($r/\delta << 1$), measures the ratio of the quadrature component of the secondary magnetic field ($Q\mathbf{H_s}$) to the free space primary magnetic field ($\mathbf{H_p}$). The instrument is designed to measure the response due to the leading term in the half-space expression of the half-space response for the normalized quadrature component, (horizontal coplanar configuration), (McNeil, 1980). This term can be written as:

$$Qh_z \approx \frac{1}{2}\left(\frac{r}{\delta}\right)^2 = \frac{\omega\mu_0\sigma r^2}{4} \qquad (3.7)$$

It follows from equation 3.7 that Qh_z is directly proportional to the terrain conductivity and the receiver is calibrated in terms of apparent conductivity (McNeil, 1980).

The EM34 is a moving source (transmitter) - moving receiver type instrument. It consists of a transmitter coil and receiver coil, both small enough to be easily handled by a two man team. It has three standard coil separations, 10m, 20m and 40m, corresponding to three different frequencies and different depths of investigation , Table 1.

Table 1. Investigative properties associated with different EM34 coil separations.

Coil separation	*Frequency*	*Depth of investigation (Horizontal coils)*	*Depth of investigation (Vertical coils)*
10m	6400Hz	15m	7.0m
20m	1600Hz	30m	15m
40m	400Hz	60m	30m

If measurements are taken with the horizontal coil configuration the EM34 can be seen as a quadrature-phase HLEM (Horizontal Loop Electromagnetic) system. It is capable of detecting steeply dipping plate-like structures with a low conductivity-thickness product in resistive ground. If the target thickness is much less than the inter coil spacing a characteristic HLEM response as shown in figure 10, will be mapped. These anomalies can be interpreted to yield conductance, depth and dip, (McNeil, 1983).

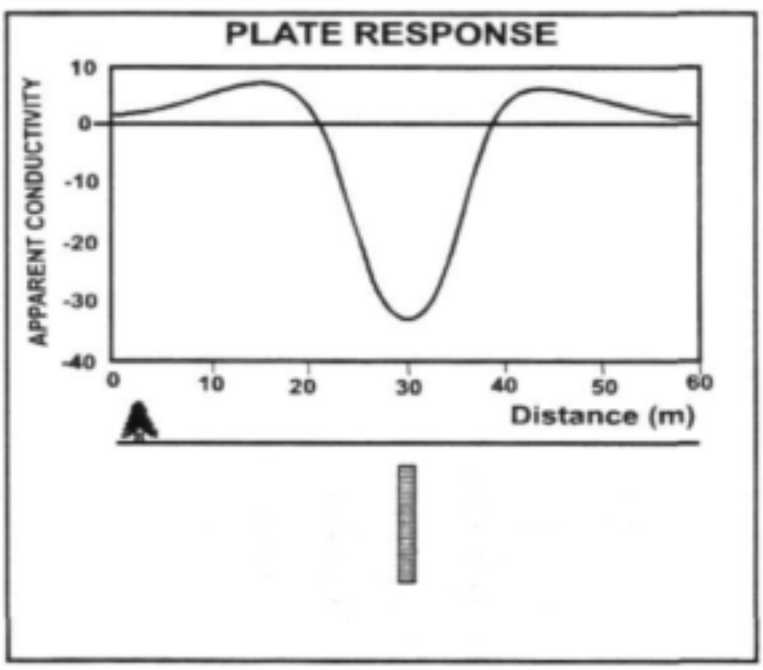

Figure 10: A typical horizontal loop response over a vertical conductor.

The EM34 system allows easy and rapid measurements, is sensitive to changes in conductivities in the order of 5 or 10 percent and the data can be interpreted fast and accurately. The maximum coil separation of 40m limits the depth of investigation to 60m, but in the study area this was found to be sufficient.

3.4 MAGNETICS

The earth's magnetic field, from an exploration geophysicist's perspective, is composed of three parts:

- the main field (internal origin)
- a small field with external origin
- spatial variations of the main field which are caused by local magnetic anomalies in the near-surface crust of the earth.

The main field varies relatively slowly and can be shown to have an internal origin using spherical harmonic analysis. The present theory is that the source of this field is convection currents of conducting material circulating in the liquid outer core. The field closely represents that of a bar magnet with the two poles being close to, but not exactly on, the geographical north and south poles of the earth. This field contributes to more than 99% of the total magnetic field, (Telford et al, 1990).

The relatively small external field is caused by electric currents in the ionized layers of the upper atmosphere. Time variations of this part are much more rapid than for the main field. Variations are caused by solar and lunar variations as well as magnetic storms which correlate with sunspot activity, (Telford et al, 1990).

Local changes in the main field result from variations in the magnetic mineral content of near-surface rocks often indicating the presence of dykes and/or faults/shear zones. These anomalies do not persist over great distances and are the main targets of the groundwater explorationist.

The magnetometer used for the ground geophysics in this study is a proton-precession magnetometer. This instrument depends on the measurement of the free-precession frequency of protons that have been polarized in a direction approximately normal to the direction of the earth's field. The protons induce a voltage that is a function of the precession frequency. The magnetic field can then be determined from:

$$F = \frac{2\pi\nu}{\gamma_p} = (\ 23.487 \pm 0.002 nT / Hz\ )\nu \qquad (3.8)$$

where

F = total field intensity in nanoTesla

ν = precession frequency

γ_p= gyromagnetic ratio of the proton

Only the total field intensity (F) can be measured and the sensitivity is approximately 1nT. The field procedure consists of taking a measurement at equal intervals along a profile. The values are presented as profile plots of amplitude versus distance. The shape of the magnetic profile is a function of the geometrical shape of the causative body, the direction of the profile, the inclination and declination of the main magnetic field at that position and whether or not the body has remanent magnetization. These factors are taken into account by most standard software packages like MAGIX from INTERPREX. Using such software, a possible geological model can be derived from the data. The derived model is however non-unique and therefore has to be correlated with other techniques or known geology.

In this study the magnetic method is used to delineate the doleritic intrusions (either as dykes or sills) into the granite. These magnetic features are used as marker horizons. Faults are detected as displacements in these marker units. Once detected, these faults are then mapped in detail using the EM techniques. Due to the relative short nature of the traverse undertaken, magnetic base station data were not collected to remove diurnal magnetic variations.

3.5 ORTHOPHOTOS

Although the use of orthophotos is not a truly geophysical technique, it proves invaluable in the search for groundwater. Important information that can be derived from these 1:10 000 maps are:

- important topographical features and relationships
- rivers, seapages and catchment areas
- available infrastructure such as roads, existing dams and villages
- accurate positioning in the field when searching for target structures
- delineation of structural features such as faults and shear zones visible on the surface
- information assisting in planning of ground surveys
- vegetational trends

CHAPTER 4

INTEGRATING MULTIDISCIPLINARY DATA SETS USING GIS

4.1 INTRODUCTION

Due to the multidisciplinary nature of the study, a way was needed to incorporate data sets of different origin, different spatial attributes and different formats. Two PC based programs were used to accomplish this. The first is Arcview 3.1 and the second is Oasis Montaj 4.1 from Geosoft. Oasis was used for its data processing capabilities especially with respect to the airborne geophysical data. All relevant maps and profiles generated in Oasis are exported to Arcview 3.1 so that the end user of the database will only need Arcview.

The following data sets were incorporated into the database:

- Lithology and large scale topocadastral data
- Small scale topocadastral data
- Ground geophysical and borehole data
- Map of lineaments
- Airborne geophysics
- Orthophotos

The origin, format and importance of each set will be discussed briefly in the rest of this chapter.

4.2 GEOLOGY AND LARGE SCALE TOPOCADASTRAL DATA

The geology and large-scale topocadastral data of the test area and surroundings came from BOSGIS. This is a GIS database developed by the Bushveld Research Institute at the Geology Department, University of Pretoria. A subset of this data is shown in figure 11. This data came in Arcview format and could be incorporated into the system without any problem. The data it contains were digitised from 1:250 000 geological maps which is not as high in resolution as most of the other data sets, but due to the relative simple nature of the geology, it proved to be sufficient for the purpose of the study. The large-scale topocadastral data unfortunately did not have the resolution required. The geology is important when interpreting the geophysics, developing a model for the study area and deciding what targets should be searched for and investigated. The data consist of:

- the major lithological units - Nebo granite and dolerite intrusions for the area under investigation (polygon themes)
- faults, dykes and lineaments (line themes)

Due to the resolution problem however, these features could not be located accurately enough to serve directly as targets for ground geophysics as follow-up. The main structural directions were identified from them though, and some of these structures have been correlated with other data sets and placed more accurately on that basis.

4.3 SMALL SCALE TOPOCADASTRAL DATA

Once the test area was identified, small scale topocadastral data were digitised from the 1:10000 orthophotos. This was done on contract by GISLab at the University of Pretoria. This data also came in Arcview 3.1 format and contain the following themes, figure 11:

- villages (polygon themes)
- rivers (line themes)
- roads (line themes)
- contours at 20m intervals (line themes)

These data sets could be used to determine topographic influences, accessibility options, recharge possibilities and structural correlation, e.g. where rivers apparently follow linear features such as faults.

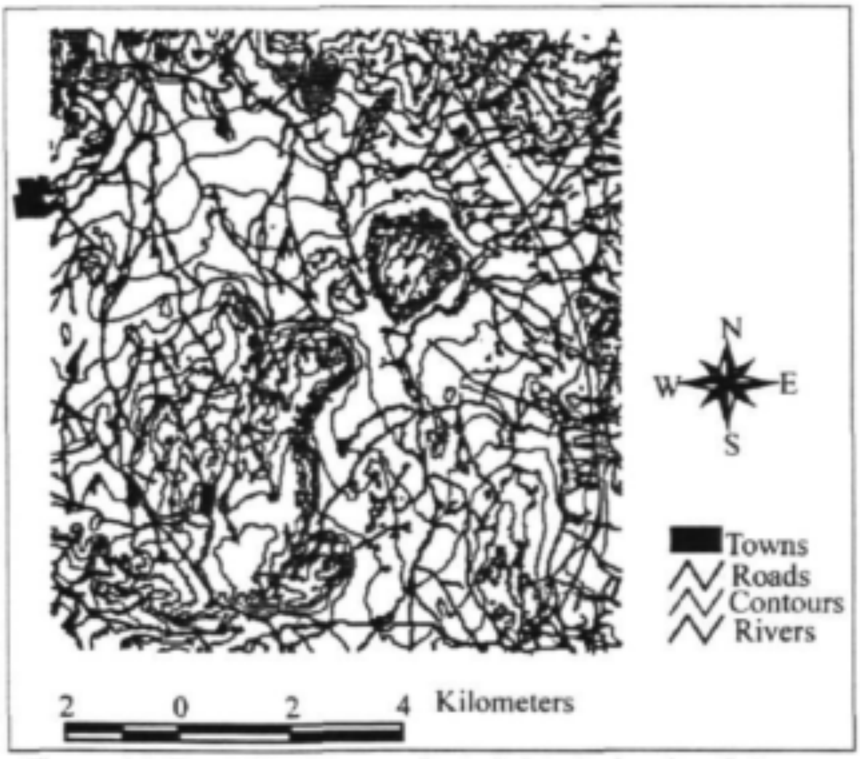

Figure 11: Example of topocadastral data in Arcview 3.1.

The contour theme data were also used by Botha (2000) to create a Digital Terrain Map (DTM) to highlight topographical and structural features.

4.4 GROUND GEOPHYSICAL AND BOREHOLE DATA

The data format and presentation of the ground geophysics and borehole information were already discussed in 2.2. Superimposing these data sets over other data sets allows one to decide whether a borehole can be associated with any visible structure on any of the other data sets. This information can then guide the further groundwater exploration. Deductions that can be made using the GIS approach are:

- which structures have groundwater development potential
- where would be the best place to explore and exploit these in terms of accessibility, needs of local population, recharge, future management and pollution/environmental dangers
- which techniques would be best suited for finding and identifying the structure
- what typical response should be expected when using such a method
- where would the optimal drilling position be on an associated geophysical anomaly

It would also assist in further hydro-geological, engineering and environmental studies.

4.5 STRUCTURAL GEOLOGY

The detailed structural geology of area 1 was mapped by Hoffman (1997) as part of a B.Sc. (Hons) project, digitized and incorporated into the Arcview 3.1 database (figure 4).

From this data the main structural directions were calculated in much more detail and possible target features such as prominent faults and shear zones were identified. As can be expected, this data show a very good correlation with the airborne geophysical data. There are, however, certain features visible which are not prominent on the geophysics and vice versa. This only serves to illustrate the point that there is no one ultimate technique in groundwater exploration and that a combination of different disciplines prove to be essential. This kind of data can be considered to be in the same category as airborne geophysical data in the sense that it is very successful in identifying large scale targets which can be followed up with groundwork. The success of this type of data set is of course proportional to the amount of outcrops visible to the geologist. In the investigation area there was fortunately an abundance of these, making a very thorough study possible. The format of this data is line themes in Arcview 3.1.

4.6 AIRBORNE GEOPHYSICS

The airborne data for area 1consist of total field magnetics, DIGHEM frequency domain EM at three frequencies and radiometric data. For area 2 it was decided, based on the results from area 1, that airborne magnetic data are sufficient.

The airborne geophysical data are in Oasis Montaj format and this is due to the fact that all the processing and interpretation is done in Oasis. In order to get this data into Arcview 3.1 it has to be exported from Oasis and imported to Arcview 3.1. This is done not in vectorised format, but in raster format (e.g. a TIFF file). This data can then be combined with other data sets, provided these other data sets are in vector format. The reason for this is that two raster format data sets occupying the same space are just like two pictures overlain. Only the top one can be seen and information on the bottom one cannot be accessed. Furthermore, seeing that there are no attributes connected to these data sets, queries cannot be performed on them and digital values for the data cannot be accessed in Arcview 3.1.

The information conveyed, however, through the raster image alone is good enough to allow spatial correlations to be made with the other data sets. In this respect Oasis Montaj can be used with much more accuracy, because these data sets can be combined by making use of linked cursors in different windows following either the grid images or profiles as shown in figure 12.

This data are used to delineate structural features and lithological units. Correlated with one another and the other data sets they prove invaluable in identifying the main structural features as well as giving information on the state of weathering of these structures. The magnetic data can also be processed (downward continued) to give an "expected profile" at any position on the ground. This proves especially helpful when looking for a certain structure in the ground follow-up stage (figure 13).

4.7 ORTHOPHOTOS

The 1:10 000 orthophotos were scanned and imported to Oasis Montaj. This data set is also in the raster format but provide very useful information when siting target areas for further ground follow-up work. Using this data set a ground survey can be planned in advance taking into account the strike direction of the target, as well as accessibility and possible obstacles such as dense vegetation or topographical features. Orientation in the field is much easier and optimal survey line lengths, directions and positions can be decided before visiting the site. This, of course, saves time and money once the ground follow-up has to be done.

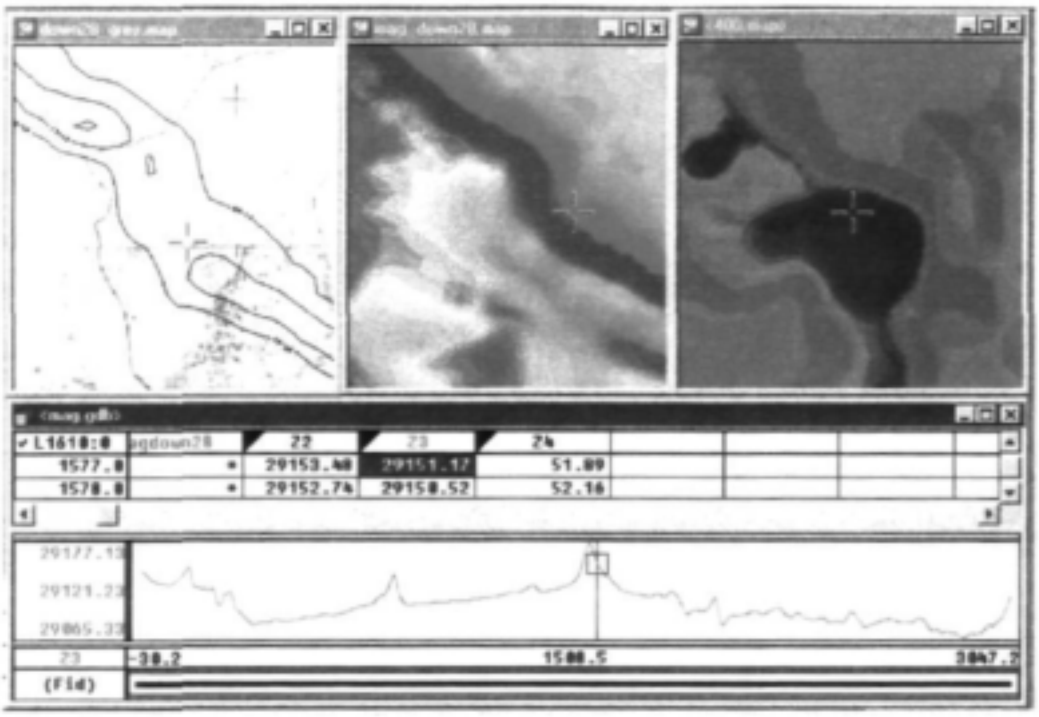

Figure 12: Window from Oasis Montaj showing different data sets of the same area (orthophotos, magnetic and EM34 data with magnetic profile), all linked by the same cursor.

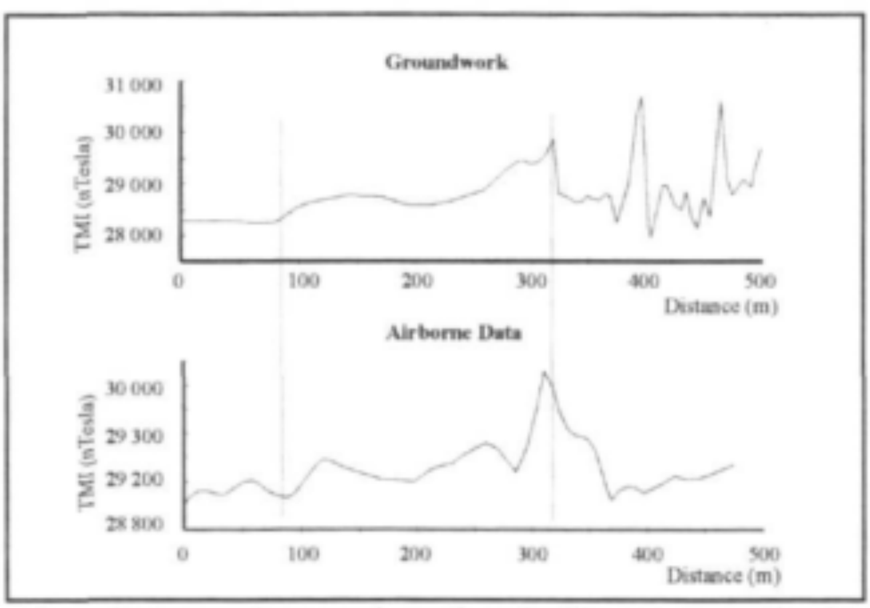

Figure 13:Comparison between downward continued airborne magnetic data and data acquired through groundwork along the same profile.

In some cases the targets are of such a nature that a drilling position can be sited from the airborne data and accurately positioned in the field from the orthophoto where there are prominent landmarks nearby. Another very helpful feature provided with Oasis Montaj is the superposition of contour data on the orthophotos. This enables the ground geophysicist to locate targets in the field and helps him/her to decide when the target structure has been identified and mapped.

4.8 SUMMARY

The GIS approach allows one to compare any two or more data sets with one another and find spatial correlation. When a promising feature is therefore identified on any one data set it can be compared to the other data sets and from that the most effective technique to find and/or map this feature can be decided. The software further allows one to use the mouse to readily obtain the exact coordinates of a identified feature and a prediction as to what should be found when doing the fieldwork can be made.

Furthermore, all available geophysical data previously used in the area, as well as all the information on existing boreholes can be accessed with the click of a button. Not only can promising targets be identified, but management decisions such as which areas have to be developed first due to the greatest shortage of water or the highest risk of pollution can be made with easier and faster access to relevant information.

This type of database can of course be developed to include other data sets as well without losing or changing any of the original data, and if there is changes in the original sets they can be updated as well. This must be seen as a dynamic system, developed to aid any groundwater-related scientist to make better informed decisions in either exploration or management. The success of this whole system would of course be dependent on the accuracy and completeness of the data sets being used. This study, however, is to prove that a GIS based exploration method can be used with great success.

CHAPTER 5

PROCESSING AND INTERPRETATION OF AIRBORNE GEOPHYSICAL DATA APPLIED TO THE SITING OF BOREHOLES

5.1 INTRODUCTION

Three airborne geophysical techniques were flown on area 1 and evaluated to determine the minimum data necessary for an effective exploration program. These were:

- Frequency domain electromagnetism
- Total field magnetics
- Radiometrics (consisting of Thorium, Uranium, Potassium and Total count measurements)

The survey coverage in area 1 consisted of 1177 line kilometers, including 31 line kilometers for tie lines. Flight lines were flown in an azimuthal direction of 0°/180° with a line separation of 100m. The helicopter (Bell 206L-3 turbine helicopter) flew at an average airspeed of 136km/h, with an EM bird height of 30m, magnetic bird height of 40m and spectrometer at 80m (Pritchard, 1997). The airborne data were digitised using a 10Hz sampling frequency. This implies an average ground station spacing of approximately 4m.

5.2 AIRBORNE ELECTROMAGNETIC DATA

5.2.1 DIGHEM data aquisitioning

The EM system used was the DIGHEM^{V} model. The DIGHEM system is an airborne frequency domain electromagnetic system utilizing both co-planer and co-axial configurations. Data from the co- axial coil configurations are used to supplement the co-planar data. The system utilizes the multi-coil coaxial/coplanar technique to energize conductors in different directions. There are five coil pairs. Three co-planar (horizontal) and two co-axial (vertical with axes in flight direction) pairs. An in-phase and quadrature phase channel is measured from each transmitter-receiver coil pair. It is a towed bird type system with a symmetric dipole configuration. The coil separation is 8m for the 400Hz, 900Hz, 5500Hz and 7200Hz, and 6.3m for the 56 000Hz coil-pair, (Pritchard, 1997). The coil orientations and frequencies are given in Table 2.

Five in-phase and five quadrature channels are recorded as well as two monitor channels.

Table 2. Coil orientations and frequencies of DIGHEM system, (Pritchard, 1997).

Coil orientation	*Nominal frequency*	*Actual frequency*
Co-axial	900Hz	1 141Hz
Co-planar	425Hz	389Hz
Co-axial	5 500Hz	5 355Hz
Co-planar	7 200Hz	7 209Hz
Co-planar	56 000Hz	55 890Hz

The targets for this system, (as for all EM systems) are conductors. The DIGHEM responses fall into two general classes, discrete and broad. The first class consists of sharp, well-defined anomalies from discrete conductors such as sulphide lenses and steeply dipping sheetlike conductors (e.g. graphite sheets). The second class consists of wide anomalies from conductors having a large horizontal surface (e.g. conductive overburden and flatly dipping sheetlike conductors). The conductive earth (half space) model is suitable for the broad conductors, and this is the model used for creating the resistivity contour maps (figures 14 to 16), (Sengpiel, 1983).

The application of the DIGHEM system to groundwater exploration is motivated on the basis that weathered material usually has a higher conductivity than its unweathered counterparts. Zones of high weathering, especially if they are connected to large structural features, were the main targets being investigated in this study and the DIGHEM data were used to locate and delineate such structures in the investigation area.

5.2.2 Interpretation of the DIGHEM data

The focus of the interpretation was to identify regional structures such as faults or any other conductive features that could be correlated with zones of extensive weathering and therefore possible aquifers. The lowest frequency data (400Hz in this case) provides the deepest conductivity information according to the skin depth relation δ (Telford et al, 1990):

$$\delta = \left(\frac{2}{\omega\mu\sigma}\right)^{\frac{1}{2}} \qquad (5.1)$$

with:

ω = angular frequency

μ = magnetic permeability

σ = apparent conductivity

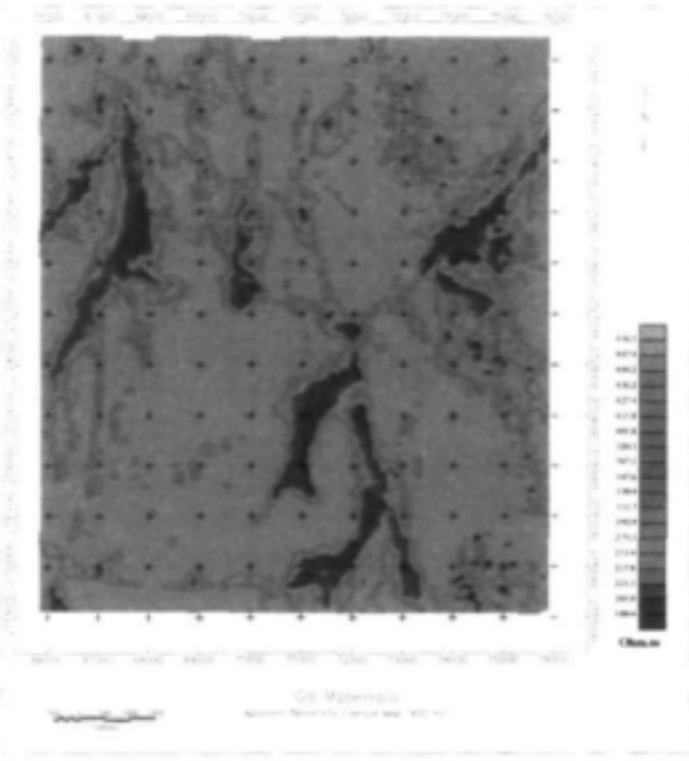

Figure 14: DIGHEM resistivity contour map for 400Hz frequency. (Blue indicates high conductivity.)

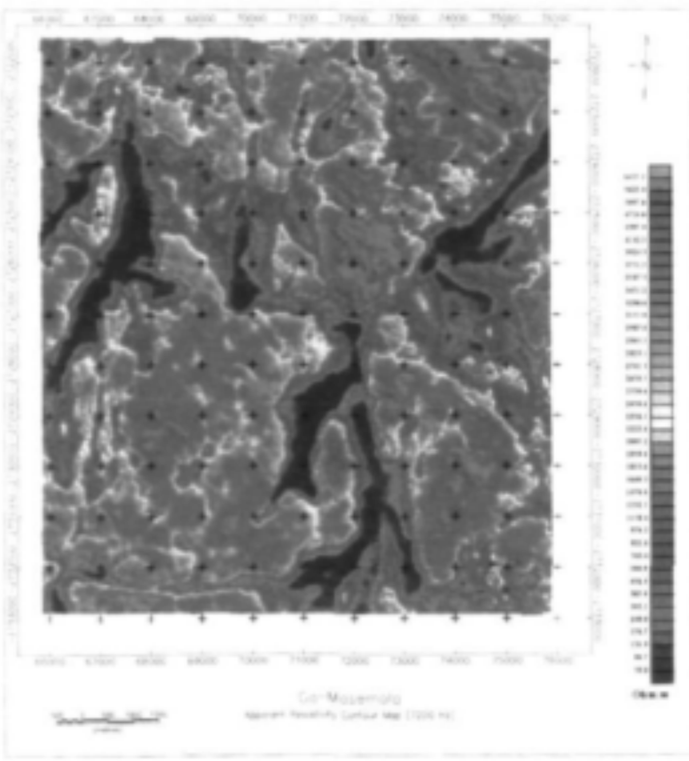

Figure 15: DIGHEM resistivity contour map for 7200Hz frequency.

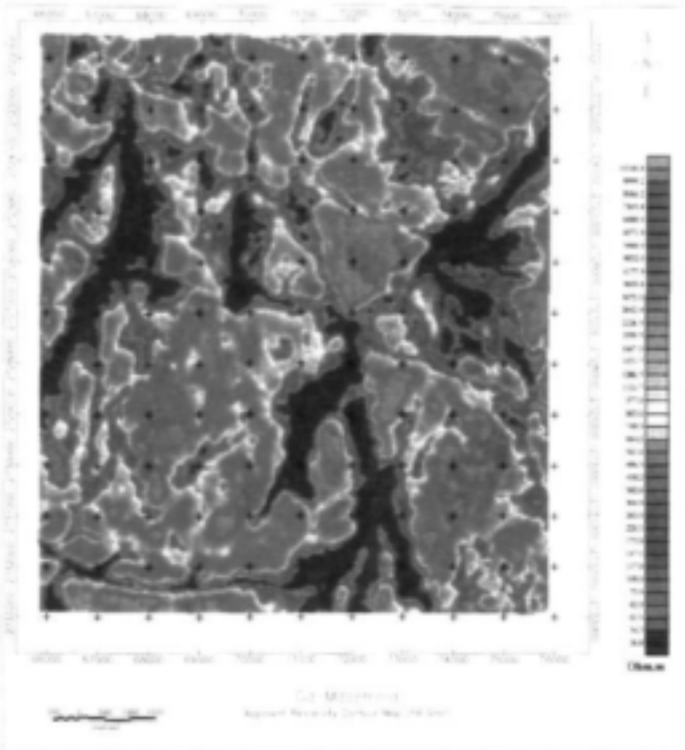

Figure 16: DIGHEM resistivity contour map for 56kHz frequency.

The deep structures were the main targets since they are ostensibly less sensitive to droughts.

The apparent resistivity contour maps were used, together with contour maps of the quadrature phase response (figures 17 and 18), to identify and map conductive linear target features. The quadrature phase contour maps enhance the smaller conductivity features that are not readily visible on the resistivity maps and also provide a more detailed delineation of the structures. Furthermore, the 900Hz co-axial data show targets perpendicular to the flight line direction more clearly.

The main targets were traced with thick black lines on the 400Hz apparent resistivity map. Smaller features were filled in with thin blue lines by making use of the 400Hz, 7200Hz and 56kHz maps. The dotted red lines show features that were defined more clearly by making use of the quadrature phase contour maps. The results of this interpretation are shown in figure 19.

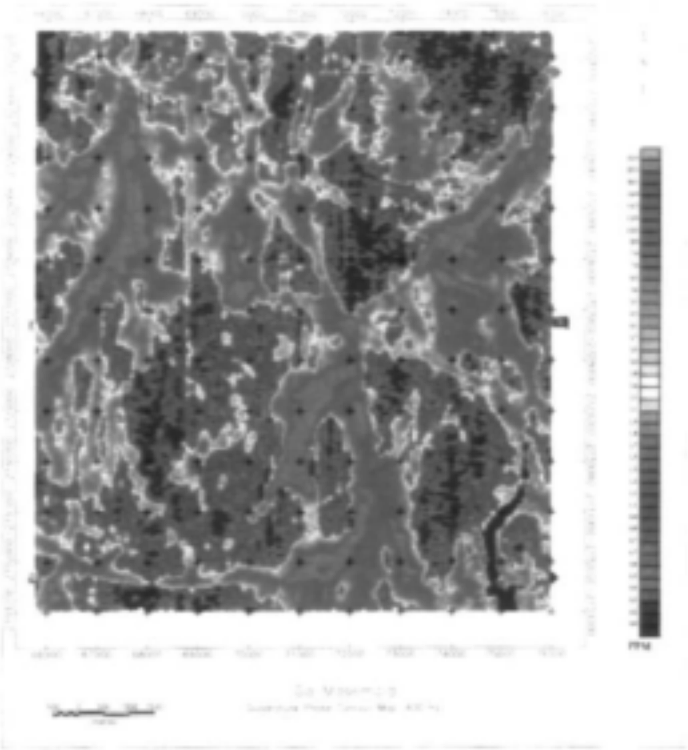

Figure 17: Contour map of the quadrature phase component (400Hz, co-planar).

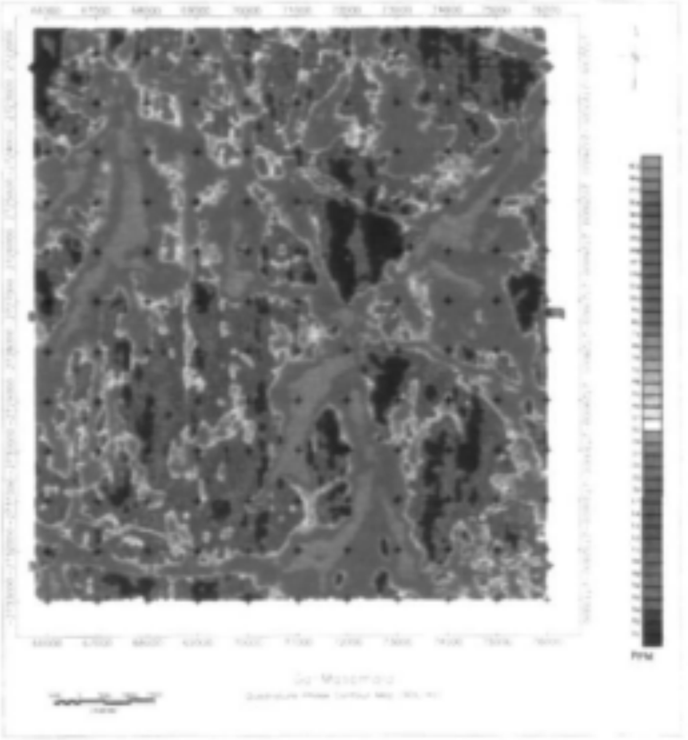

Figure 18: Contour map of the quadrature phase component (900Hz, co-axial).

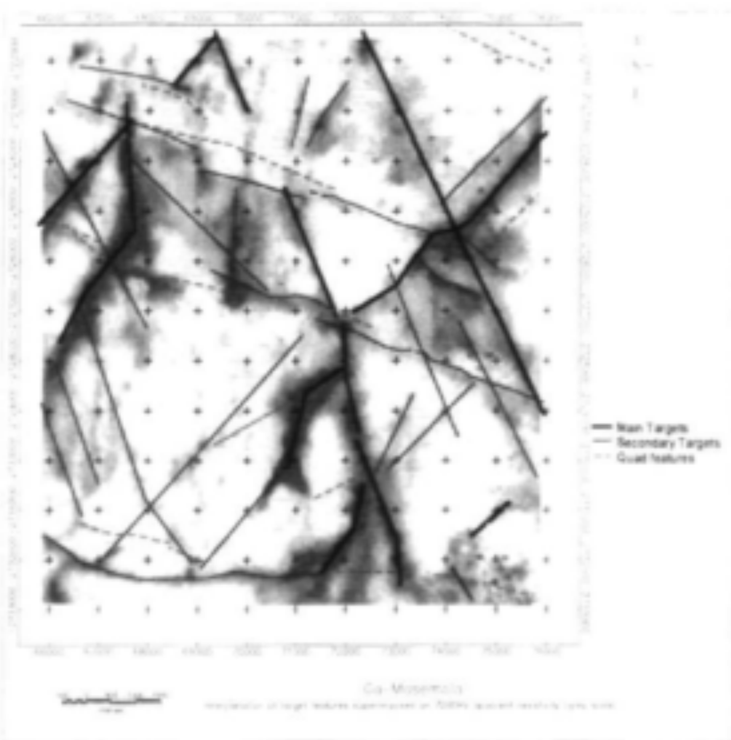

Figure 19: Interpreted structural features.

5.3 AIRBORNE MAGNETIC DATA, AREA 1

5.3.1 Magnetic data acquisitioning

The magnetometer used was a Scintrex H8 Cesium Vapour type with sensitivity of 0.005nT. A sampling rate of 10Hz was achieved and this sensor was also towed in a bird 20m below the helicopter (± 40m above the ground).

A digital recorder containing a clock synchronized with that of the airborne system, was operated together with a base station magnetometer to record, and permit subsequent removal of diurnal variations of the earth's magnetic field. The base station magnetometer was a Geometrics G856-X, proton precession instrument with a sample rate of 30 seconds, (Pritchard, 1997).

The airborne magnetic data are used to identify and map different lithological units and structural features. Different lithological units give different responses due to differences in magnetite content. Faults can be inferred from a displacement in a magnetic unit. By modeling profiles taken from the airborne data sets other important parameters such as depth, dip and depth extent can also be determined. These profiles also serve as an important "data link" between the airborne and ground follow-up data (figure 13).

5.3.2 Magnetic data processing and interpretation

By overlaying a simplified version of figure 2 (geology of the study area) on the total magnetic field map, a definite correlation can be seen with the shallow magnetic features and the geology (figure 20). The high magnetic values (red) clearly represent the dolerite sills and dykes as expected, due to the noticeable higher magnetite content in dolerite, relative to granite. On the magnetic data it is clearly seen that the dolerite sill extends to the east and intruded into the granite. There are also east-west striking dolerite dykes in the eastern half of the area. It should be noted that the magnetic amplitude variation in the study area is small, varying between 28900nT and 29400nT.

Several filters were applied to the magnetic total field data to highlight certain features.

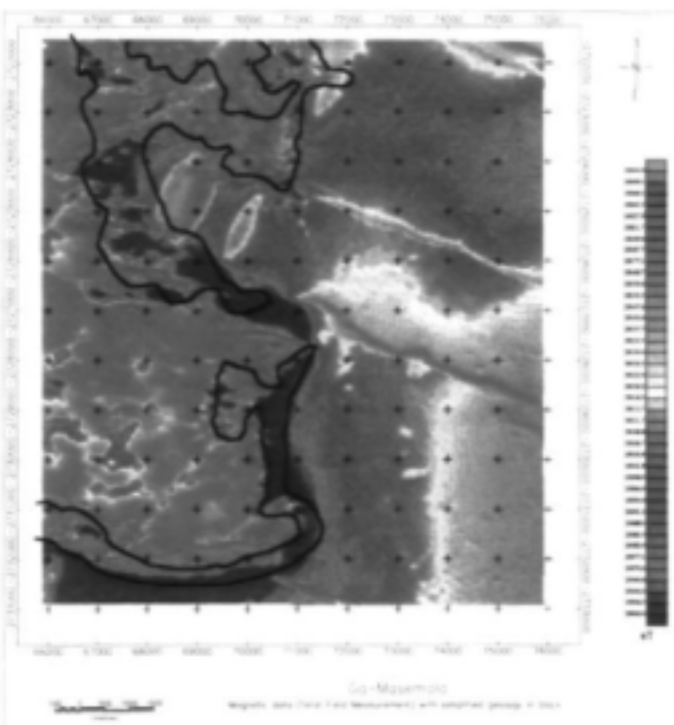

Figure 20: Magnetic total field with simplified geology superimposed

5.3.2.1 Analytical signal

Nabighian (1972) has shown that for two-dimensional bodies a bell-shaped symmetrical function can be derived which maximizes exactly over the top of a magnetic contact. The three-dimensional case was derived in 1984 also by Nabighian (1984). This function is the amplitude of the analytical signal. The only assumptions made are uniform magnetization and that the cross-section of all causative bodies can be represented by polygons of finite or infinite depth extent. This function and its derivatives are therefore independent of strike, dip, magnetic declination, inclination and remanent magnetism, (Debeglia and Corpel, 1997).

The 3-D analytical signal ***A***, of a potential field anomaly can be defined (Nabighian, 1984) as:

$$A(x,y) = \left(\frac{\partial M}{\partial x}\right)\hat{x} + \left(\frac{\partial M}{\partial y}\right)\hat{y} + \left(\frac{\partial M}{\partial z}\right)\hat{z} \qquad (5.2)$$

with :

M = magnetic field.

The analytical signal amplitude can now be calculated (Debeglia, 1997) as:

$$|A(x,y)| = \sqrt{\left(\frac{\partial M}{\partial x}\right)^2 + \left(\frac{\partial M}{\partial y}\right)^2 + \left(\frac{\partial M}{\partial z}\right)^2} \qquad (5.3)$$

This filter was applied to the airborne magnetic total field data, yielding figure 21. Comparing this with figure 20 (total field), the difference is most obvious along the edge of the dolerite sill in the southwestern quarter. Using the superimposed geology as standard, it is seen that the analytical signal amplitude maximizes over the edge of the sill. In interpreting the data, the edges of three-dimensional bodies and the centers of two-dimensional bodies were delineated using the peak values of the analytical signal amplitude.

{In the discussions below, the following parameters are used. (Geosoft Inc., 1996):

μ	*wavenumber in the X direction (complex, radians/m)*
v	*wavenumber in the Y direction (complex, radians/m)*
$r = \sqrt{\mu^2 + v^2}$	*Wavenumber (radians/m)*
$\theta = \tan^{-1}(\mu/v)$	*Wavenumber direction}*

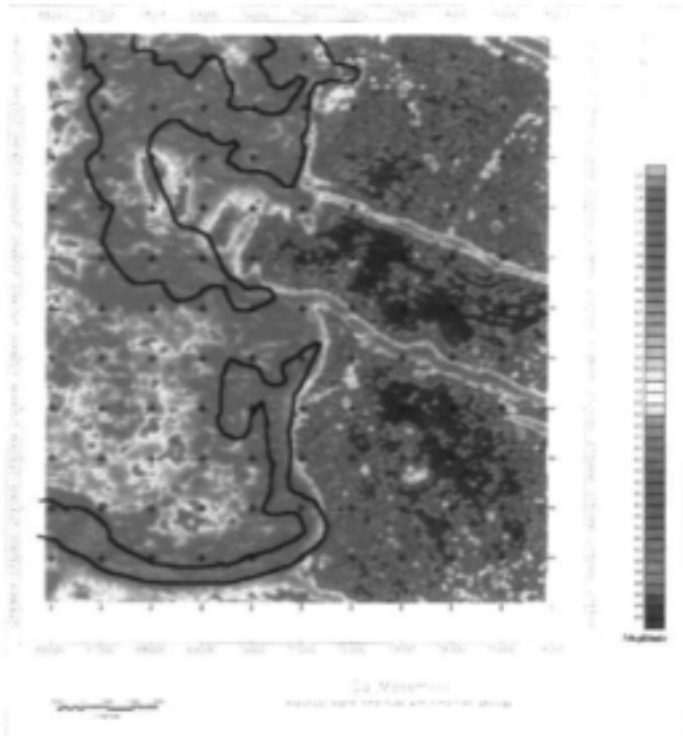

Figure 21: Analytical signal amplitude.

5.3.2.2 Reduction to the magnetic equator

Reduction to the magnetic equator is used in regions of low latitude to center the peaks of anomalies over the causative bodies. This allows for more accurate interpretation of the data under certain physical conditions. Unlike the analytical signal filter, this procedure is subject to the influences of remanent magnetization. The filter expression is given as, (Geosoft Inc., 1996):

$$L(\theta) = \frac{-\cos^2(D-\theta)}{\left[\sin I + i.\cos I.\cos(D-\theta)\right]^2} \qquad (5.5)$$

with:

- I geomagnetic inclination
- D geomagnetic declination

The result of this filter is shown in figure 22. Features striking northeast are more clearly delineated on this map, especially in the western half of the area.

5.3.2.3 Reduction to the magnetic pole

A reduction to the pole transform (figure 23) will provide a symmetrical anomaly over a vertically dipping, non-remanent body and is again used to improve interpretability under certain conditions. At low latitudes, however, an amplitude correction is required to prevent north-south signals from dominating the data. This filter can be described as (Geosoft Inc., 1996):

$$L(\theta) = \frac{1}{\left[\sin(I_a) + i\cos(I).\cos(D-\theta)\right]^2} \tag{5.6}$$

with:

I	geomagnetic inclination
I_a	inclination for amplitude correction ($I_a > I$)
D	geomagnetic declination

For two-dimensional structures the anomaly peaks correlate very closely with the analytical signal peaks, indicating that the effect of remanent magnetism is relatively small.

5.3.2.4 Downward continuation

Downward continuation is used to enhance features at a specified depth/level (lower than original acquisition level) by bringing the plane of measurement closer to the sources. The procedure is susceptible to high frequency noise. This data is especially useful for ground follow-up work when downward continued to ground level. The expression (Geosoft Inc., 1996) is:

$$L(r) = e^{hr} \tag{5.7}$$

with:

h	distance in meters, to continue downward.

Figure 24 shows the airborne data downward continued to ground level (h=38m). This map enhanced features in the low amplitude eastern half of the area, and gives an overall sharper image with more detail on the shallow features.

5.3.2.5 Upward continuation

Upward continuation attenuates high frequency data while enhancing the deeper basement anomalies (figure 25). Depending on the distance (h) used to upward continue the data, it can also be used to define a regional or background field. Upward continuation is described (Geosoft Inc., 1996) as:

$$L(r) = e^{-hr} \qquad (5.8)$$

with:

h distance in meters, to continue upward.

5.3.2.6 Vertical Derivatives

The first vertical derivative (figure 26) is used to enhance the shallow geologic sources in data and often is useful in delineating high frequency features more clearly where they are shadowed by large amplitude, low frequency anomalies. The expression (Geosoft Inc., 1996) is:

$$L(r) = r^n \qquad (5.9)$$

with:

n order of differentiation

This map shows much more detail in the eastern half of the area than any other map, and also enhances magnetic low features that are superimposed on magnetic high structures.

5.3.2.7 Attenuating low frequency anomalies

From the perspective of prospecting for groundwater bearing structures the features at depths less than 150m are important and it is necessary to isolate their response for interpretation. This can be done in several ways. One approach is to use the upward continued data as a background or regional data set. By subtracting the upward continued grid file from the original data the anomalies caused by shallow features are enhanced, (figure 27). The maps created through the application of these filters were used interactively in Oasis Montaj to do an interpretation of the data. Magnetic units, dykes, faults and various lineaments were identified and mapped (figures 28 and 29).

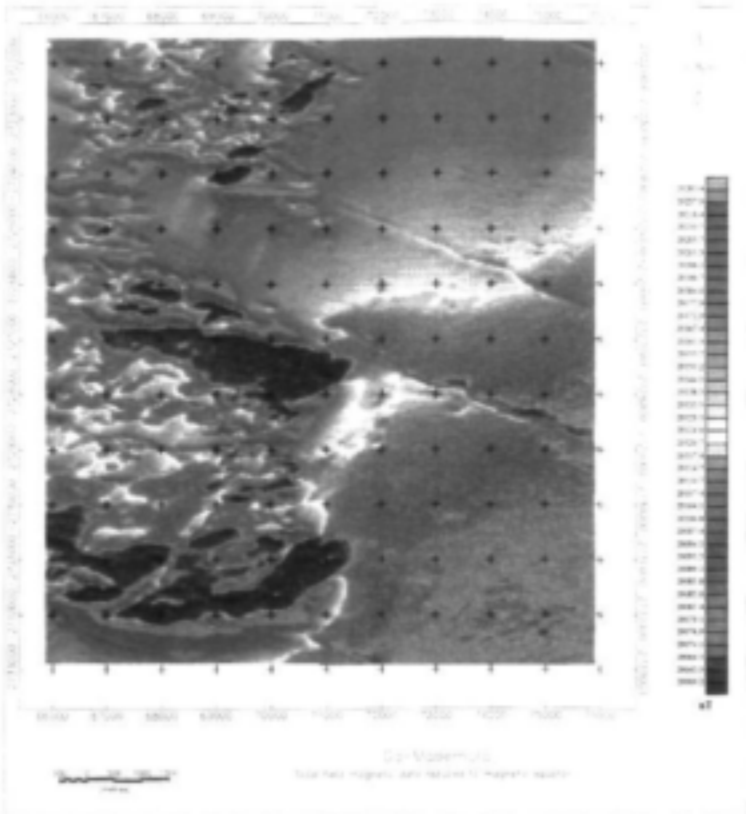

Figure 22: Total field data reduced to the magnetic equator

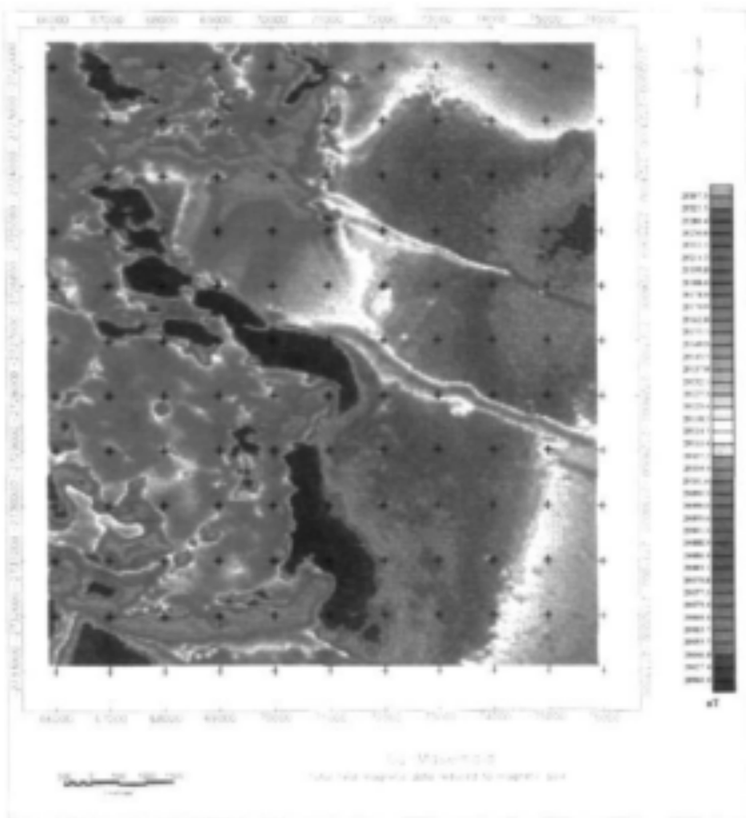

Figure 23: Total field data reduced to the magnetic pole.

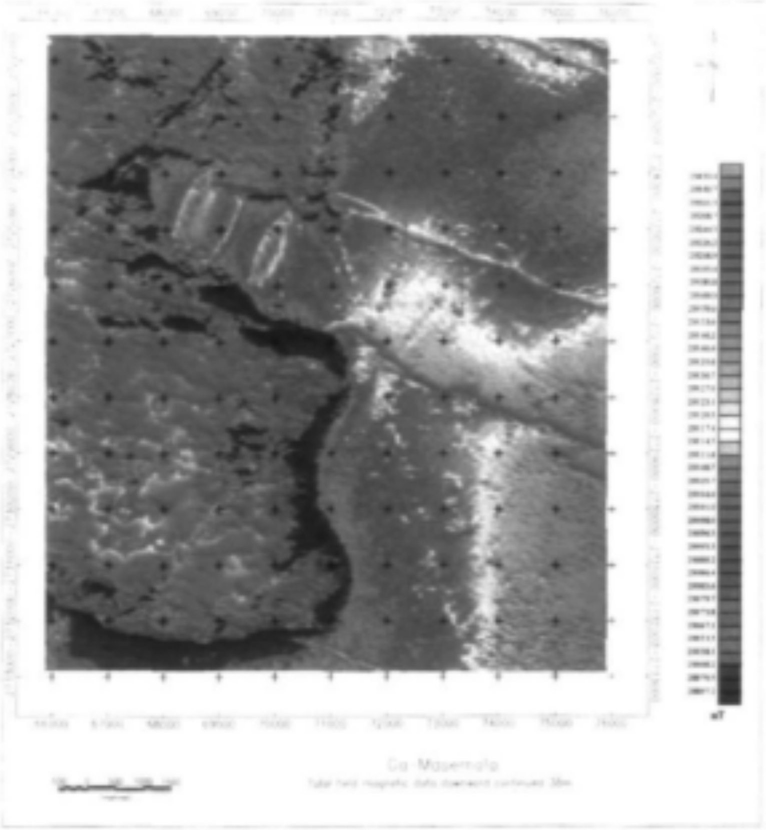

Figure 24: Total field data downward continued 38m.

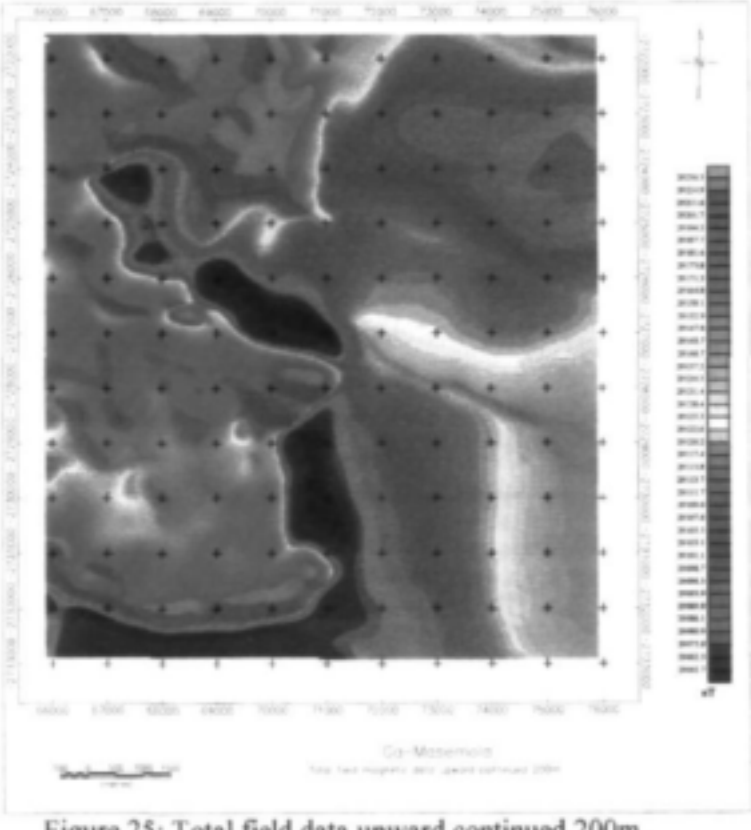

Figure 25: Total field data upward continued 200m.

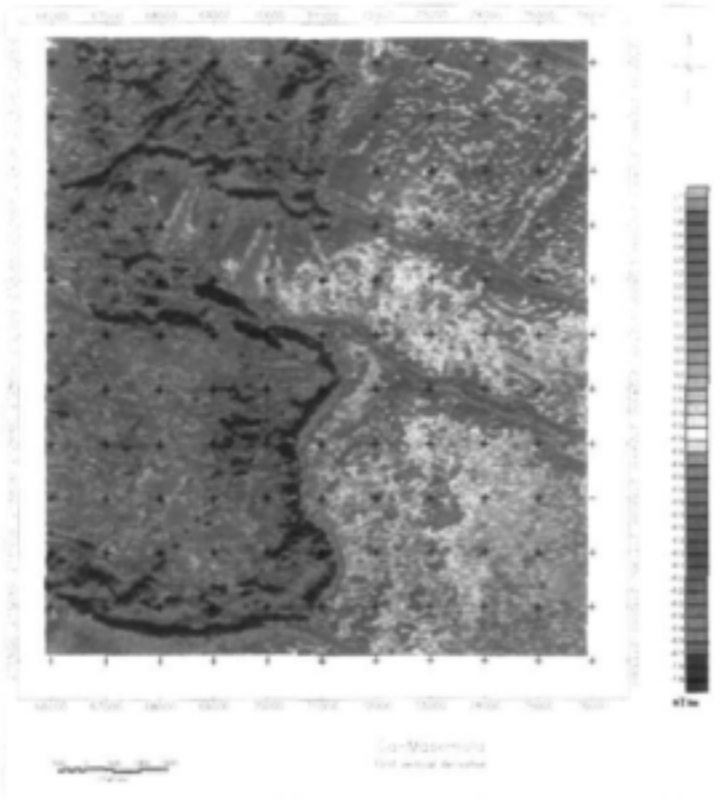

Figure 26: First vertical derivative

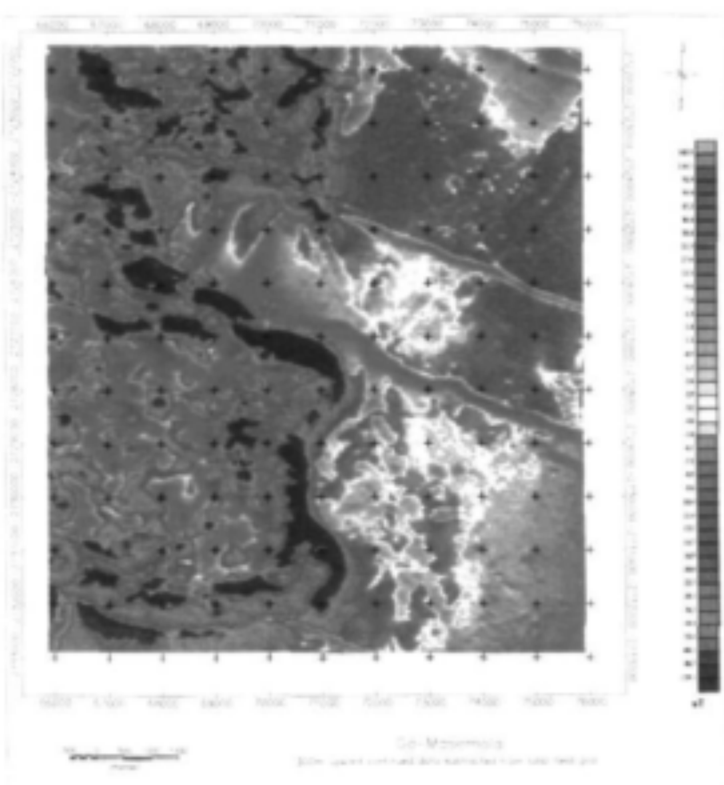

Figure 27: Map showing the residual after the 300m upward continued data is subtracted from the total field data.

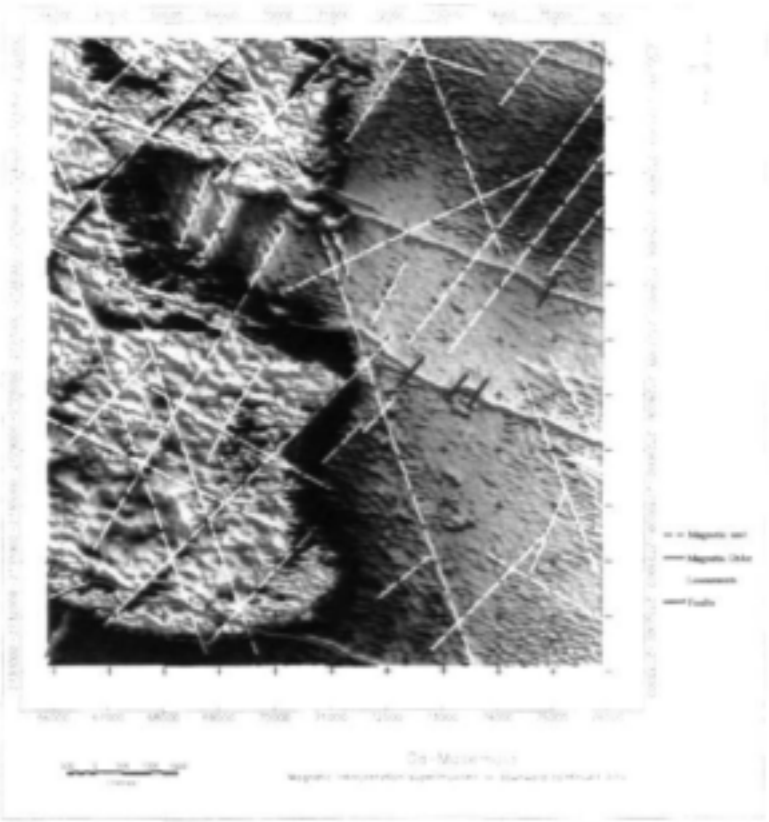

Figure 28: Magnetic interpretation superimposed on downward continued data.

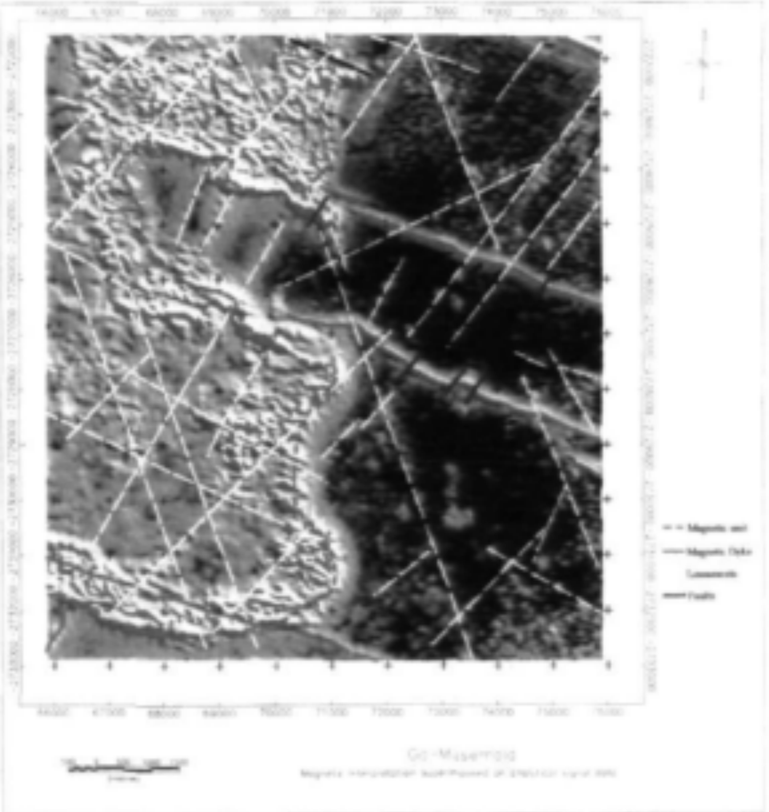

Figure 29: Magnetic interpretation superimposed on analytical signal

5.3.2.8 Euler deconvolution

Three dimensional Euler deconvolution is an algorithm which can be applied to magnetic or gravity survey data that are in grid form. The algorithm solves for source positions and depths by deconvolution using Euler's homogeneity relation and geological constraints imposed through the use of a structural index (SI) (Reid et al, 1990).
From Thompson (1982) the Euler's homogeneity relation is given as:

$$(x-x_0)\frac{\partial T}{\partial x}+(y-y_0)\frac{\partial T}{\partial y}+(z-z_0)\frac{\partial T}{\partial z}=N(B-T) \quad (5.10)$$

where (x_0, y_0, z_0) is the position of a magnetic source whose total field T is detected at (x,y,z). The total field has a regional value of B and the degree of homogeneity (N) may be interpreted as a structural index, which is a measure of the rate of change with distance of a field (Thompson, 1982). Data need not be pole-reduced and therefore remanence does not influence the technique. The corollary is that the method cannot yield any dip information (Reid et al, 1990).

When implementing the algorithm three important parameters have to be specified. These are the maximum depth tolerance to allow, the window size and the structural index. The maximum depth tolerance to allow (given in percentage), controls which solutions are accepted (i.e. solutions with error estimates smaller than the specified tolerance) (Geosoft Inc., 1995). The window size determines the area in terms of grid cells used to calculate the Euler solutions. For high resolution data and shallow targets window sizes of 3X3 to 6X6 are common, while larger window sizes are used for regional data and to define basement structures (Reid et al, 1990). The structural indices (SI) depend on the source geometry and are summarized in the following table.

Table 3: Summary of structural indices for simple models in a magnetic field (Geosoft Inc. 1995).

SI	*Magnetic field*
0.0	Contact
0.5	Thick step
1.0	Sill/dyke
2.0	Pipe
3.0	Sphere

The results of the Euler solutions are plotted as small circles that are colour coded for depth. A given geological structure will show up on maps created with different values for SI and correspondingly different depths. In order to decide which value of SI to accept, the map on which the symbols (circles) are clustered the closest together are assumed to give the best fit. An index that is too low gives depths that are too shallow and vice versa. Lower indices have lower relative precisions and the parameters obtained from these data are therefore also less precise (Reid et al, 1990).

Three maps were created using a depth tolerance of 15%, 5X5 window size and SI values of 0, 0.5 and 1 respectively. The results are shown in figures 30-32. The data are seen to correspond very well with interpretations made from the previously mentioned maps. The dykes are extremely well matched on the SI=1 and SI=0.5 maps. Furthermore it is noticed that the prominent magnetic unit (sill) in the western half of the area is associated with depths up to 170m which is much deeper than the other features. The SI values were chosen because faults, sills and dykes were the target features. As mentioned in the previous paragraph, small indices lead to lower precision and therefore the maps have a noisy character. However, when the solutions are restricted to yield a cleaner map, the structural trends become less visible.

5.4 AIRBORNE RADIOMETRIC DATA, AREA 1.

Almost all the γ-ray radiation measured from rock and overburden originates in the upper 0.5 meters of the earth. Radioelement counts are the rates of detection of the gamma radiation from specific decaying particles corresponding to products in each radioelement's decay series. Radiometric data applied to groundwater exploration are used to discriminate between lithological units and to identify faults. Faults can exhibit radioactive highs due to increased permeability that allows Radon migration, or as lows due to structural control of drainage and fluvial sediments that attenuate gamma radiation from the underlying rocks (Pritchard, 1997). Changes in radioelement concentrations due to alteration will also define faults.

The spectrometer used in this survey was a GR-820, 256 multichannel, Potassium stabilized model manufactured by Exploranium. It has an accuracy of 1 count/second. The spectrometer employs four downward looking crystals (recording the radiometric spectrum from 410 KeV to 3 MeV over 256 discrete energy windows, as well as a cosmic ray channel detecting photons with energy levels above 3 MeV) and one upward looking crystal (to measure and correct for Radon). From this data the standard Total Count, Potassium, Uranium and Thorium channels are extracted. The GR-820 provides raw or Compton stripped data that have been automatically corrected for gain, base level, ADC offset and dead time (Pritchard, 1997).

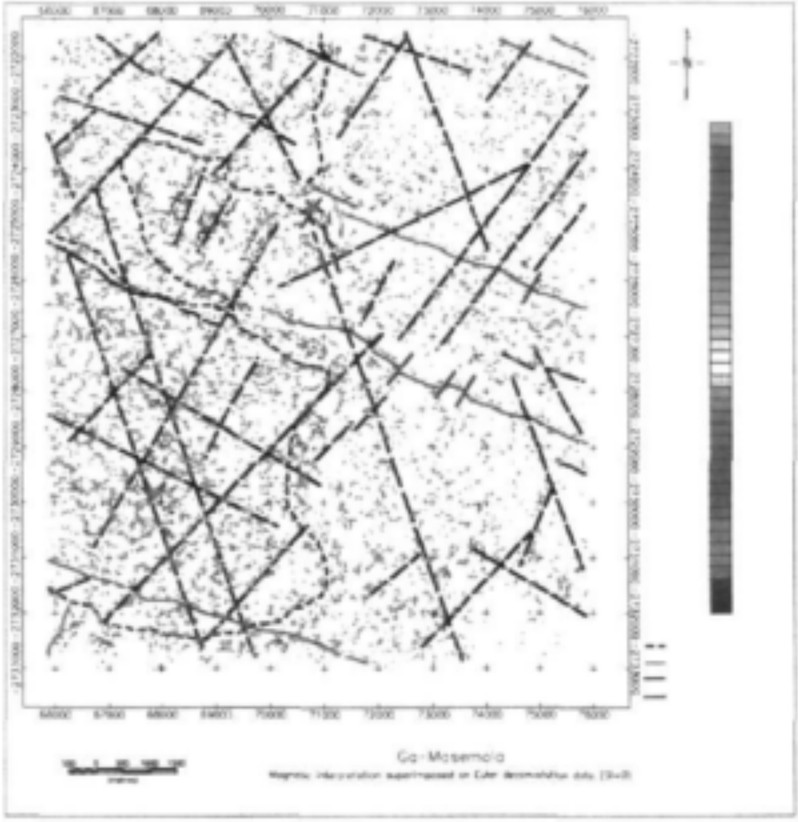

Figure 30: Magnetic interpretation superimposed on Euler deconvolution resluts (SI=0).

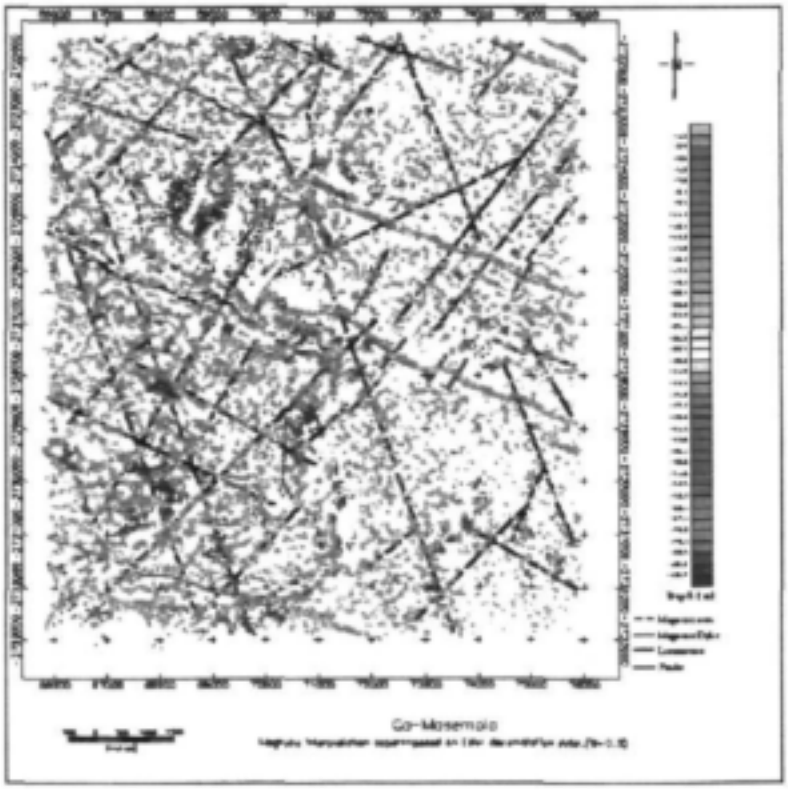

Figure 31:Magnetic interpretation superimposed on Euler deconvolution resluts (SI=0.5).

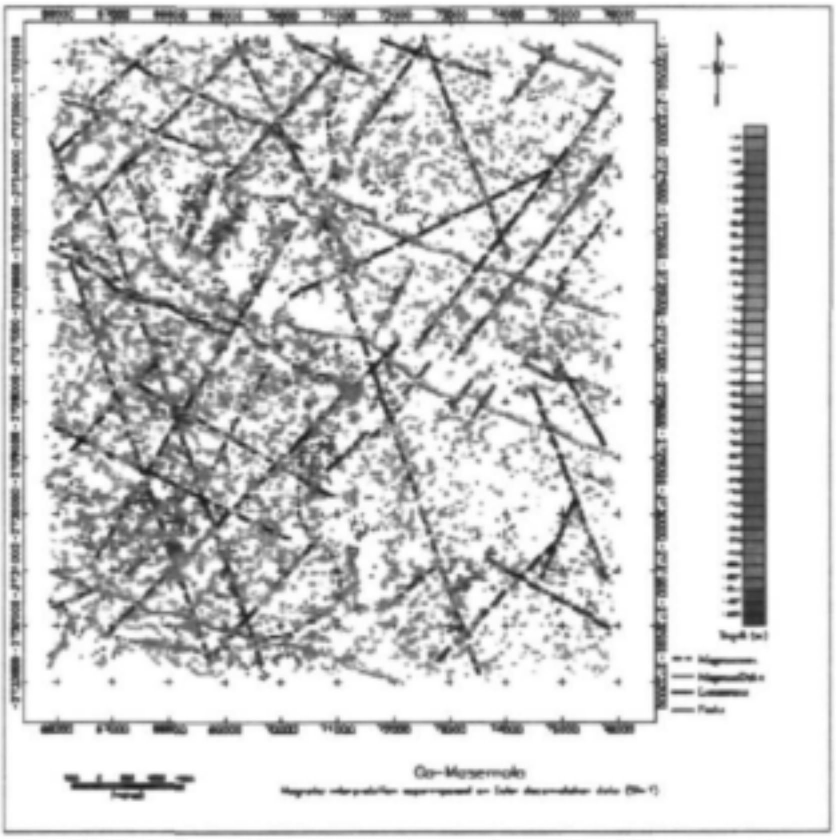

Figure 32: Magnetic interpretation superimposed on Euler deconvolution resluts (SI=1).

Figure 33: Ternary image of radiometric data with simplified geology outline.

The data are presented as a ternary image (figure 33) with Thorium in yellow, Potassium in magenta and Uranium in cyan.

The data can be clearly correlated with the geological outcrops. The white areas indicate the dolerite while the magenta and green indicate higher total count concentrations indicative of the granites in the region. Some of the major structural features can be identified on this map, especially in the eastern half.

5.5 ANCILLARY EQUIPMENT

The following ancillary equipment were used to aid in the survey (Pritchard, 1997):

- radar altimeter (0.3m sensitivity measuring the vertical distance between the helicopter and the ground)
- barometric altimeter (0.1m accuracy at sea level)
- analog recorder
- digital data acquisition system
- tracking camera
- navigation system (12 channel, simultaneous receiver; 1m accuracy in differential mode)
- field workstation

5.6 DETERMINATION OF OPTIMUM DATA ACQUISITION PARAMETERS

The initial approach to this project was to obtain all possible relevant data at 100m line spacing. After interpretation of the data it was necessary to determine the most cost-effective set of data that would yield the same information that was obtained from the initial set. In order to do this the following was investigated:

- optimum line spacing
- optimum data set
- optimum ground follow-up

5.6.1 Optimum line spacing

The optimum line spacing was determined by reprocessing the 100m line spacing data using every second, every third and every fourth line. This corresponds to 200m, 300m and 400m line spacing respectively. The optimum line spacing would then be the largest one on which the interpreted structures can still be distinguished clearly. A comparison of these data sets is shown in figure 34.

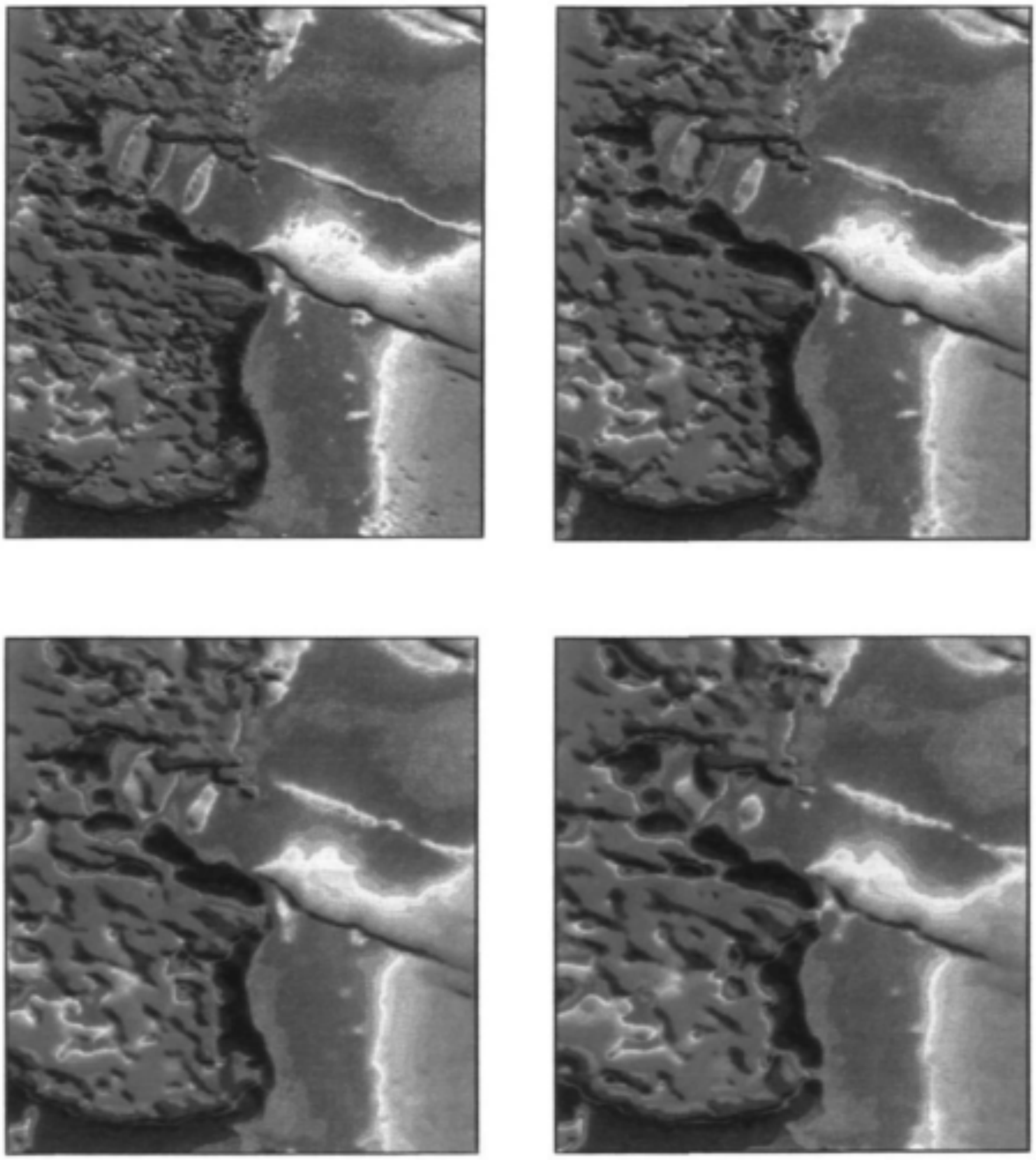

Figure 34: Total field magnetic data processed at 100m (top left), 200m (top right), 300m (bottom left) and 400m (bottom right) flight line spacing.

At first glance there seems little to choose between the 100m and 200m line spacing data. Based on the fact that this study is focused on the granites and that our main targets are faults rather than dykes, sills and dolerite-granite contacts, the measure of resolution was chosen as a north-west striking feature in the eastern half of the area. This feature is much more clearly visible on the EM data and was confirmed by drilling to be a fault in granite (no dolerite visible in drill samples) which yielded 3l/s (blow test yield). On the 200m line spacing this feature is still just visible (provided that its position is already known!). Even when applying filters to the 200m data that enhanced this feature on the 100m data, it cannot be distinguished to satisfaction.

Unfortunately the data could not be processed at 150m line spacing interval without re-sampling the data and introducing possible artifacts. Based on the available data however, the recommended line spacing for future surveys is 100m although even 50m line spacing should be strongly considered if at all possible.

5.6.2 Optimum data set

Comparing the different data sets, it is noted that almost all of the prominent electromagnetic features (especially on the 400Hz frequency) are evident on the magnetic data as well. The radiometric data resemble the geological map very well and also confirm the major features visible on the other data sets, but do not add any exclusive features to the overall structural interpretation. Taking into account the cost of each type of survey (the EM still being very expensive at this point in time), the information conveyed by each method and the specialised type of interpretation (mapping faults and fracture zones with weathering shallower than 200m), the magnetic data are by far the best suited for this kind of exploration. High density magnetic data are therefore recommended as the best option for an economically viable regional groundwater exploration program. This assumption was tested by doing an airborne magnetic survey only of area 2.

CHAPTER 6

GROUND FOLLOW-UP AND TARGET IDENTIFICATION, AREA 1

6.1 Ground follow-up procedure

From the interpretation of the airborne data, certain target areas have been selected. Depending on the airborne data type anomaly, ground follow-up work was done to map the target areas in greater detail in order to site drilling positions.

The groundwork consisted of magnetic and frequency domain electromagnetic (EM34) profiles done along survey lines determined from the airborne geophysical data sets. The target positions were found in the field with the aid of a global positioning system (GPS) and the 1:10 000 orthophotos. Due to the high resolution of the airborne data and the convenience of overlaying the geophysical anomalies onto the orthophotos (figure 12), the fieldwork could in most cases be limited to a 400m long profile or less to identify the targets. Because the target strike direction is known beforehand from the airborne data, one profile usually proved sufficient to site a borehole on. The magnetic surveys consisted of total field measurements at 5m station spacing while the EM34's 20m and 40m coil spacing were used where possible, with 10m and 20m station spacing respectively. The 40m coil spacing configuration yielded very noisy data in areas of low conductivity (<5 mS), and therefore was only included in areas of relatively higher conductivities.

A typical field survey to find an airborne target was finished on average in 4 hours. Once the readings were taken, the profiles were plotted and interpreted. Because the main target features were already known from the airborne data, this interpretation usually only consisted of determining a dip and exact field location of the target structure. The areas that were chosen as investigation sites from the airborne data are shown in figure 35. In this figure, a square box was drawn around each of the anomalous areas chosen for ground follow-up work. Detailed maps and profiles showing all the groundwork that were done as well as the borehole positions associated with each target are found in figures 36-59.

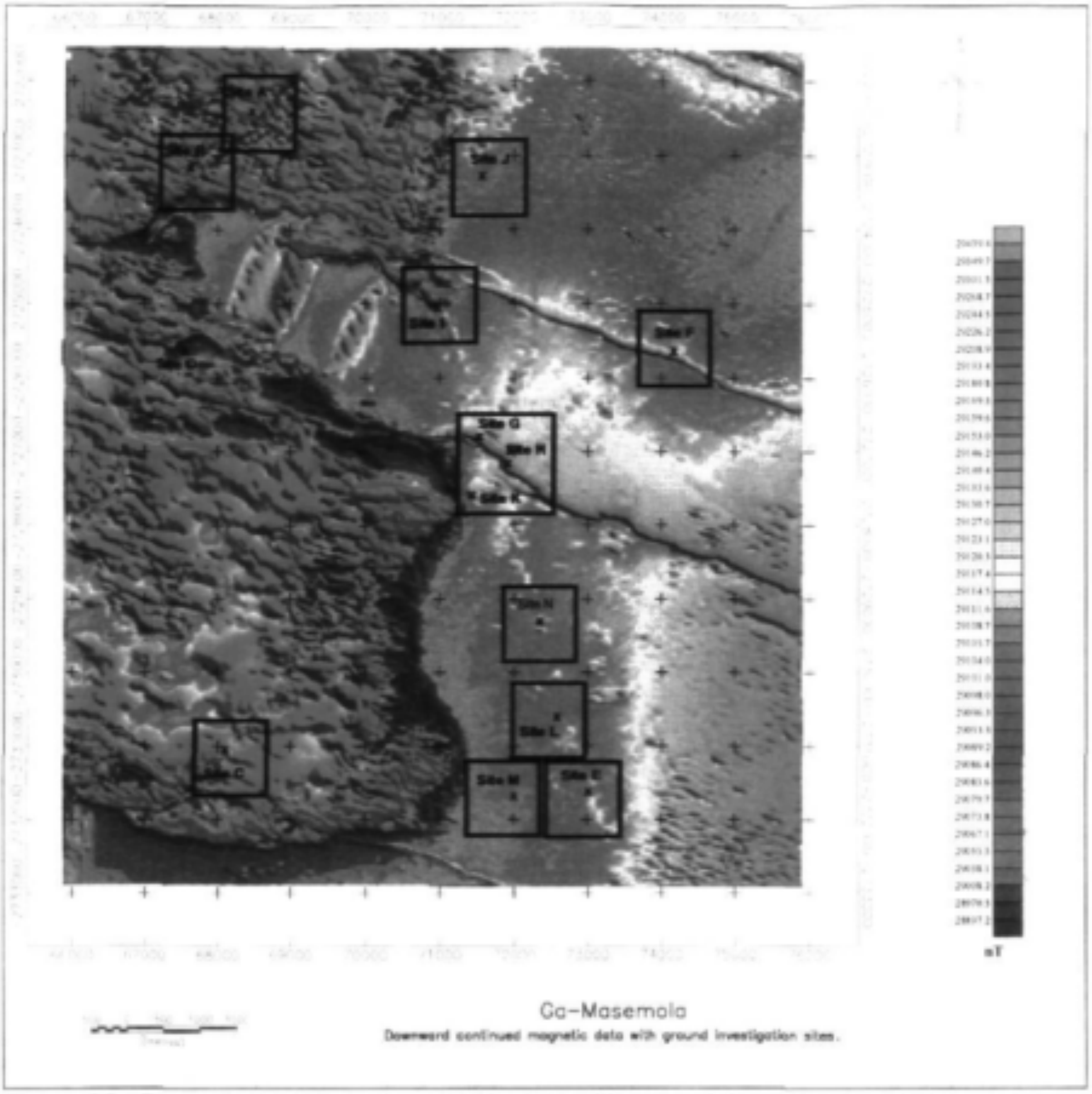

Figure 35: Downward continued magnetic data with ground investigation sites.

All borehole positions were finally chosen, based on the EM34 data. Attention was given to a maximum value on the vertical loop data, corresponding to a minimum value on the horizontal loop data. For more detail on the interpretation, see the Geonics technical note on the EM34 that accompanies the purchase of the instrument.

6.2 LOCATION MAPS AND GROUNDWORK PROFILES

Site A

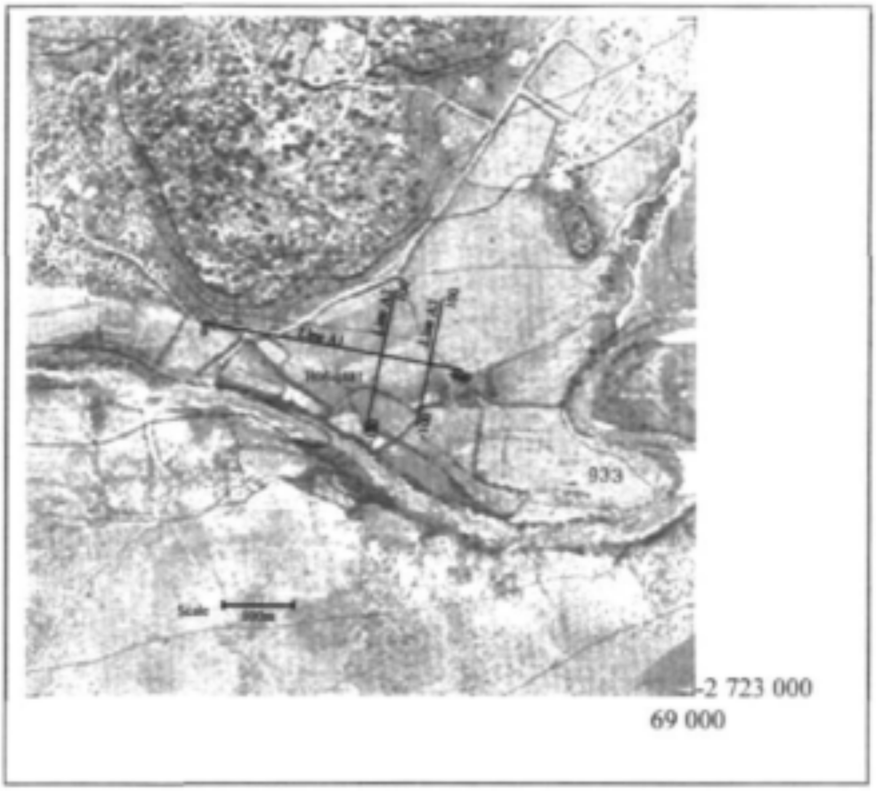

Figure 36a: Location map with field profiles and borehole position (Orthophoto series, 1983)

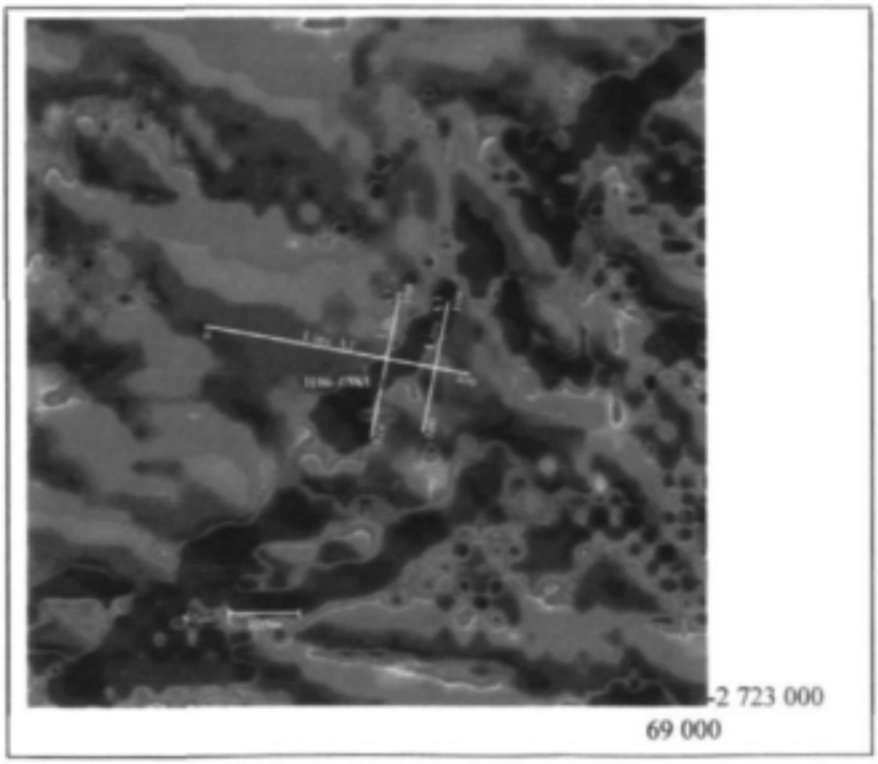

Figure 36b: Airborne magnetic data for the same area as shown above.

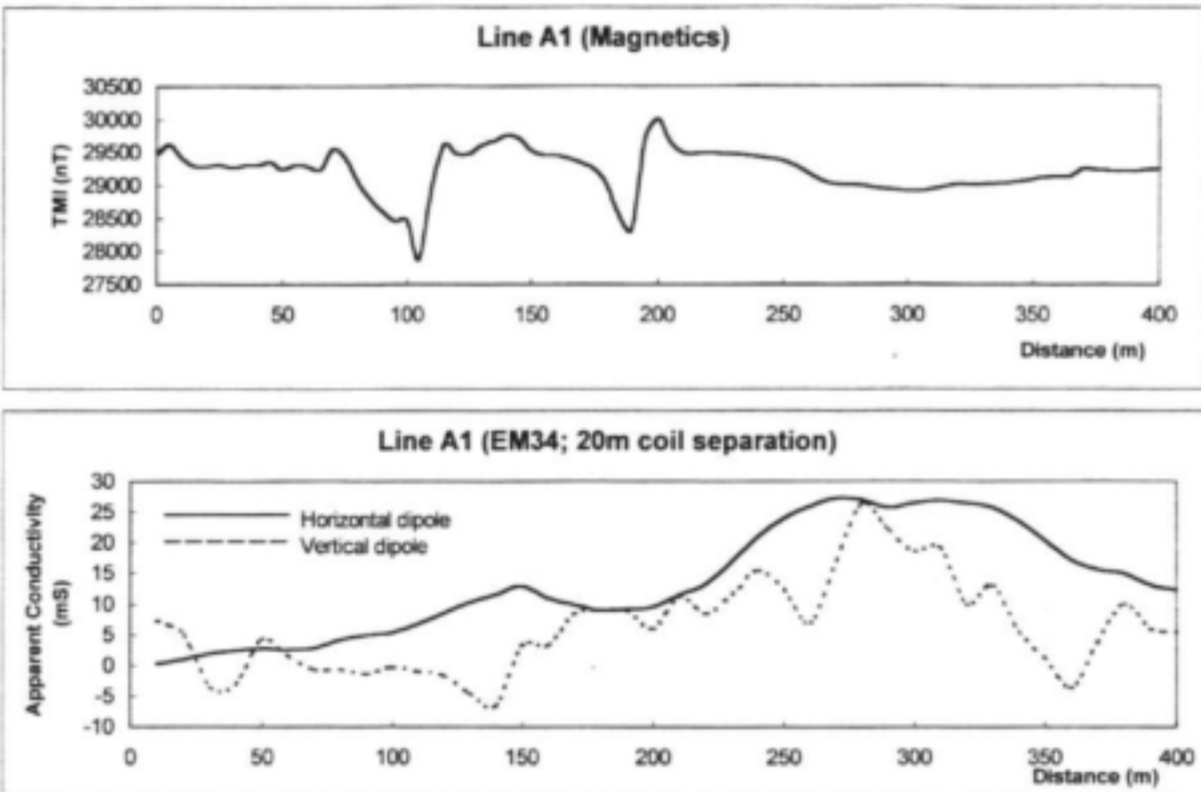

Figure 37a: Profiles for line A1

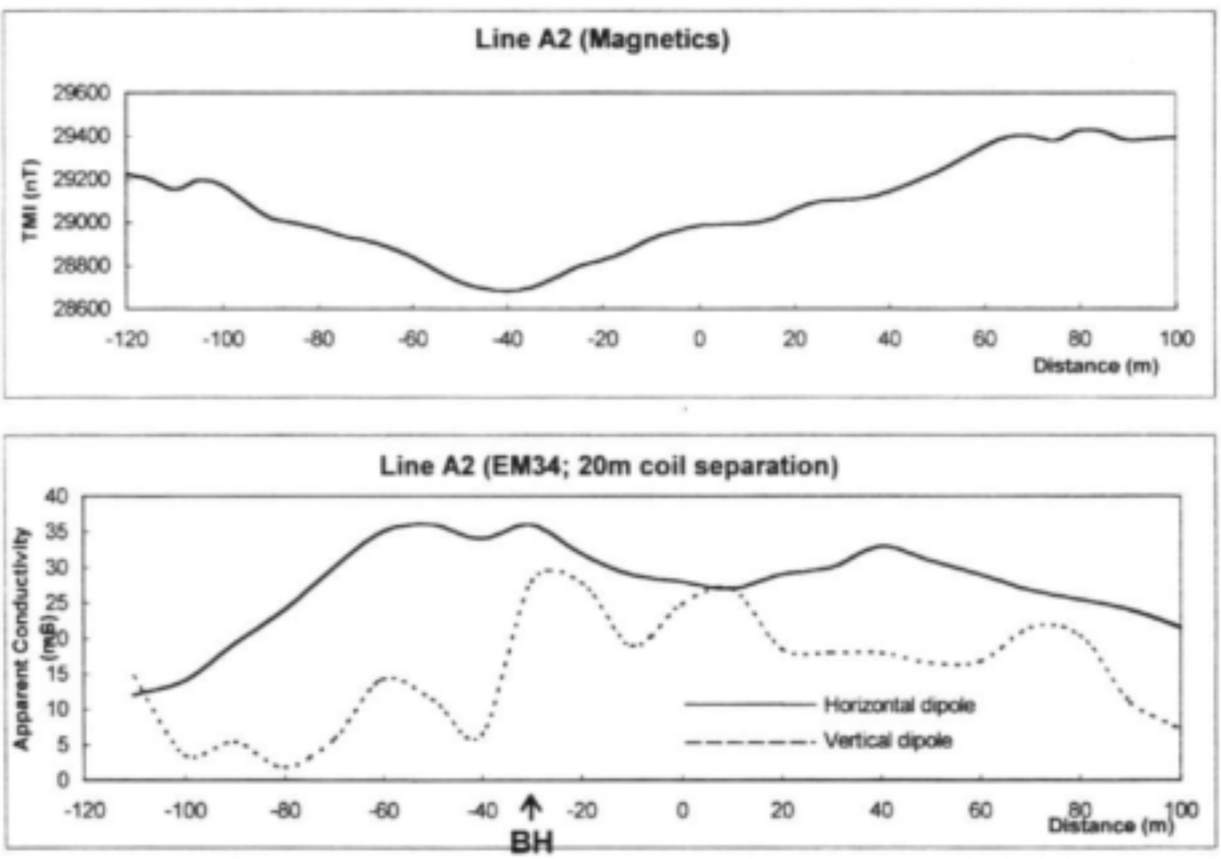

Figure 37b: Profiles for line A2

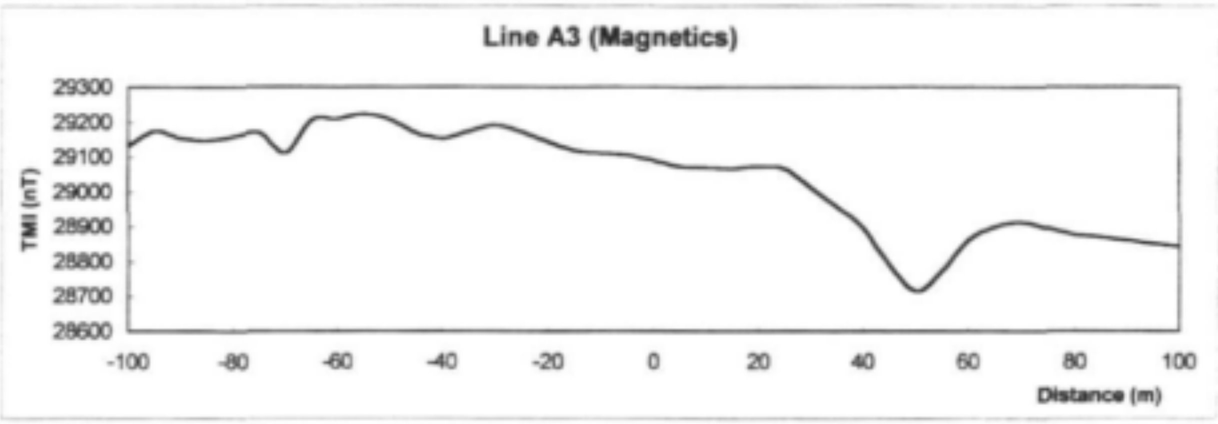

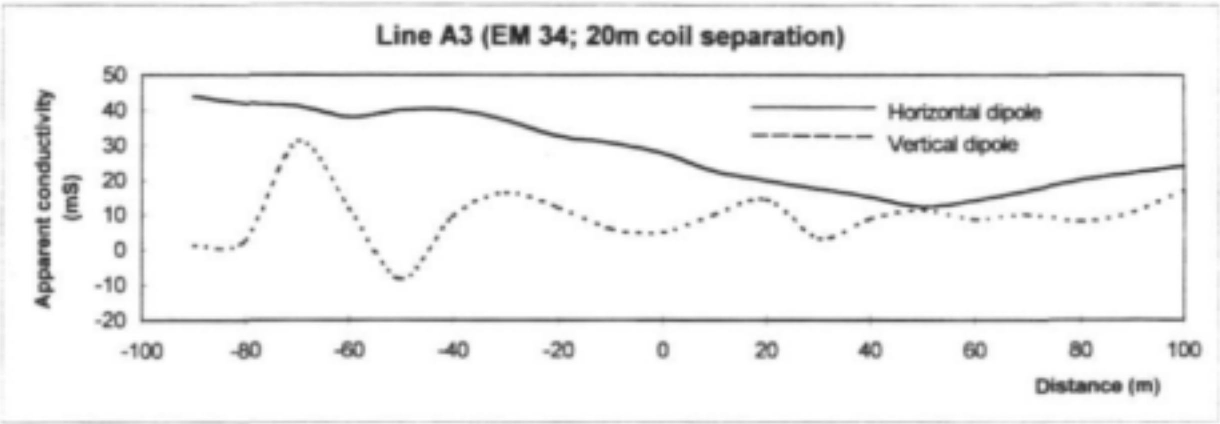

Figure 37b: Profiles for line A3

Site B:

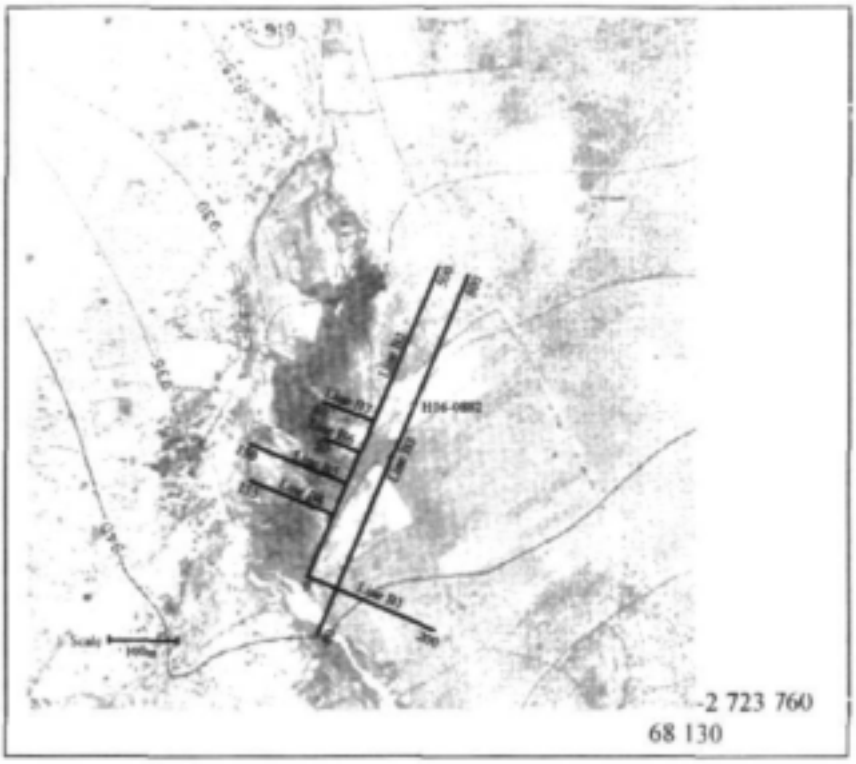

Figure 38a: Location map with field profiles and borehole position (Orthophoto series, 1983)

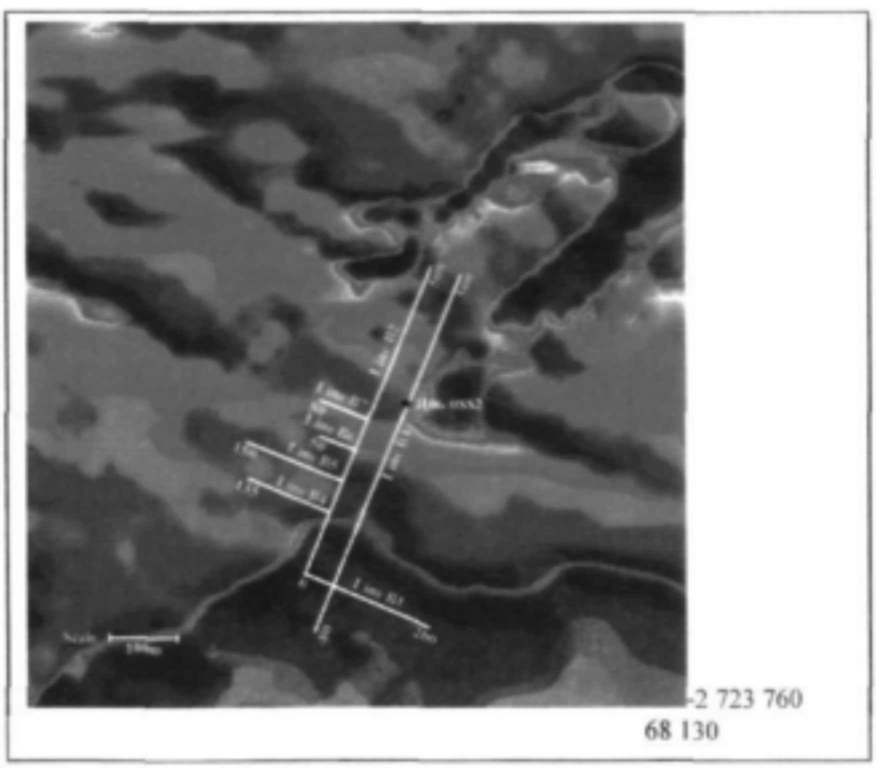

Figure 38b: Airborne magnetic data for the same area as shown above.

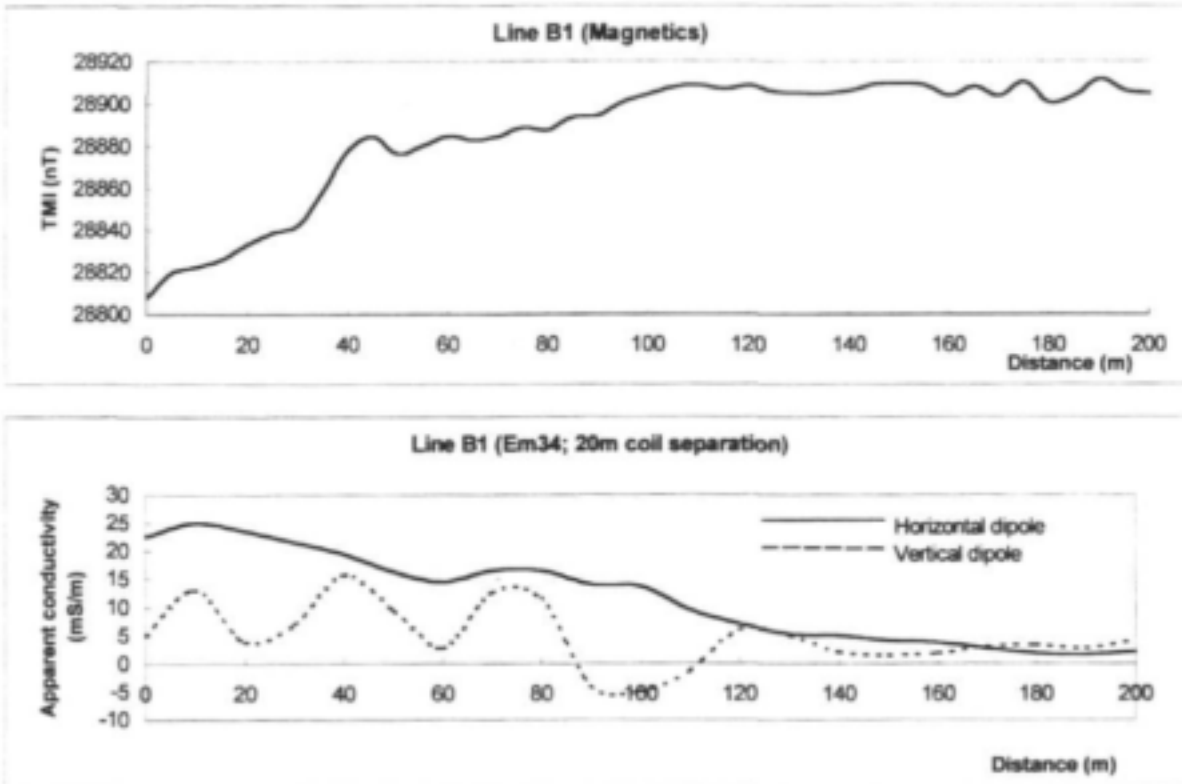

Figure 39a: Profiles for line B1

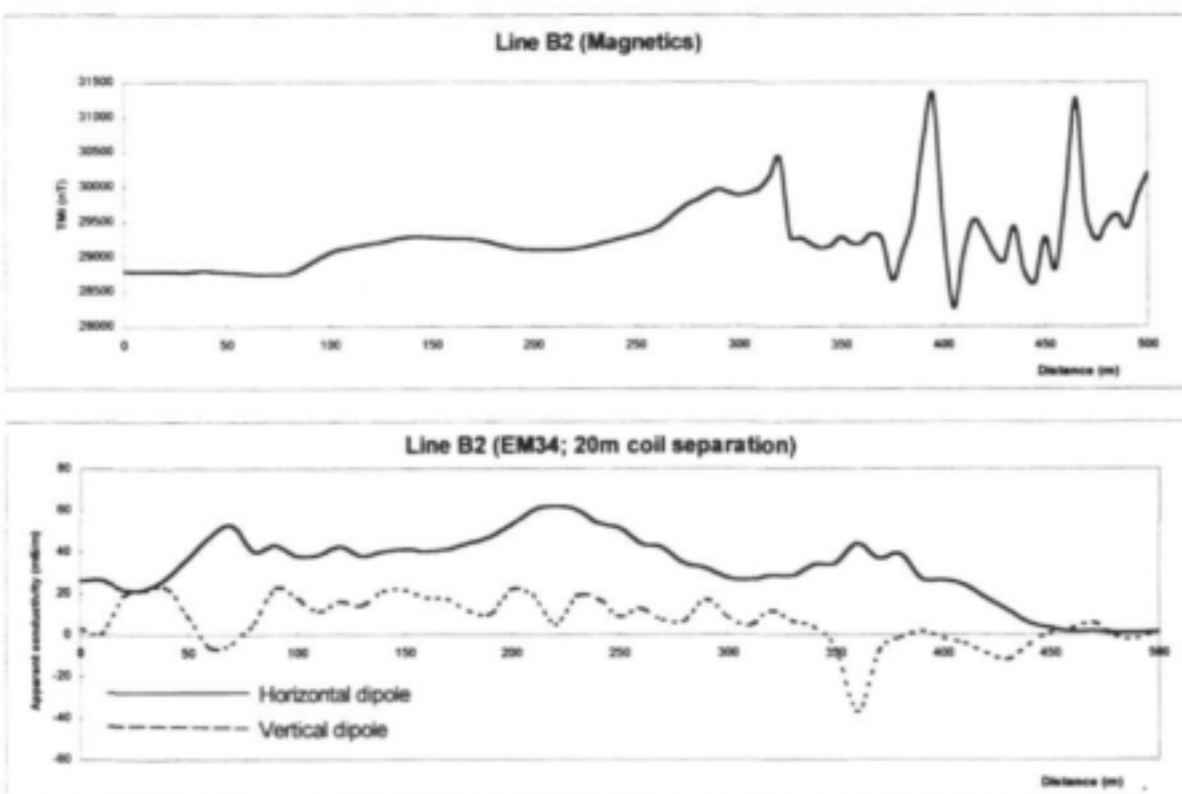

Figure 39b: Profiles for line B2

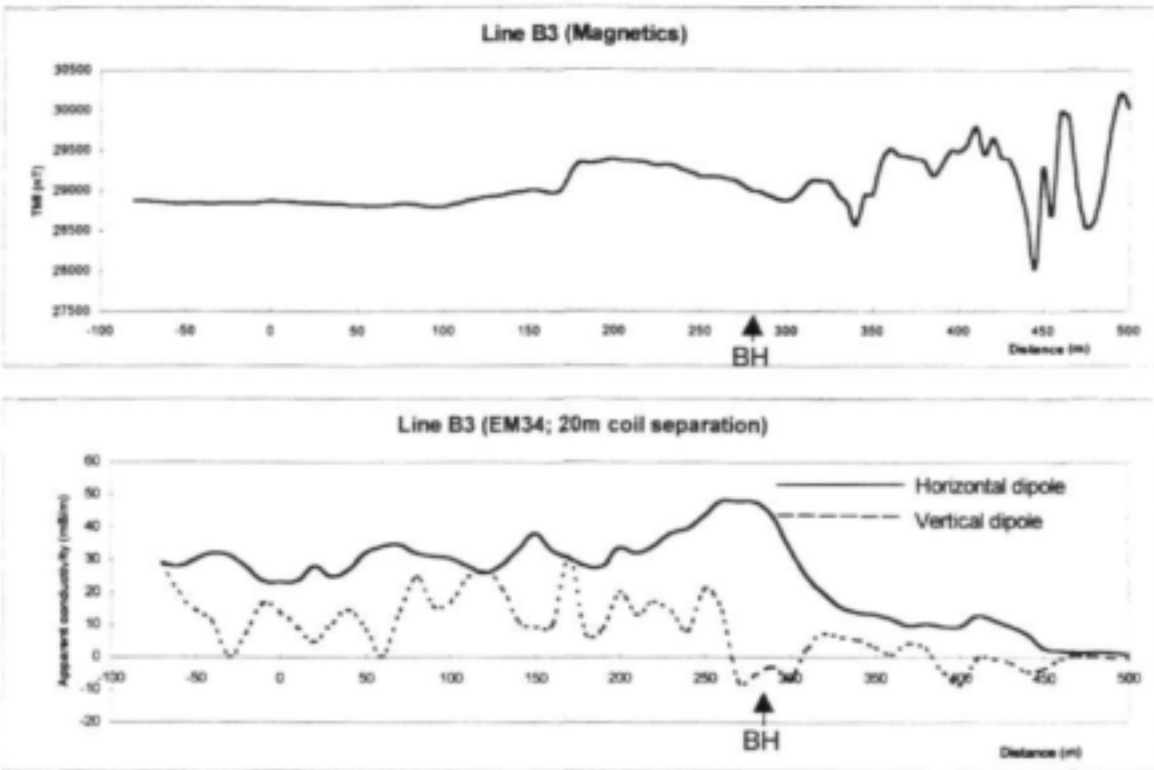

Figure 39c: Profiles for line B3

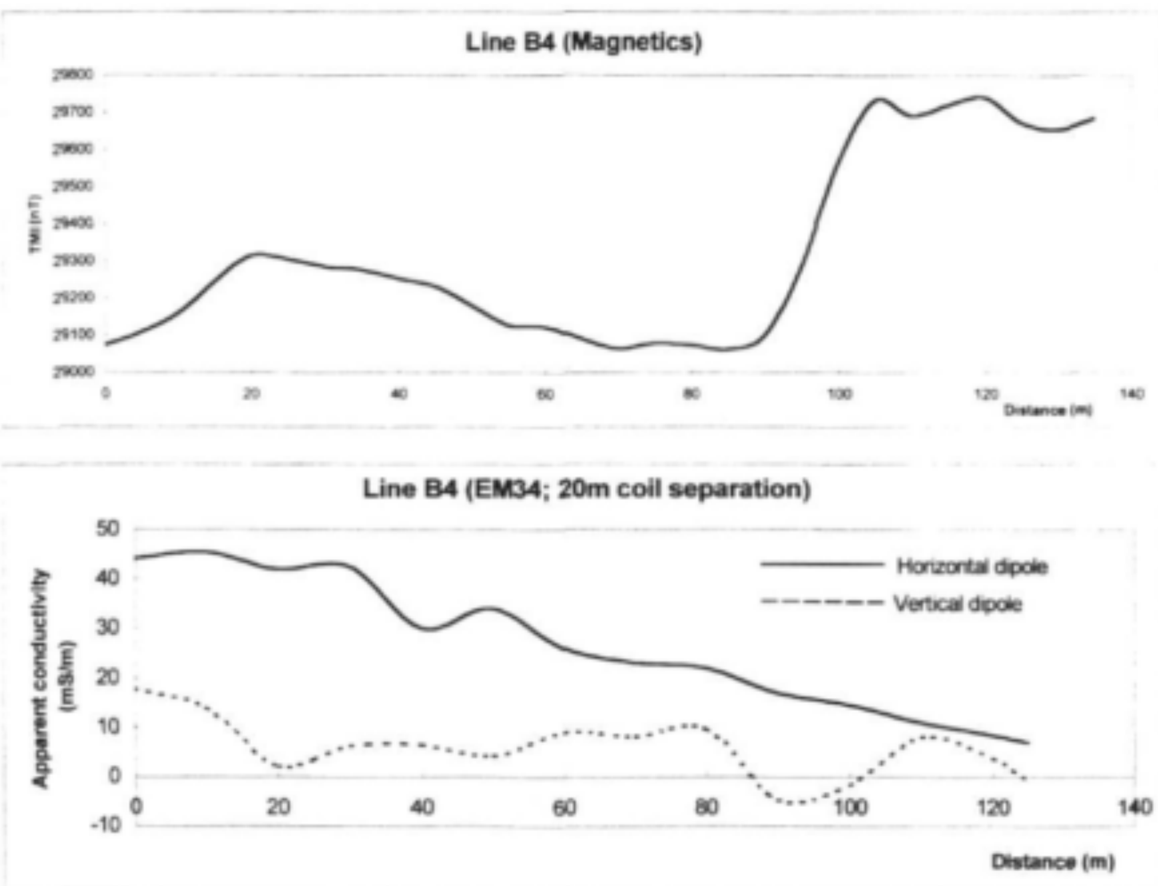

Figure 39d: Profiles for line B4

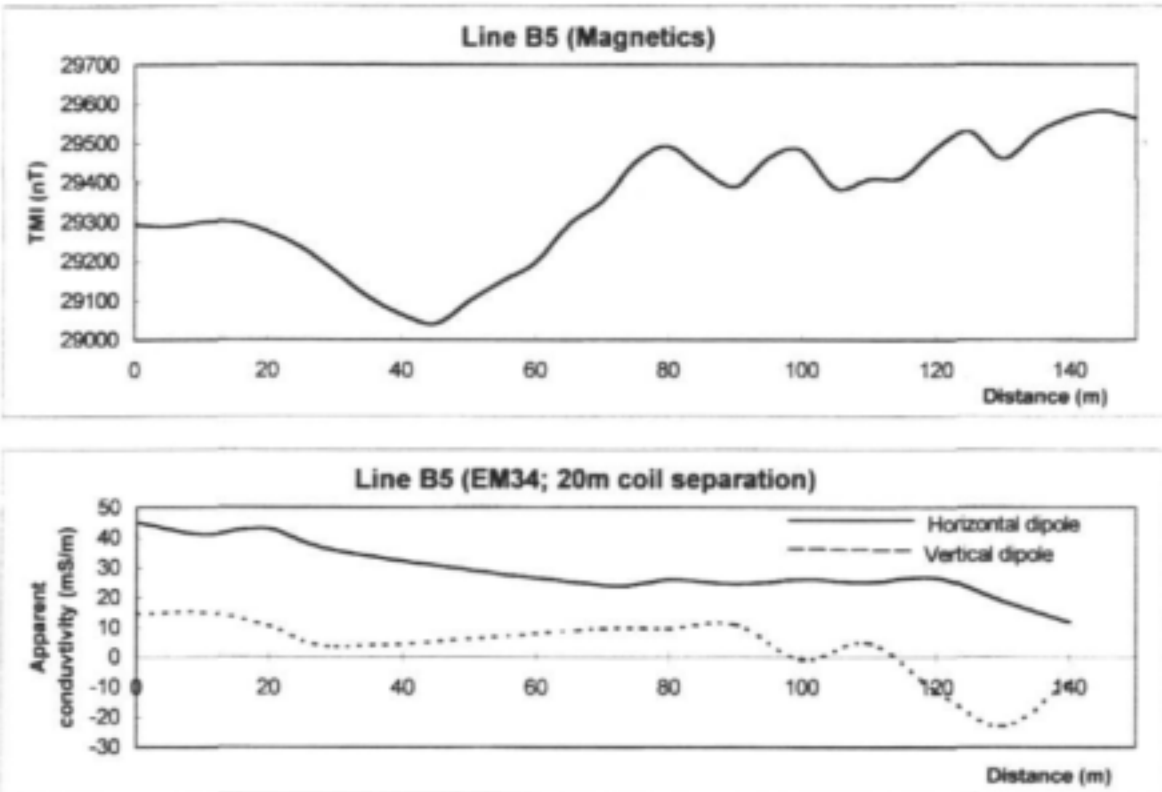

Figure 39e: Profiles for line B5

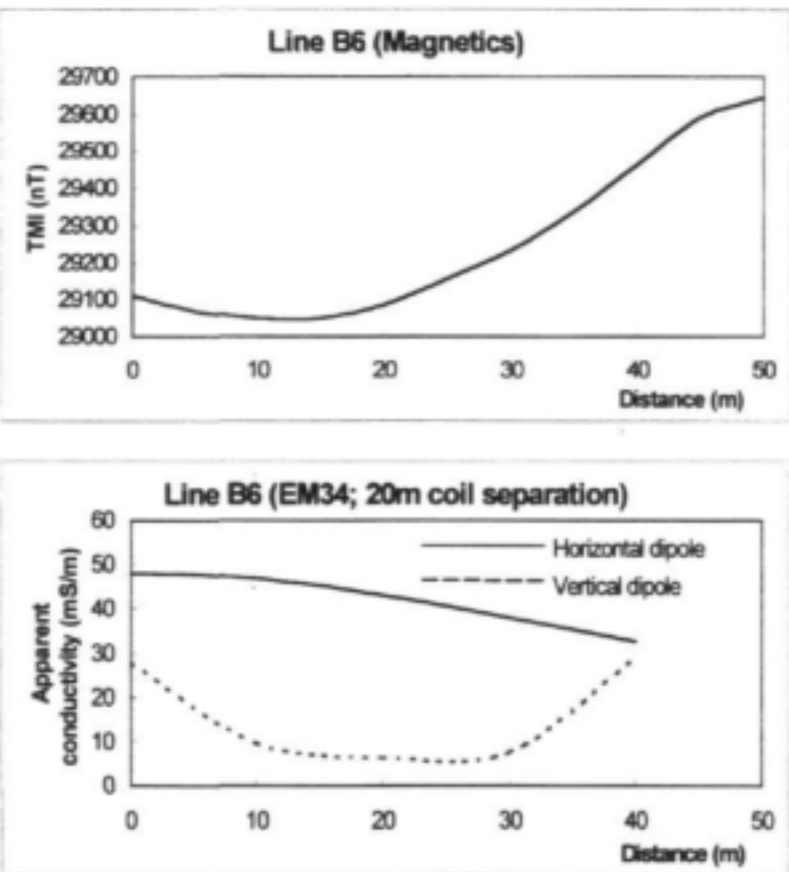

Figure 39f: Profiles for line B6

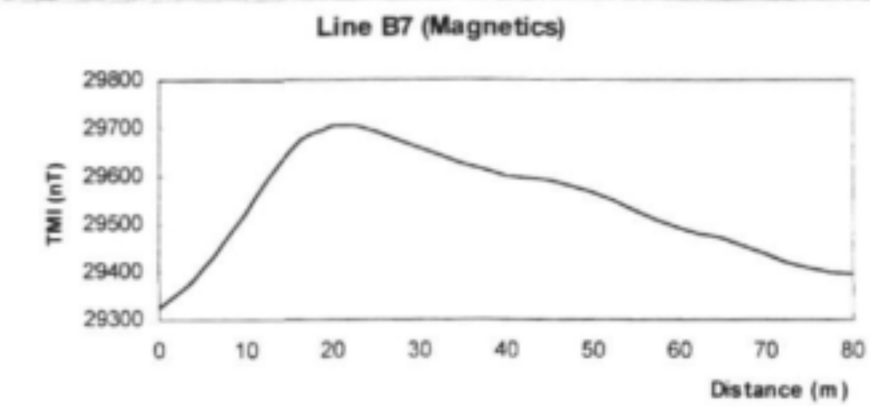

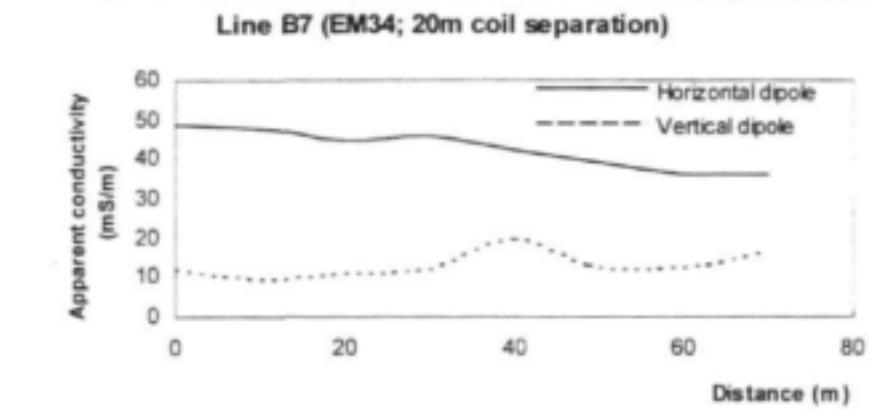

Figure 39g: Profiles for line B7

Site C:

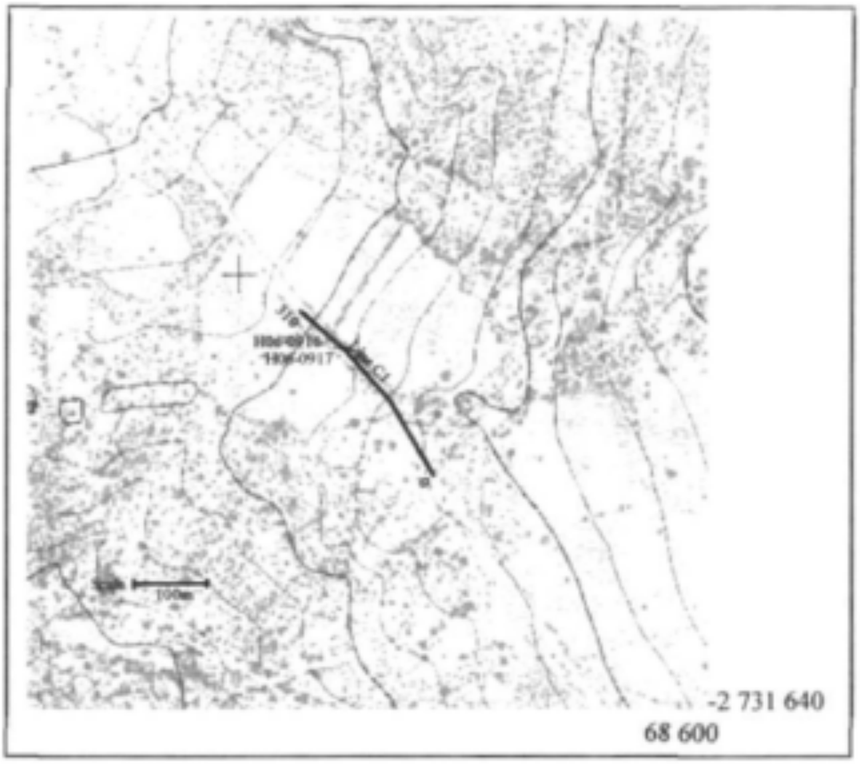

Figure 40a: Location map with field profiles and borehole position (Orthophoto series, 1983)

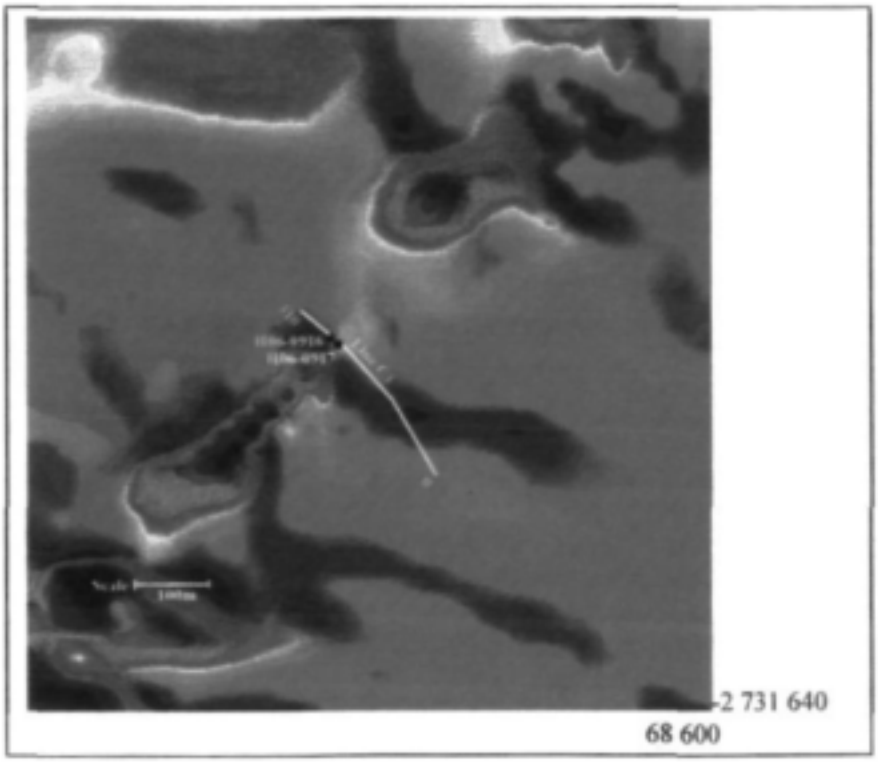

Figure 40b: Airborne magnetic data for the same area as shown above.

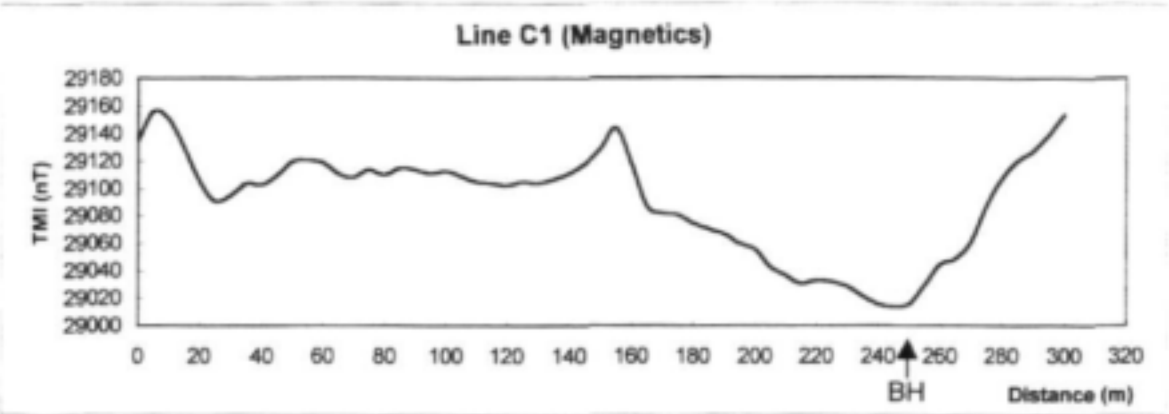

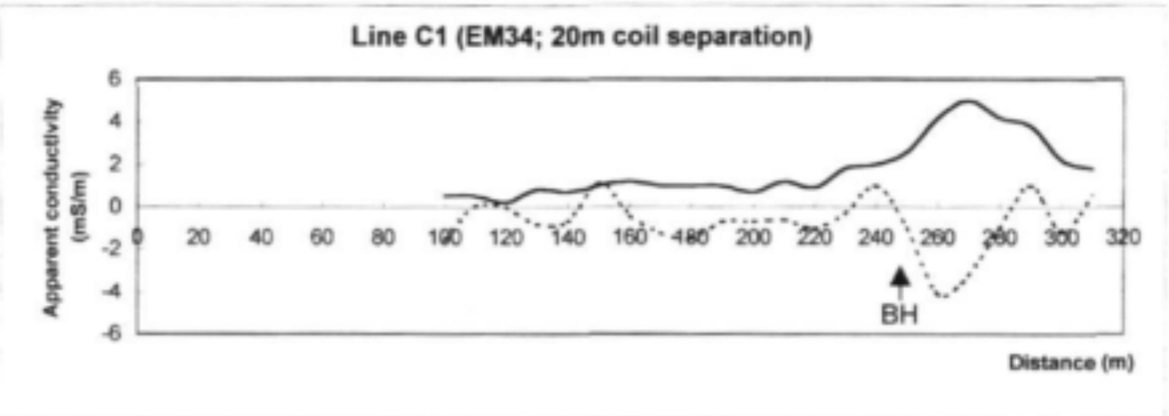

Figure 41: Profiles for line C1

Site D:

No fieldwork was done because the site was inaccessible.

Site E:

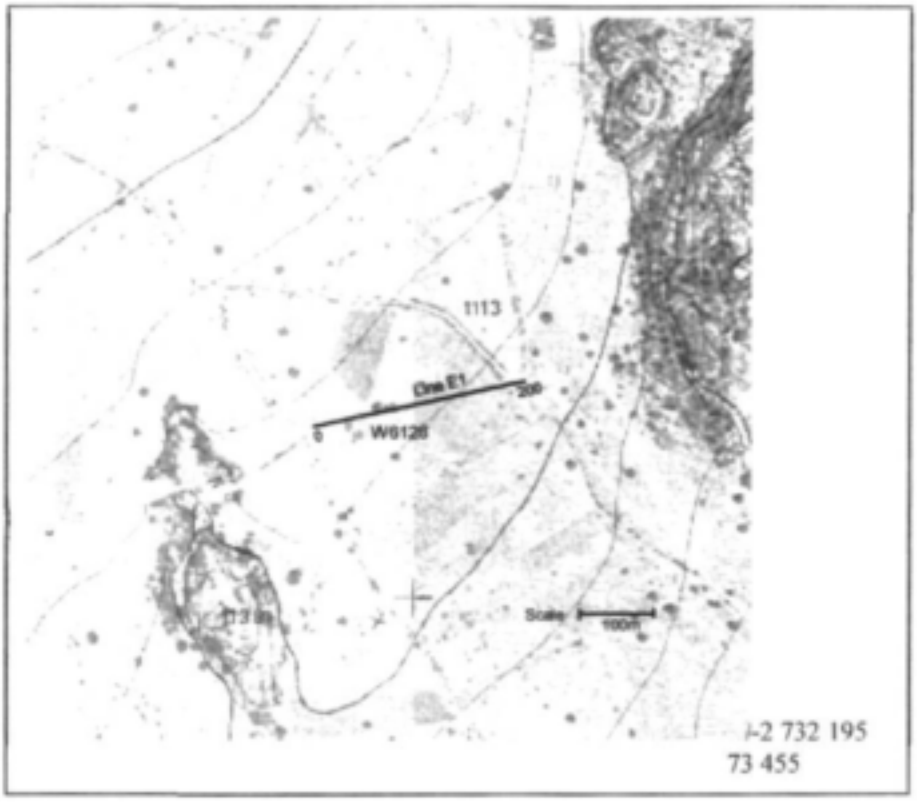

Figure 42a: Location map with field profiles and borehole position (Orthophoto series 1983).

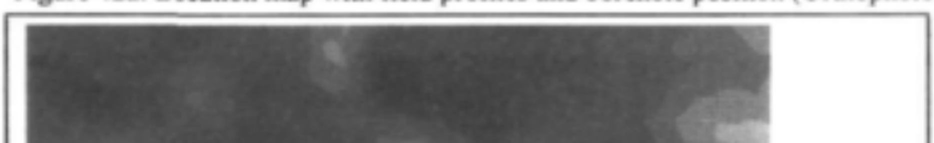

Figure 42b: Airborne magnetic data for the same area as shown above.

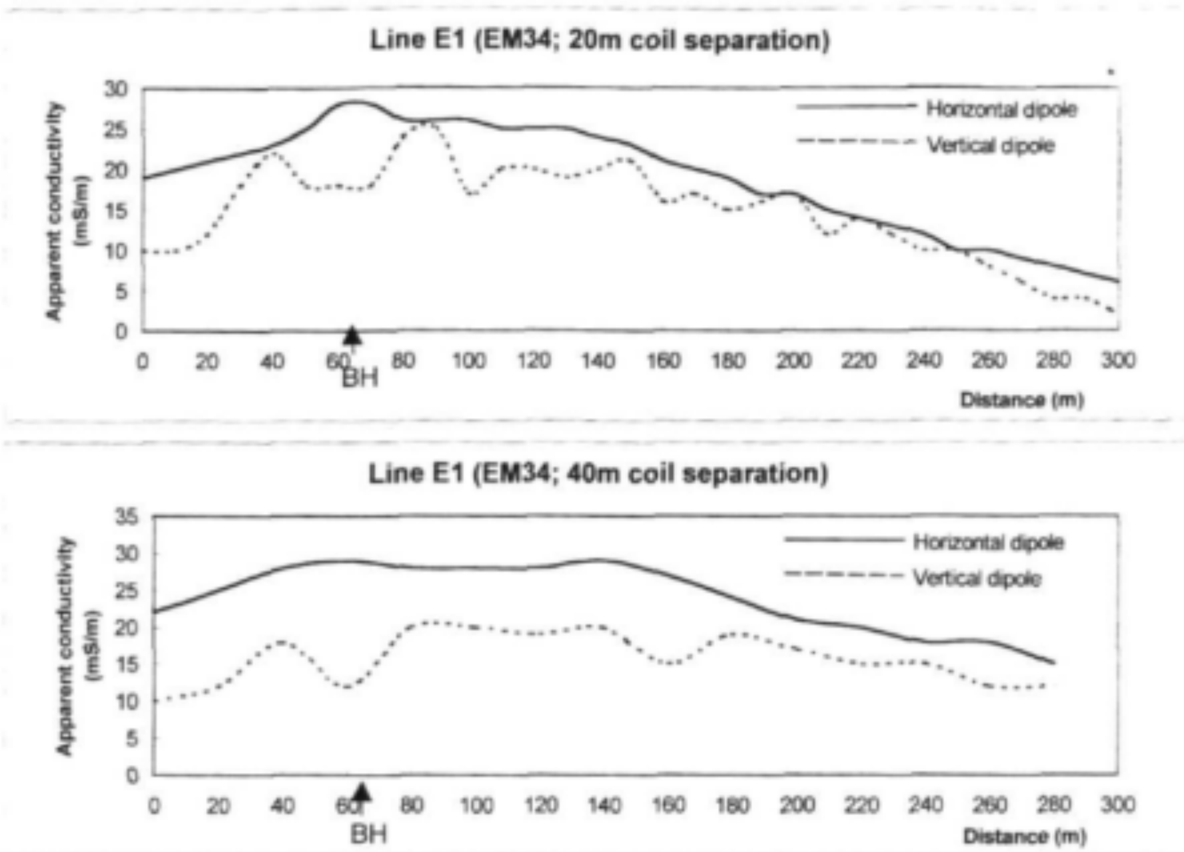

Figure 43: Profiles for line E1

Site F:

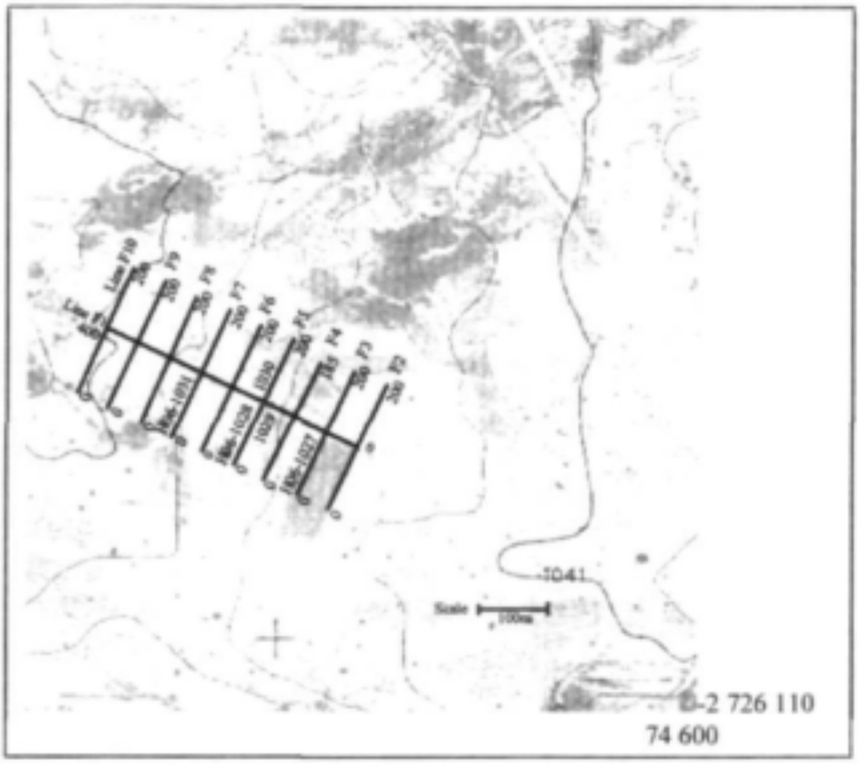

Figure 44a: Location map with field profiles and borehole position (Orthophoto series, 1983)

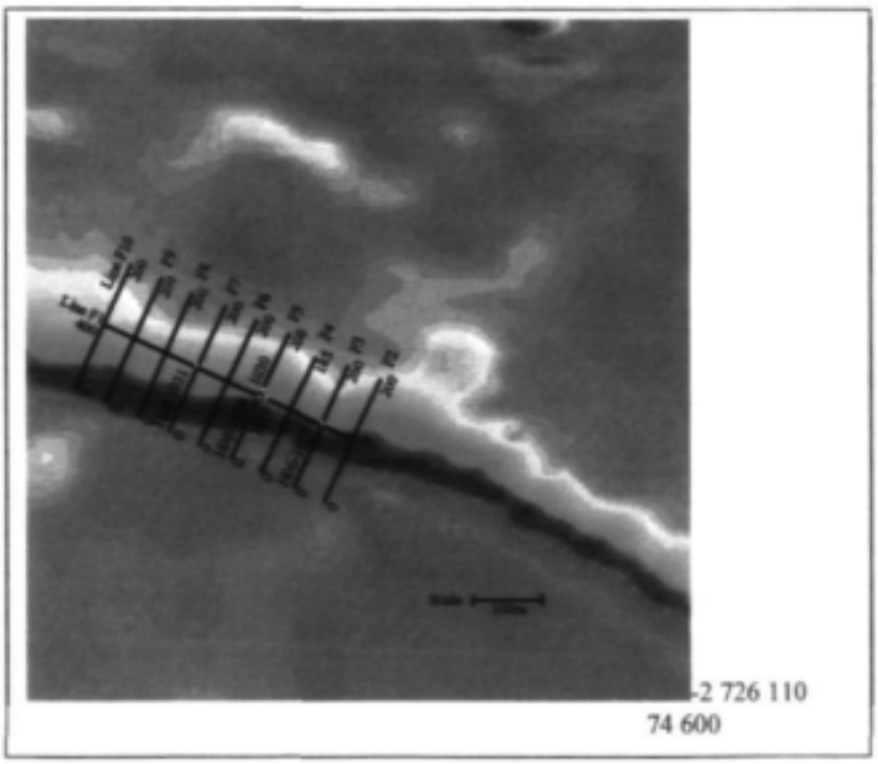

Figure 44b: Airborne magnetic data for the same area as shown above.

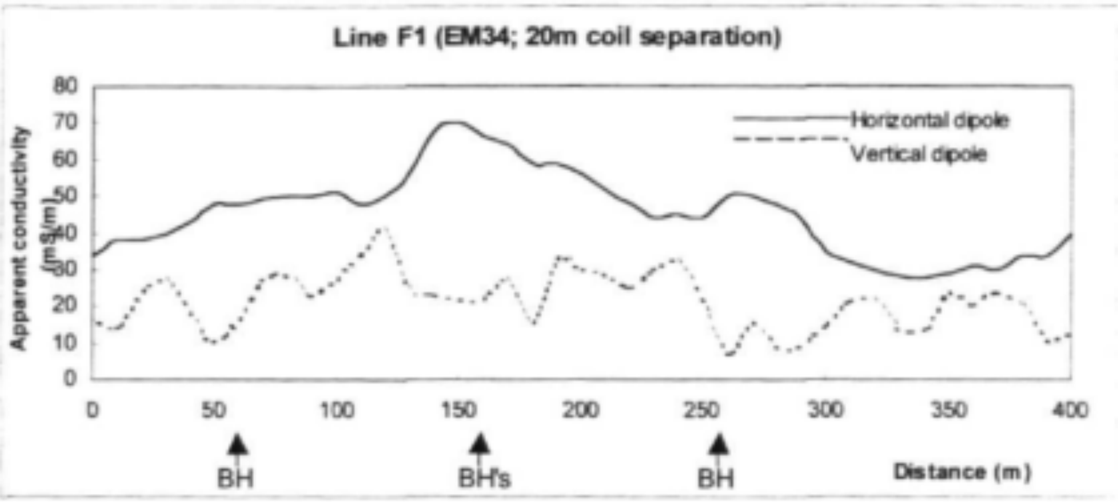

Figure 45a: Profiles for line F1

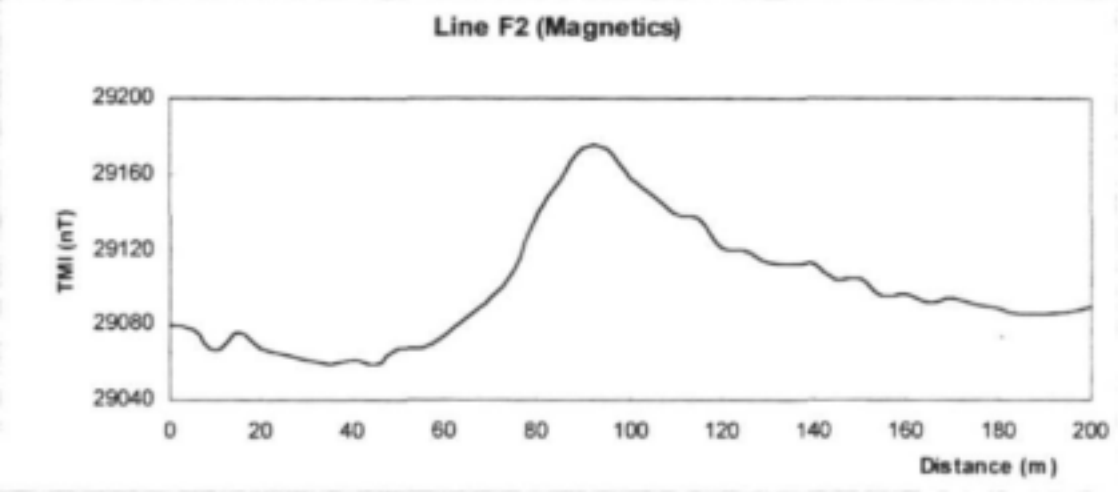

Figure 45b: Profiles for line F2

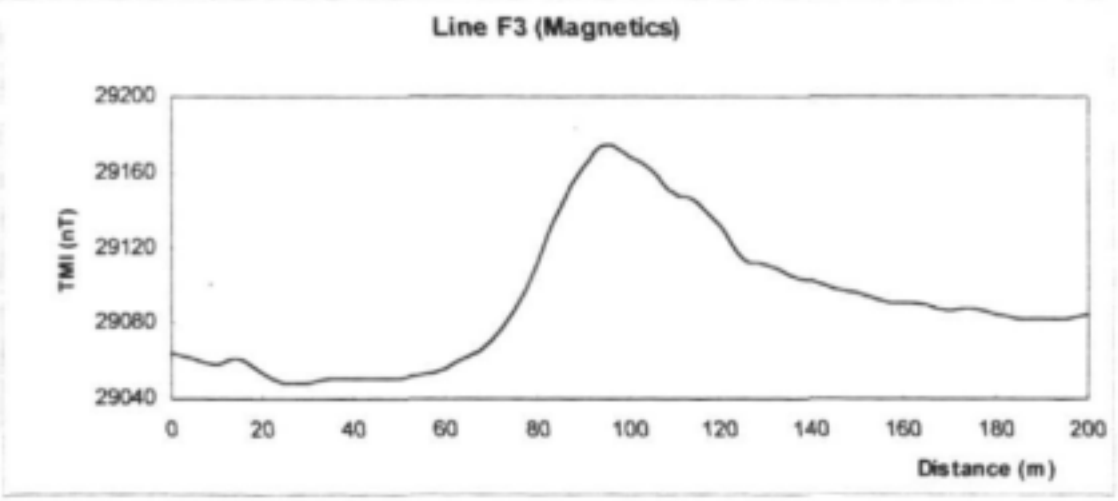

Figure 45c: Profiles for line F3

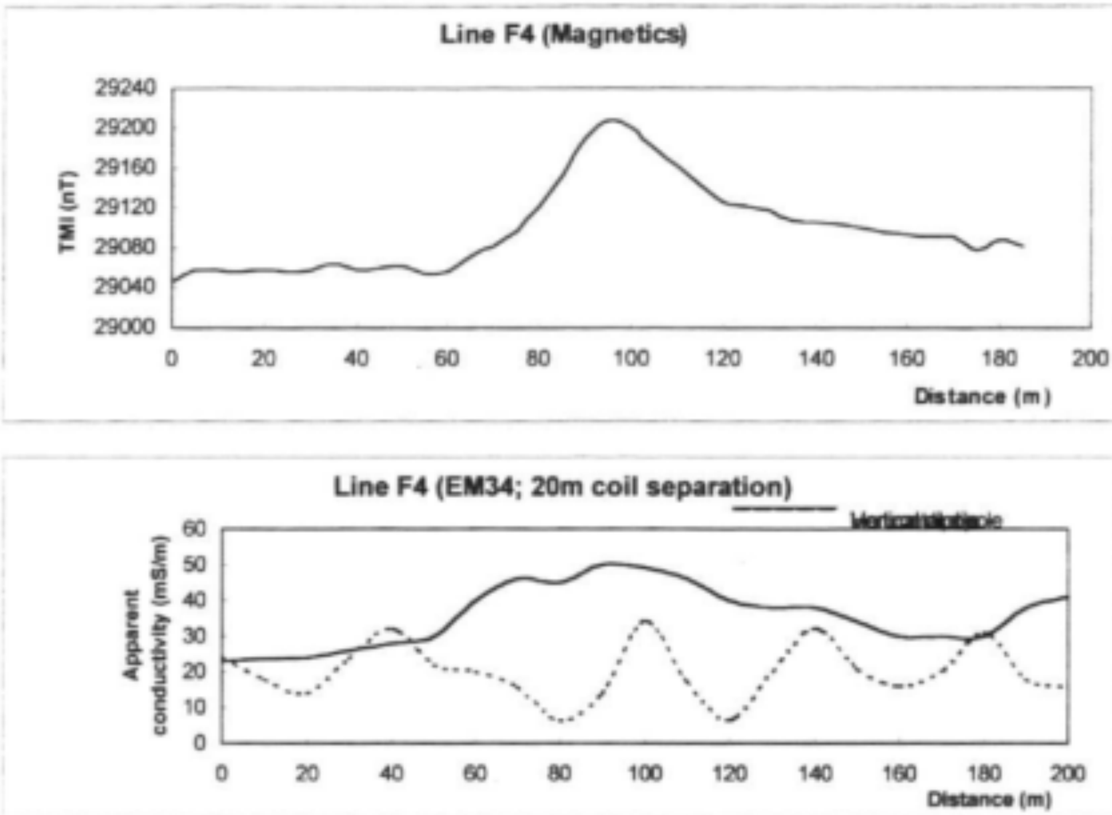

Figure 45d: Profiles for line F4

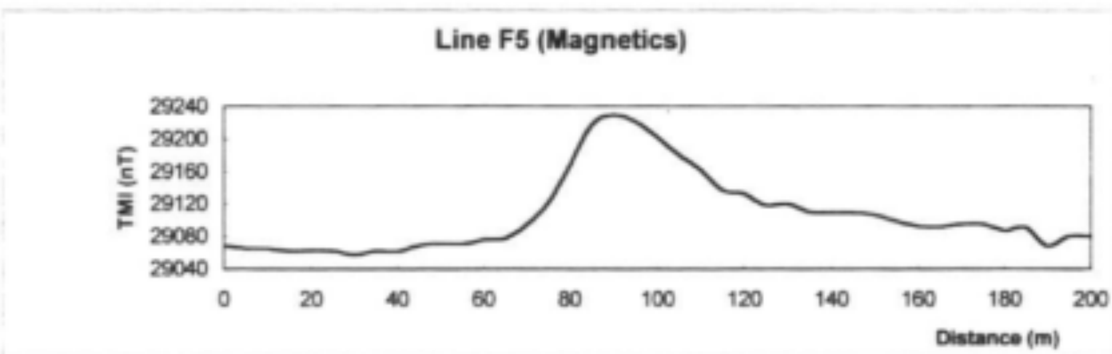

Figure 45e: Profiles for line F5

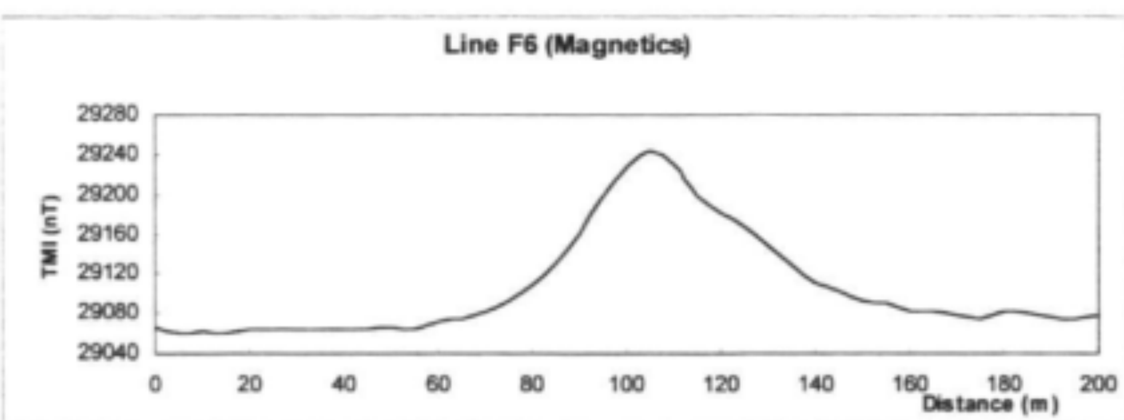

Figure 45f: Profiles for line F6

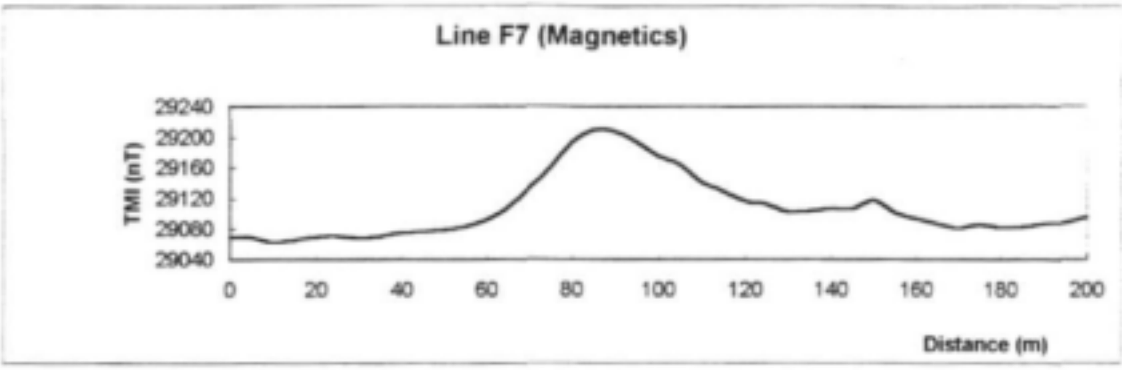

Figure 45g: profiles for line F7

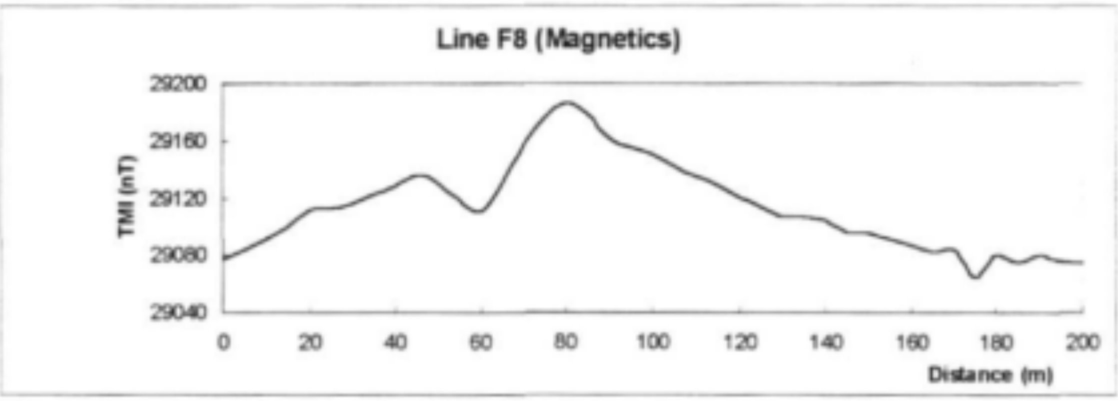

Figure 45h: profiles for line F8

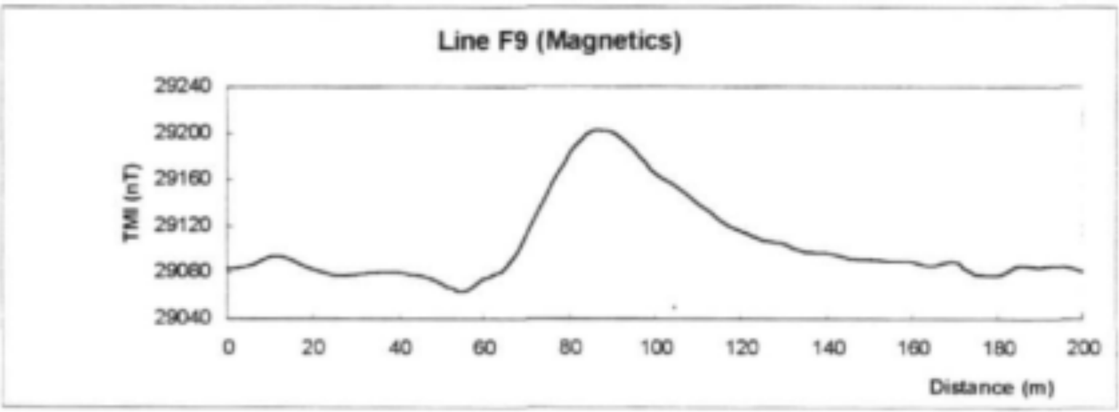

Figure 45i: profiles for line F9

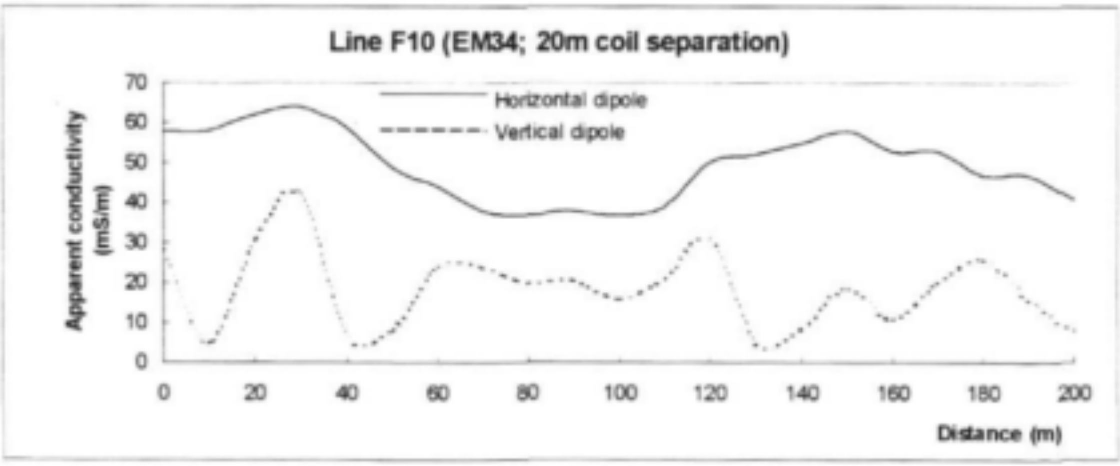

Figure 45j: profiles for line F10

Site G,H&K:

Figure 46a: Location map with field profiles and borehole positions (Orthphoto series, 1983).

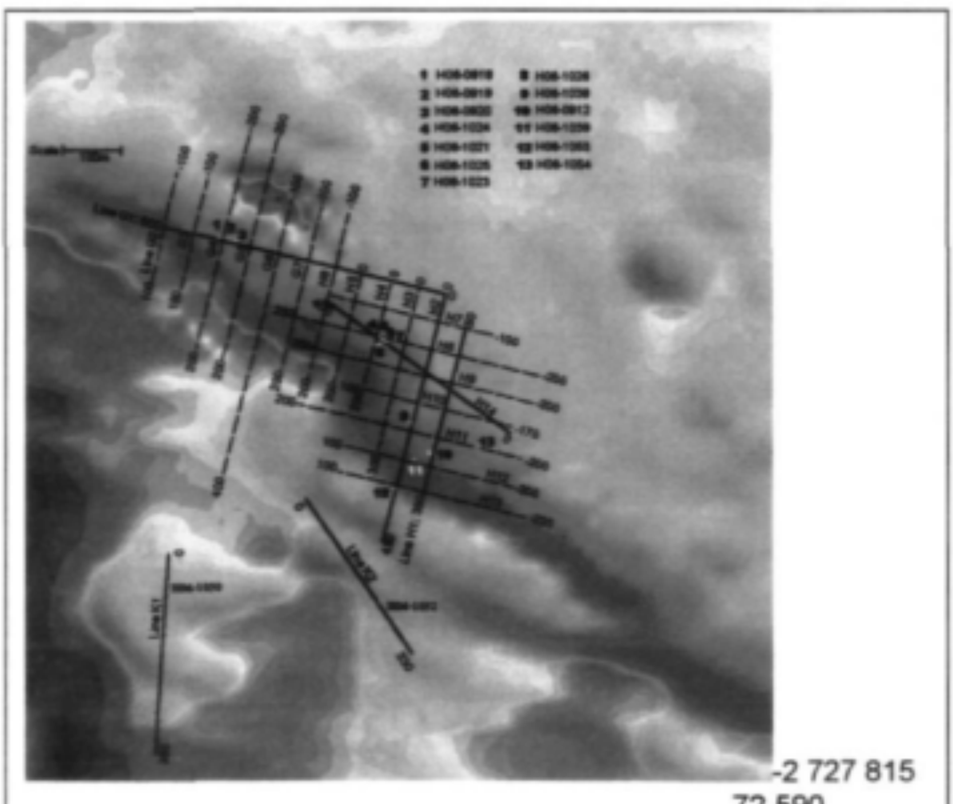

Figure 46b: Airborne magnetic data for the same area as shown above.

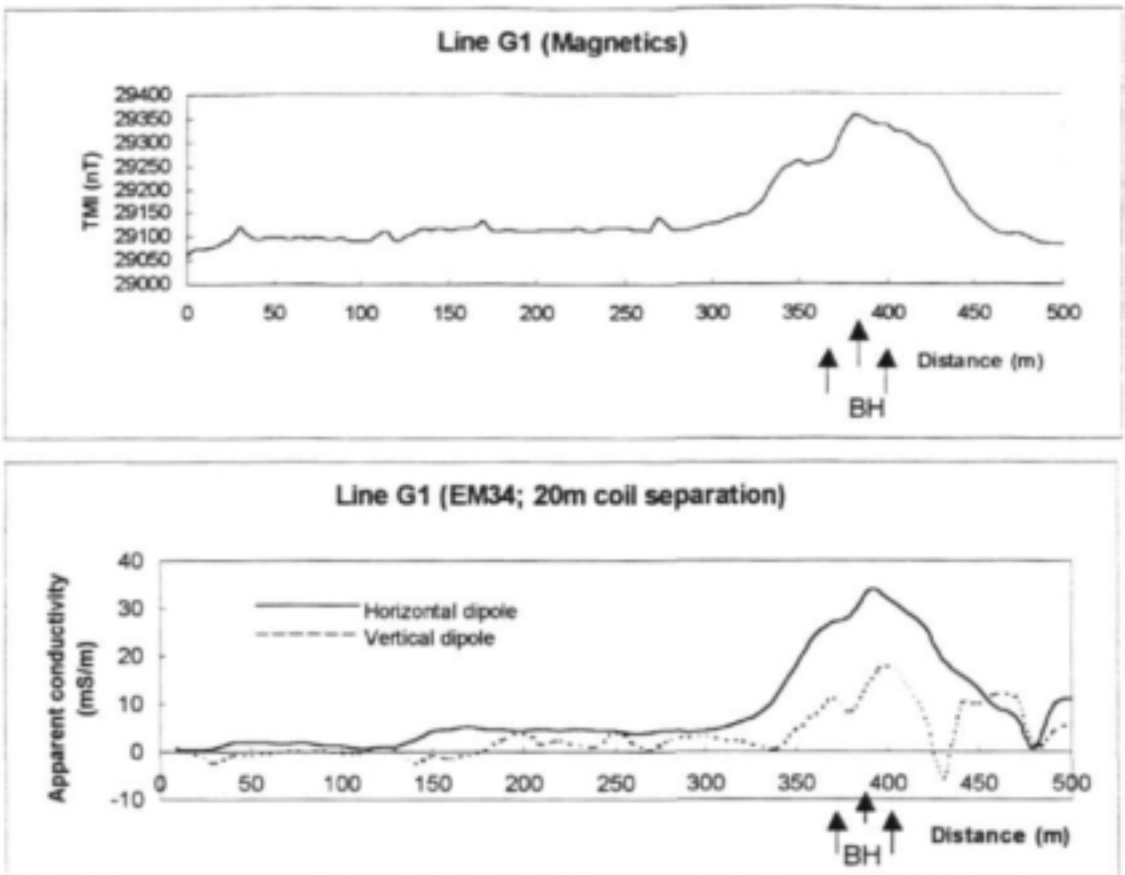

Figure 47a: Profiles for line G1

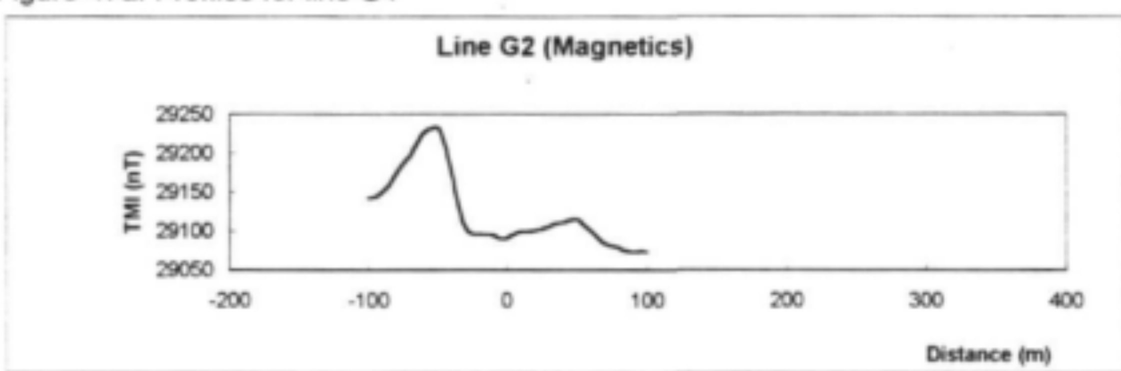

Figure 47b: Profiles for line G2

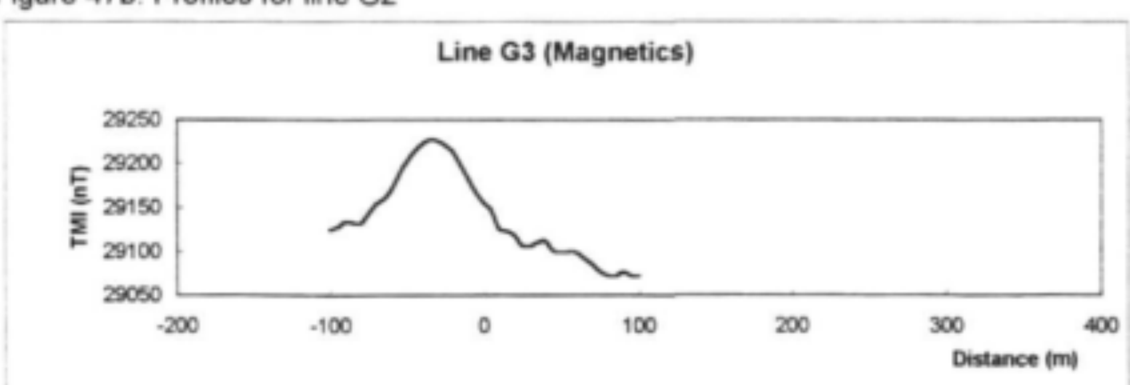

Figure 47c: Profiles for line G3

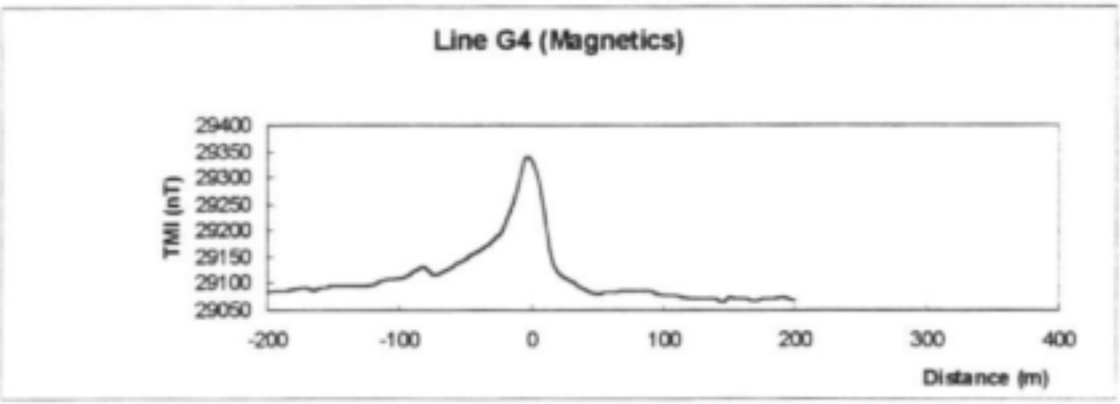

Figure 47d: Profiles for line G4

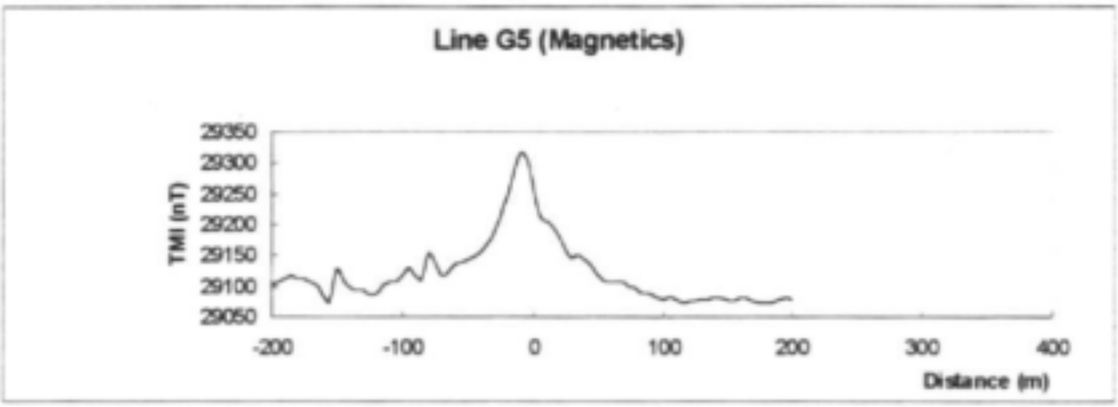

Figure 47e: Profiles for line G5

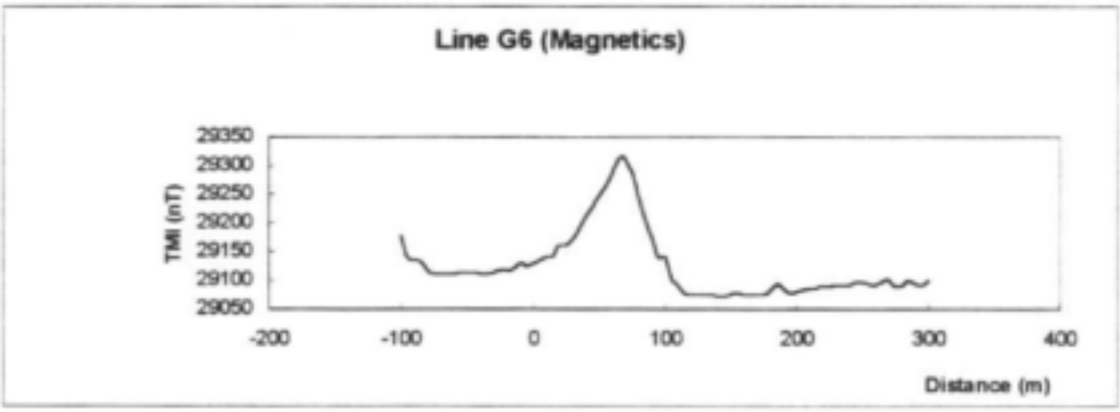

Figure 47f: Profiles for line G6

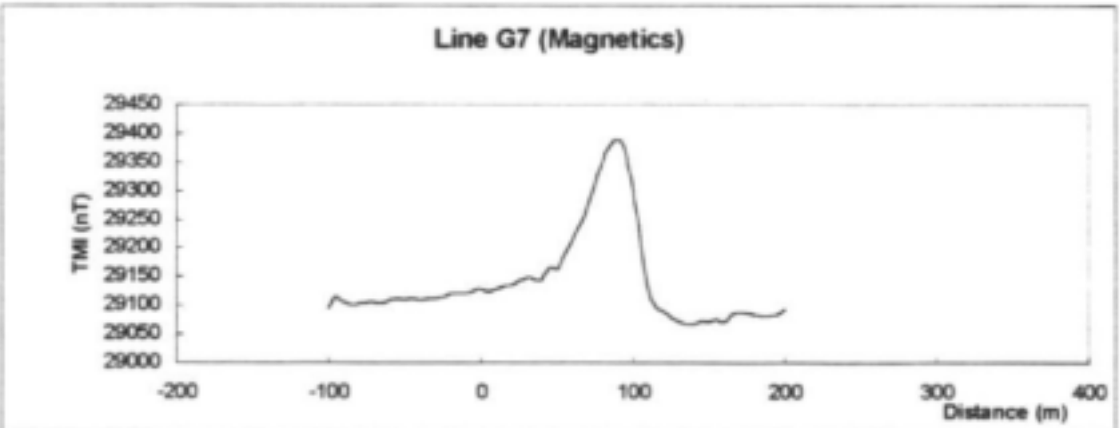

Figure 47g: Profiles for line G7

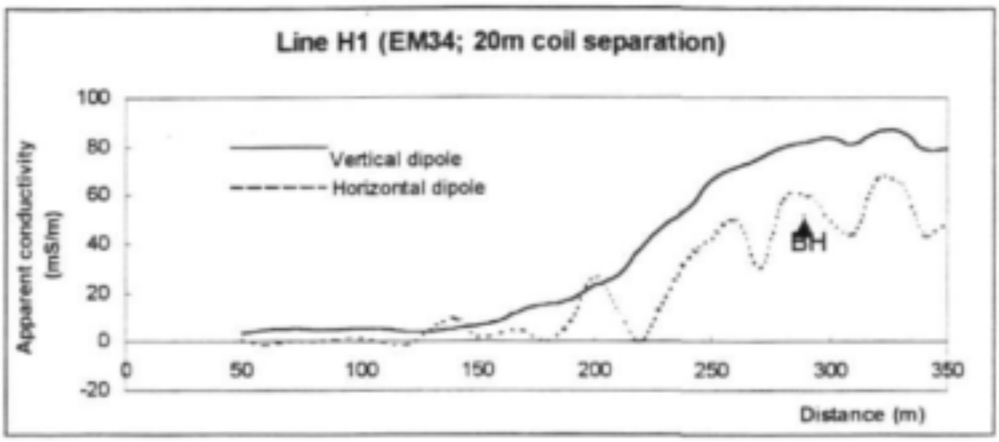

Figure 48a: Profiles for line H1

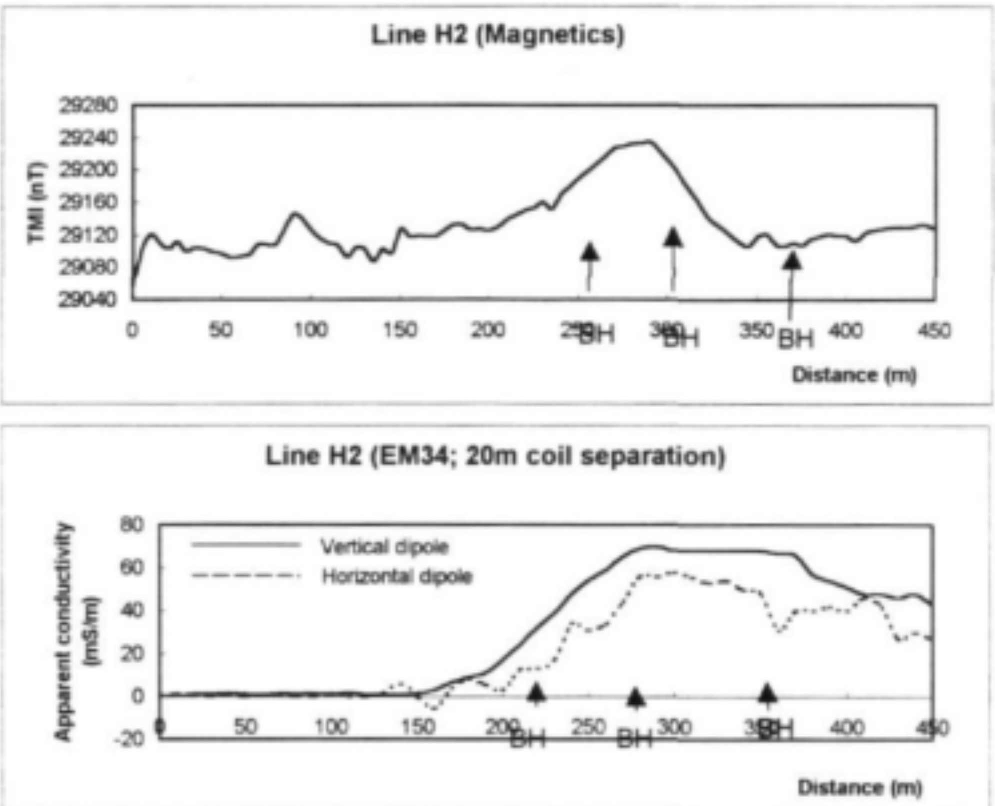

Figure 48b: Profiles for line H2

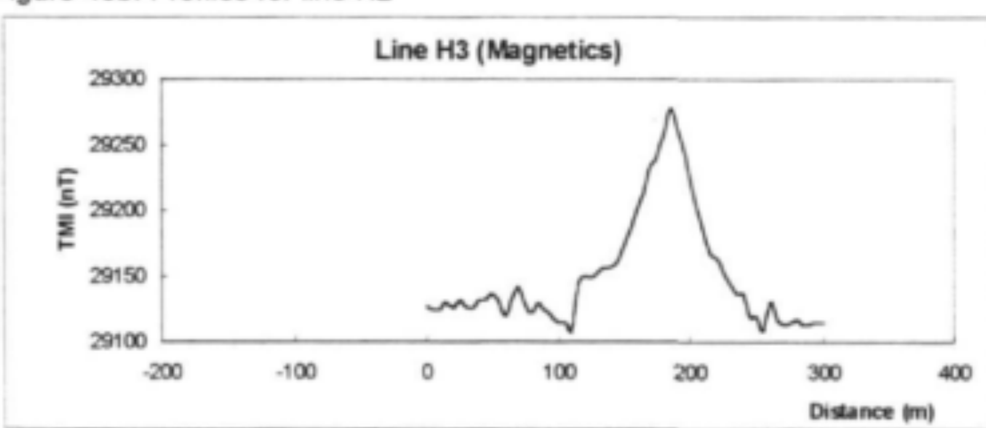

Figure 48c: Profiles for line H3

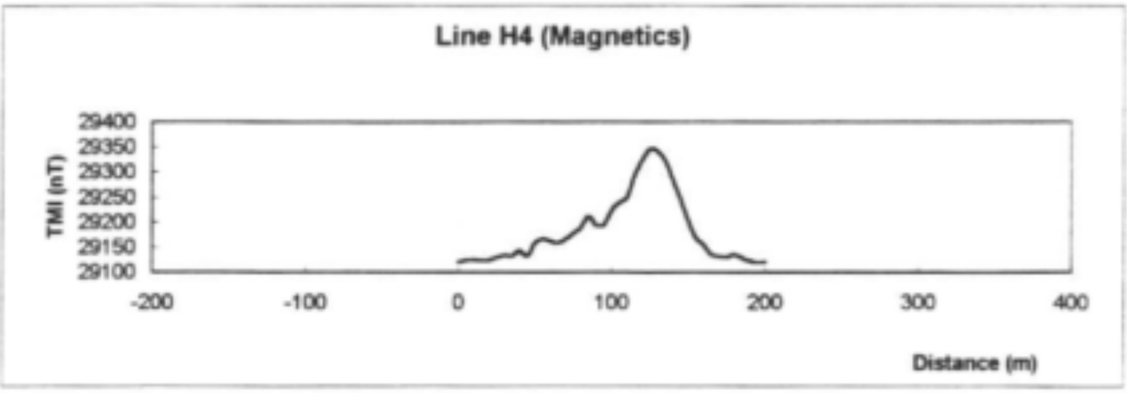

Figure 48d: Profiles for line H4

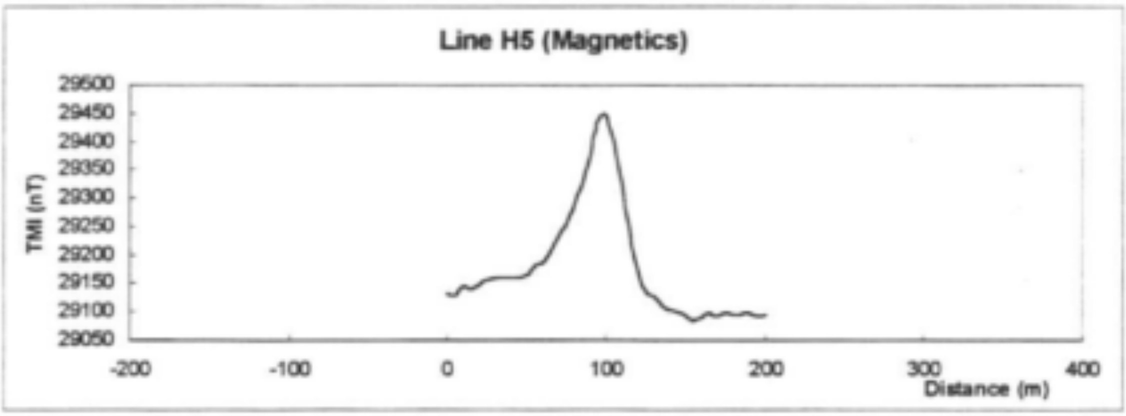

Figure 48e: Profiles for line H5

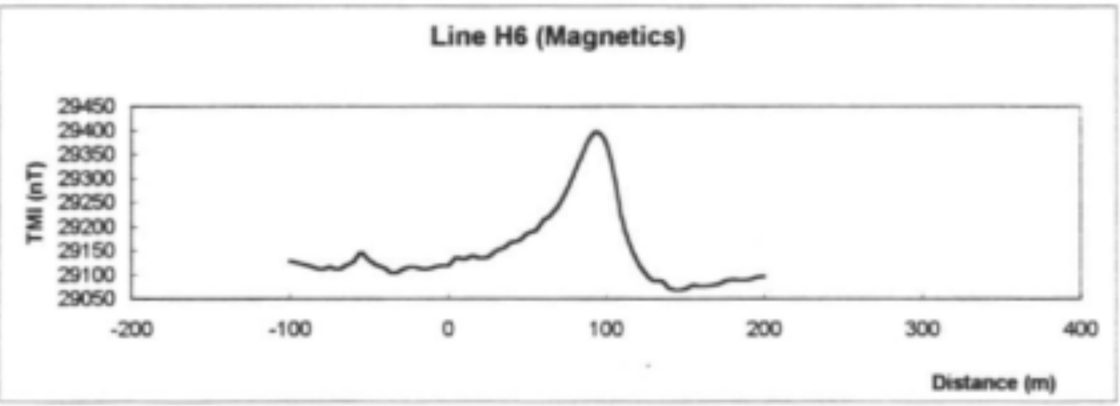

Figure 48f: Profiles for line H6

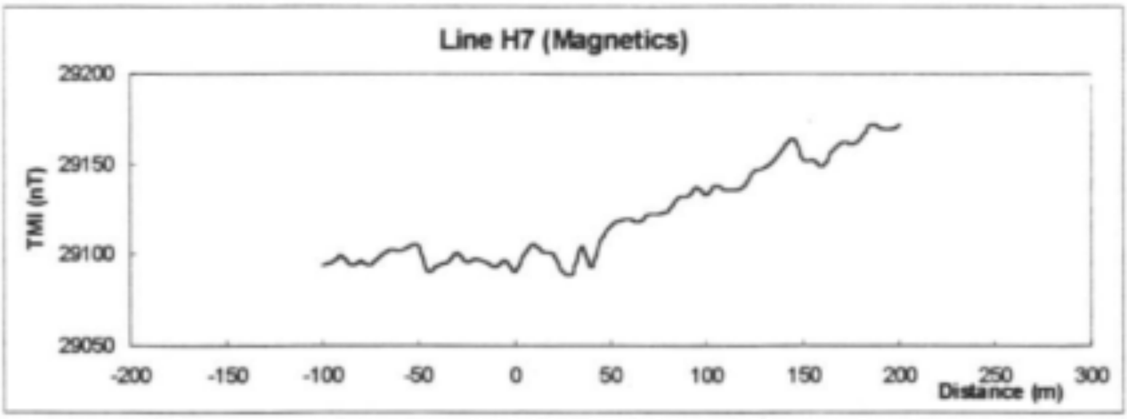

Figure 48g: Profiles for line H7

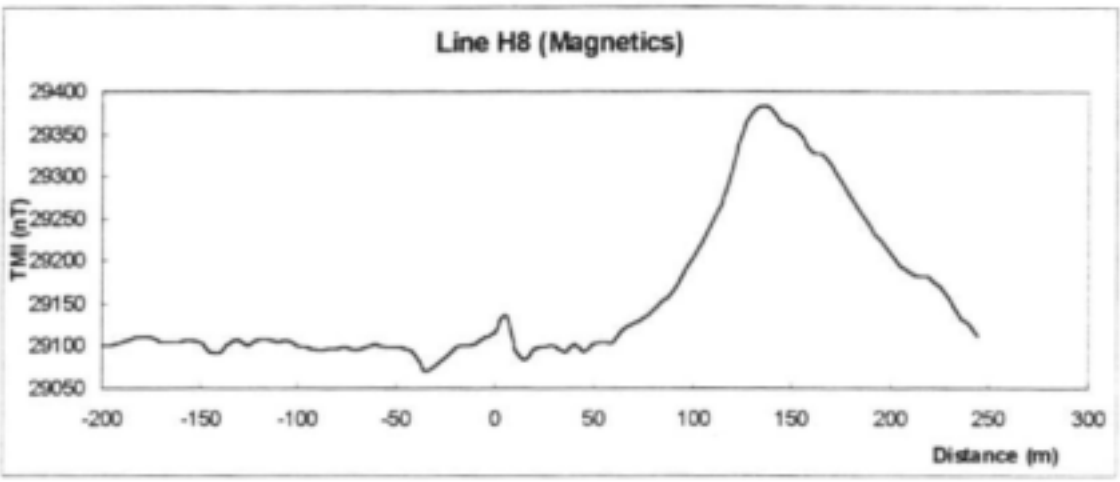

Figure 48h: Profiles for line H8

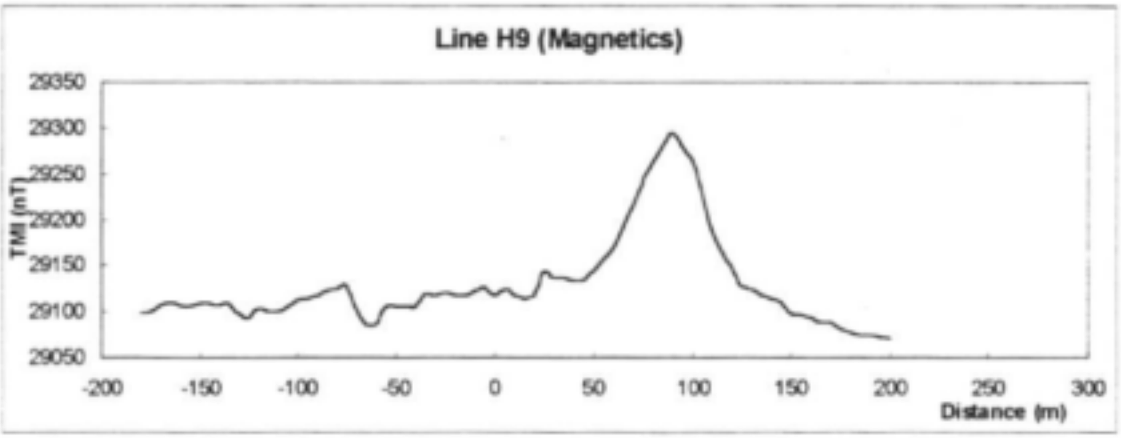

Figure 48i: Profiles for line H9

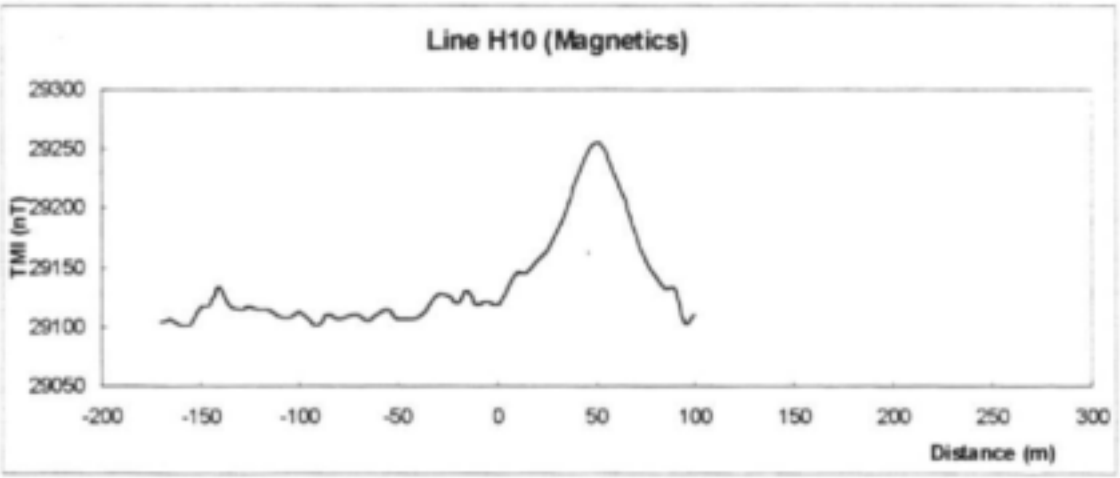

Figure 48j: Profiles for line H10

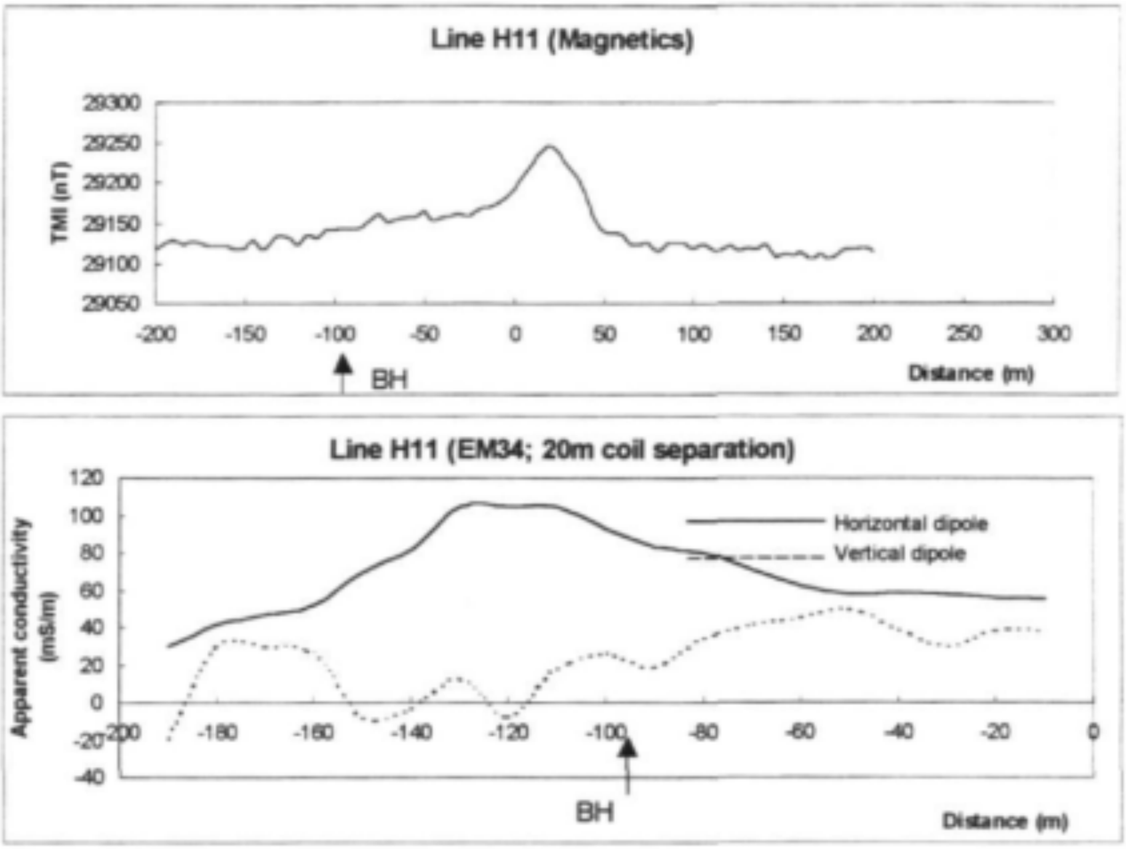

Figure 48k: Profiles for line H11

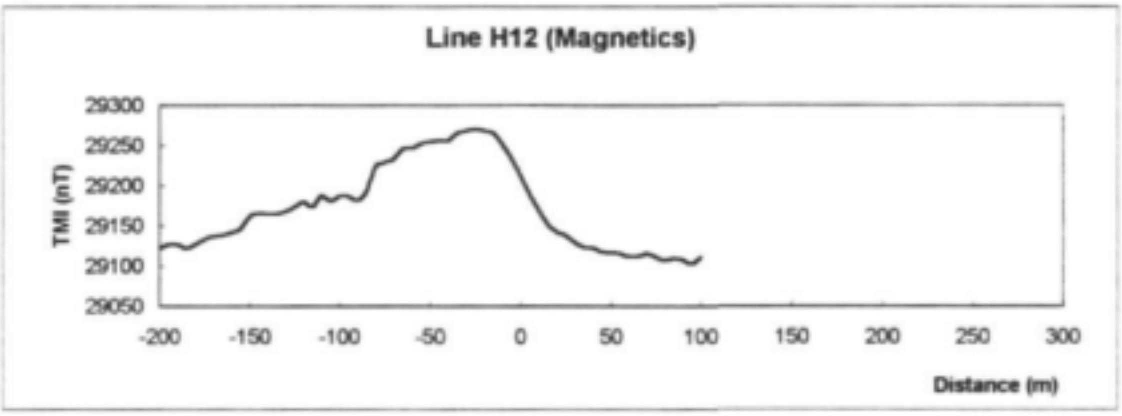

Figure 48l: Profiles for line H12

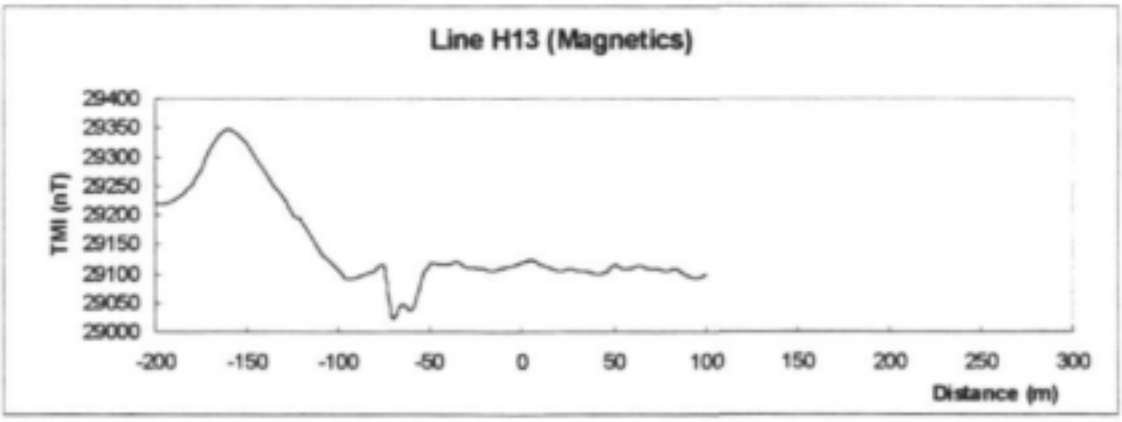

Figure 48m: Profiles for line H13

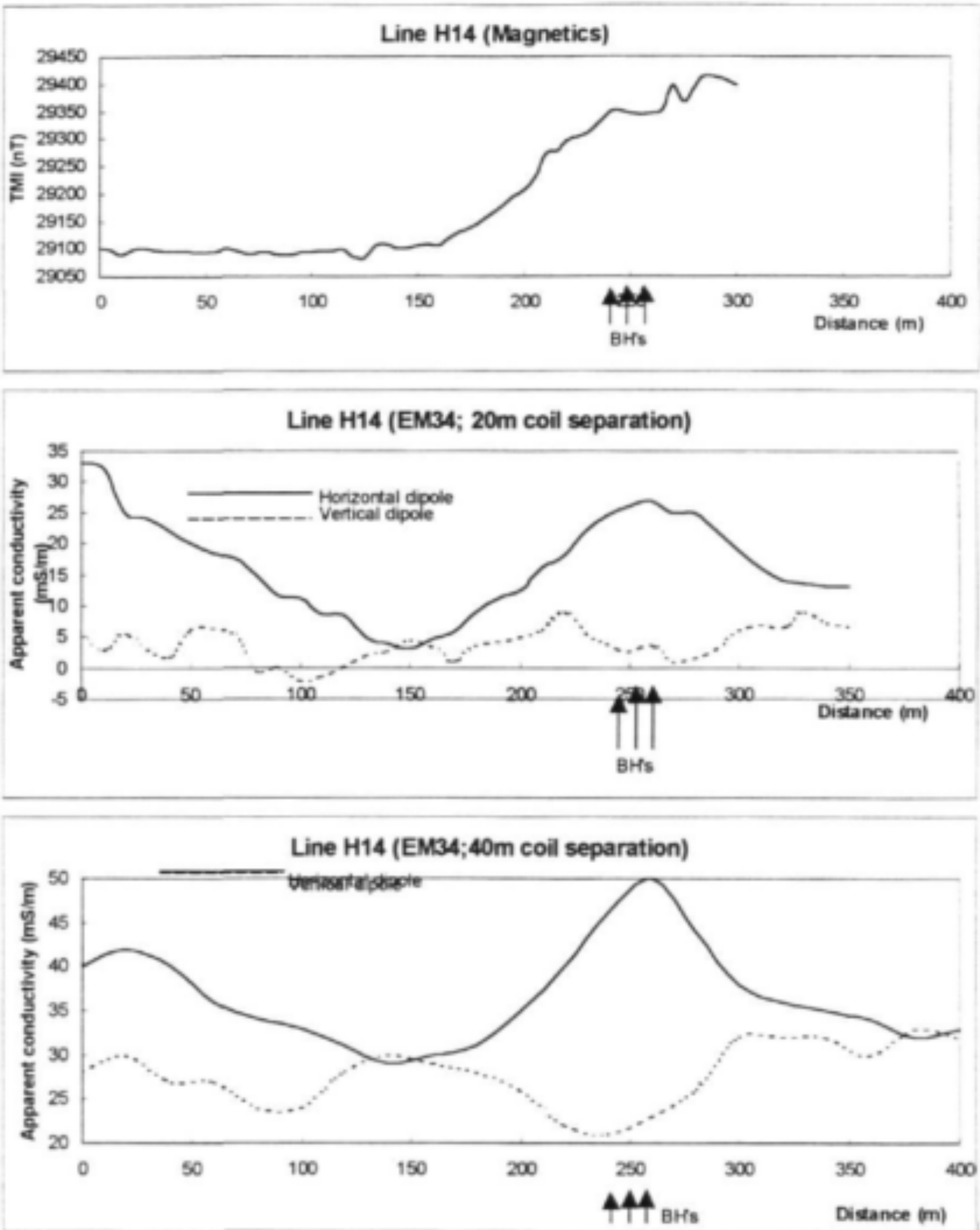

Figure 48n: Profiles for line H14

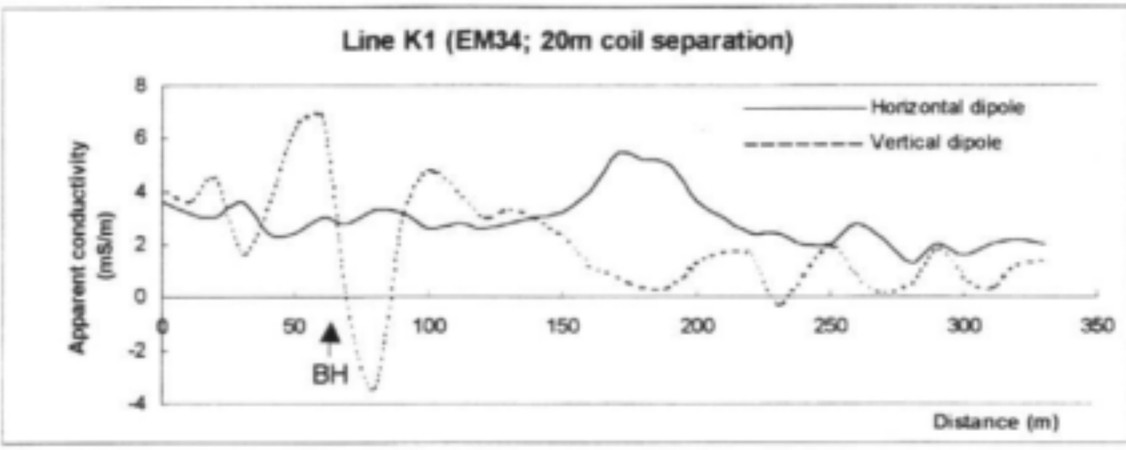

Figure 49a: Profiles for line K1

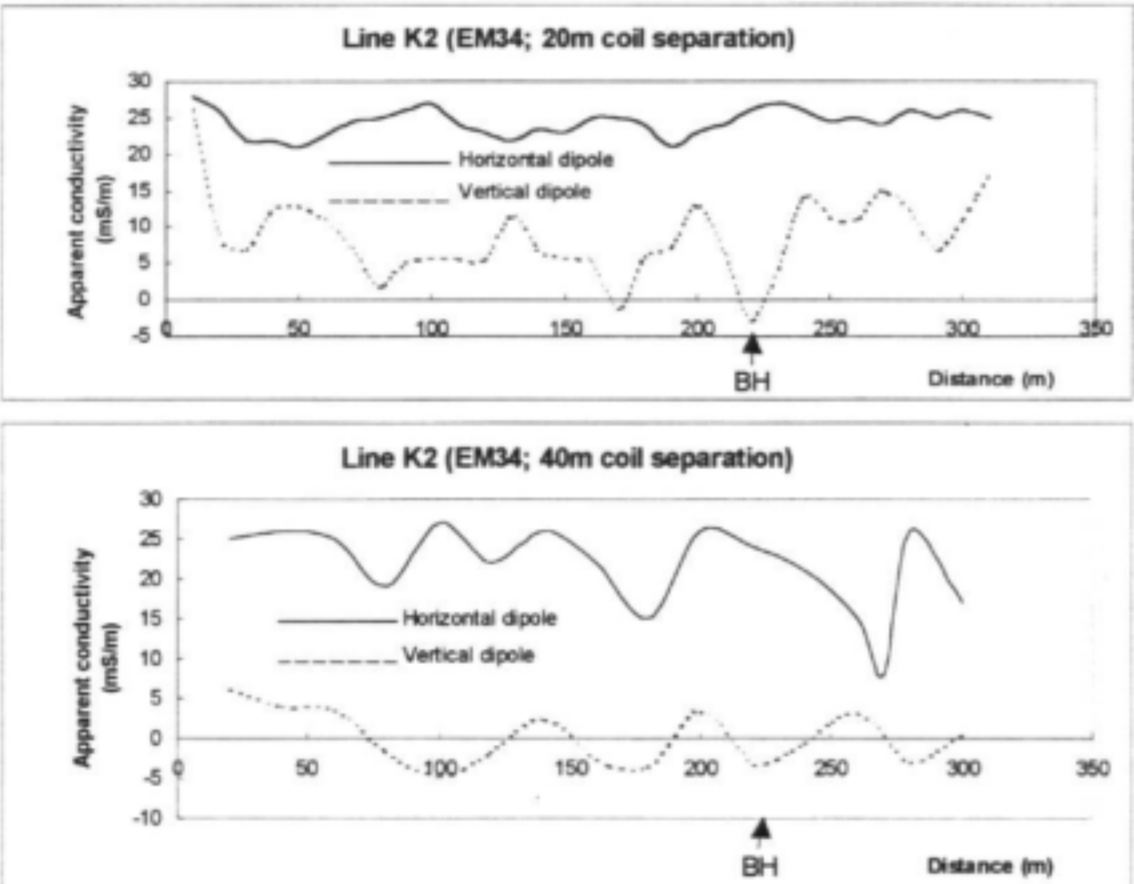

Figure 49b: Profiles for line K2

Site I

Figure 50a: Location map with field profiles and borehole positions (Orthophoto series, 1983).

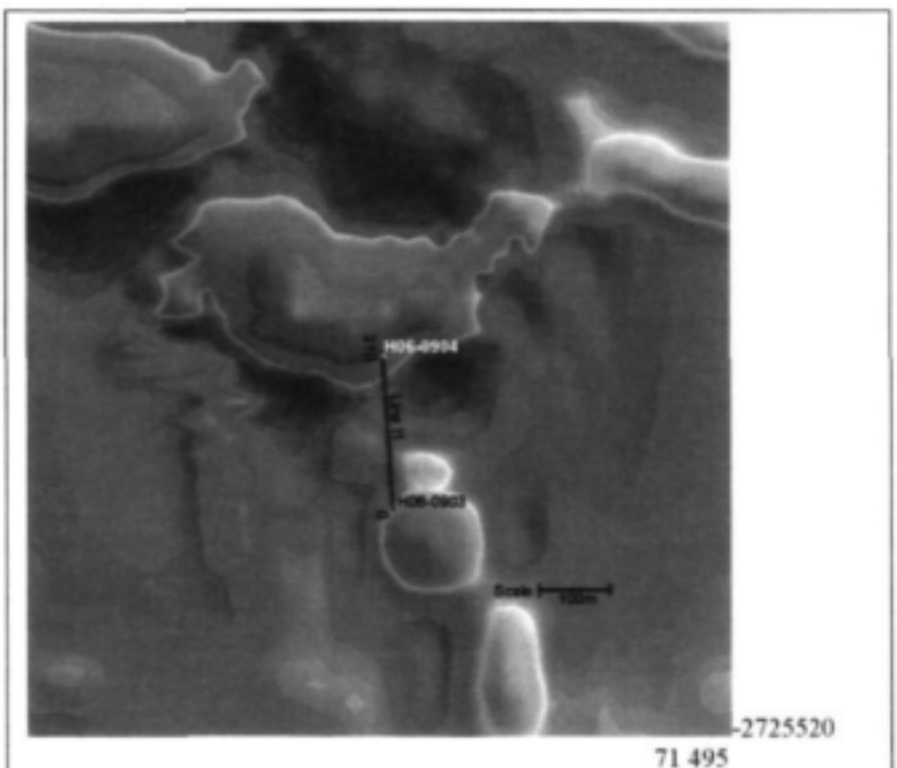

Figure 50b: Airborne magnetic data for the same area as shown above.

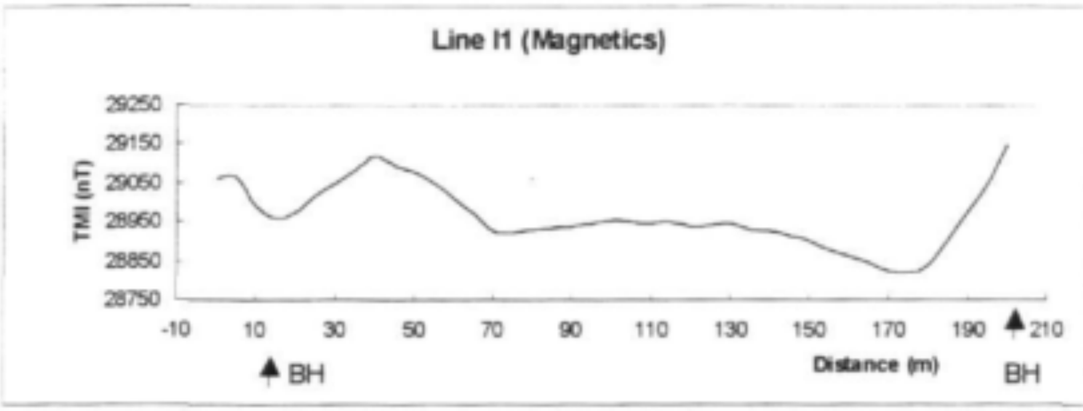

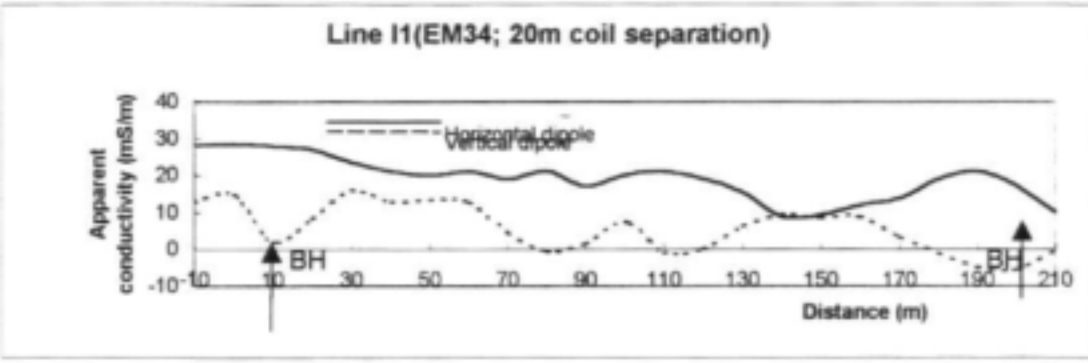

Figure 51: Profiles for line I1

Site J:

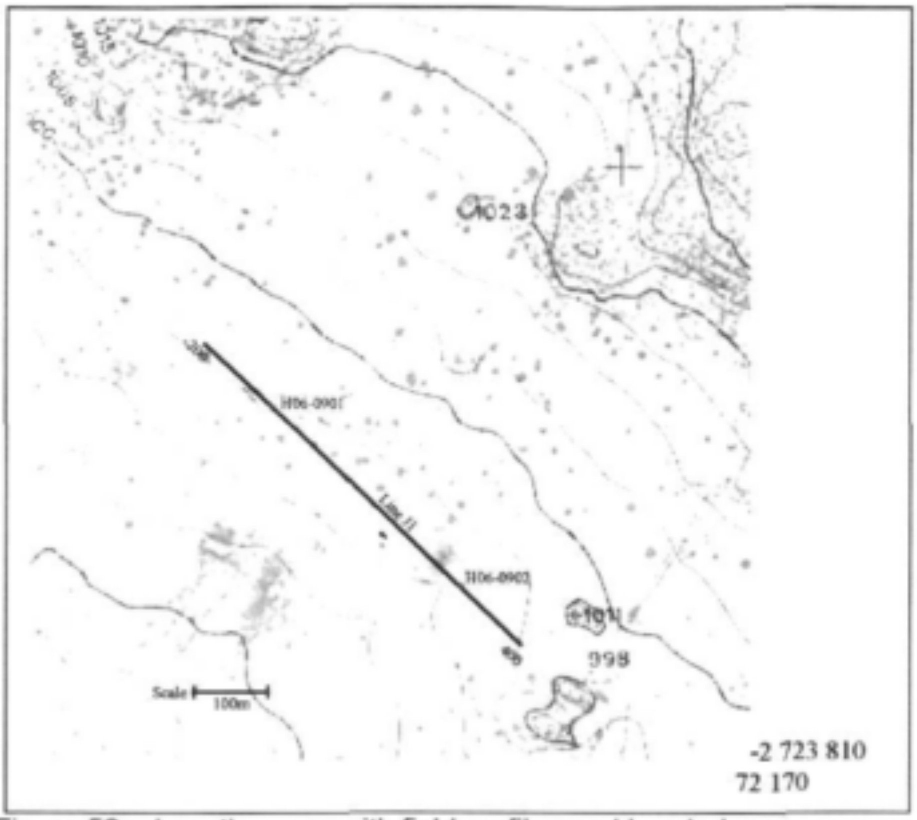

Figure 52a: Location map with field profiles and borehole positions (Orthophoto series, 1983).

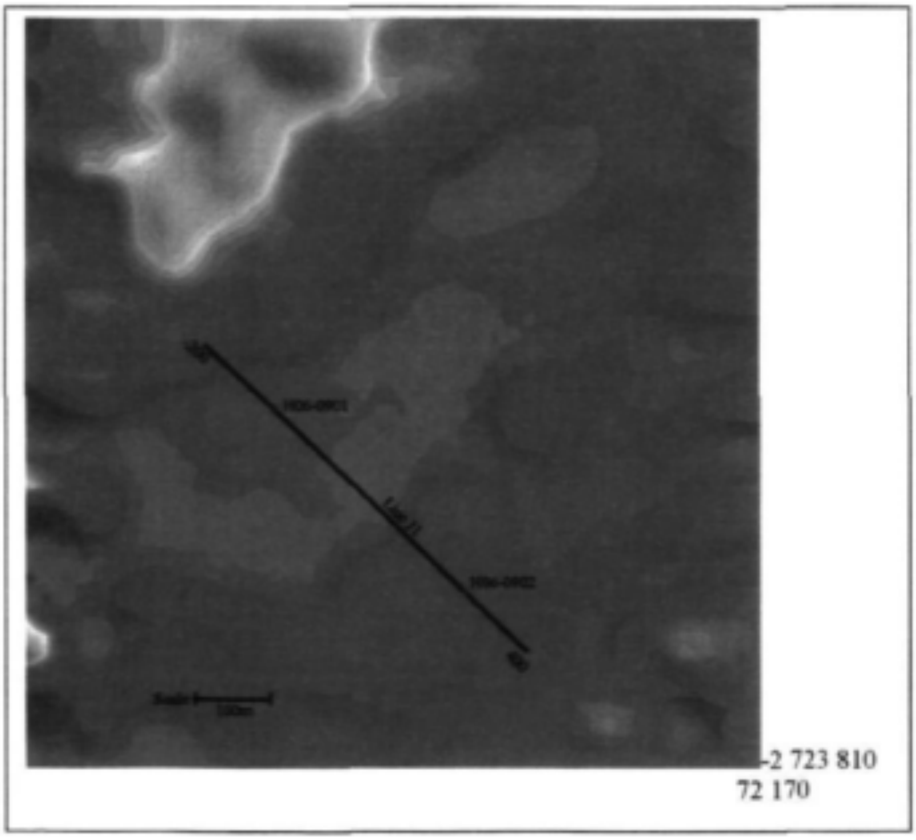

Figure 52b: Airborne magnetic data for the same area as shown bove.

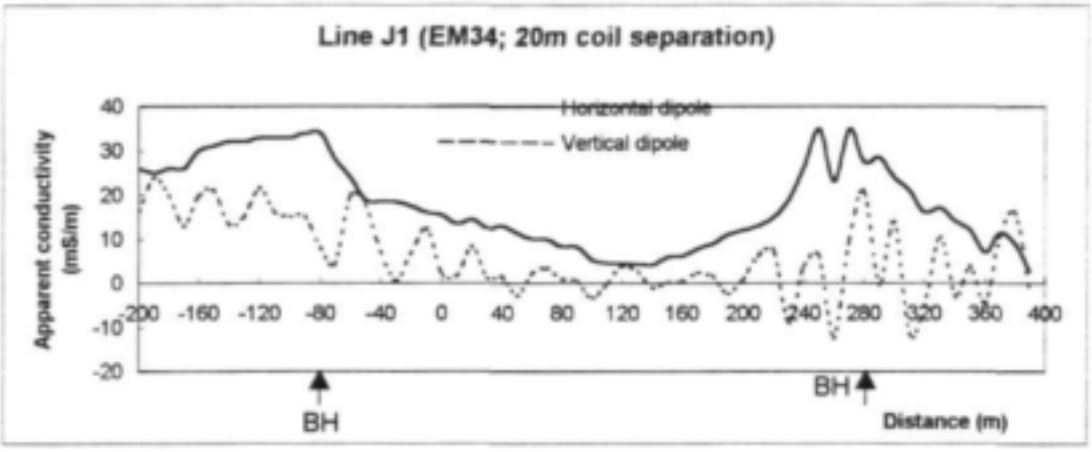

Figure 53: Profile for line J1

Site L:

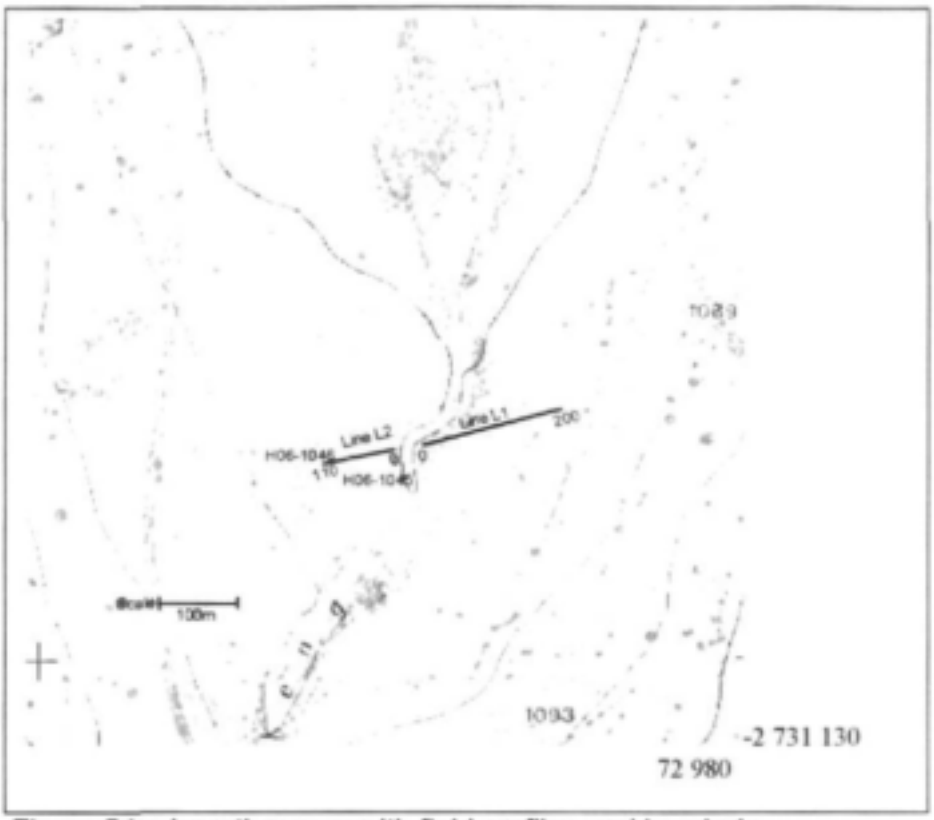

Figure 54a: Location map with field profiles and borehole positions (Orthophoto series 1983).

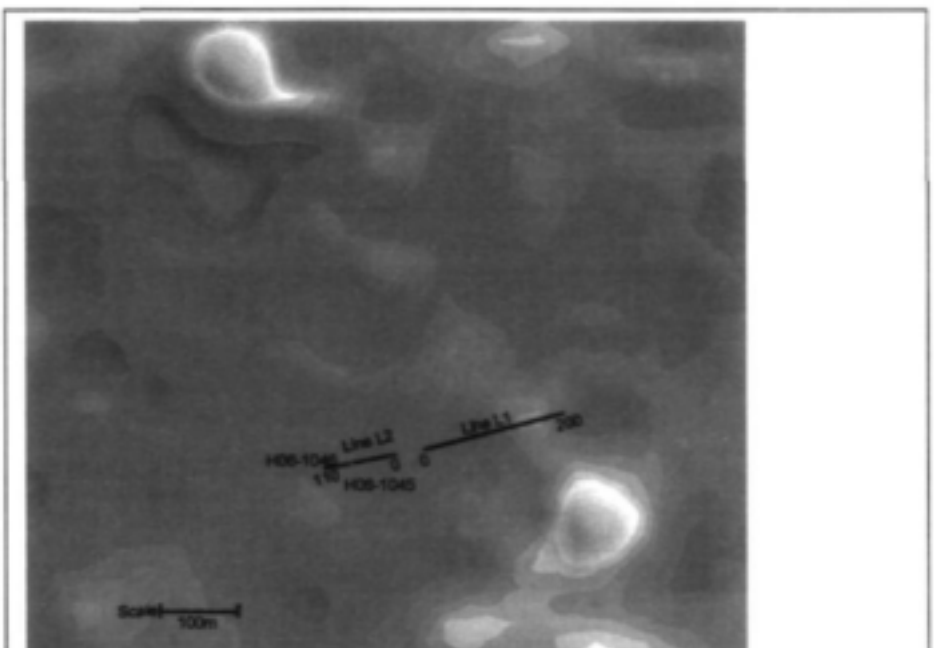

Figure 54b: Airborne magnetic data for the same area as shown above.

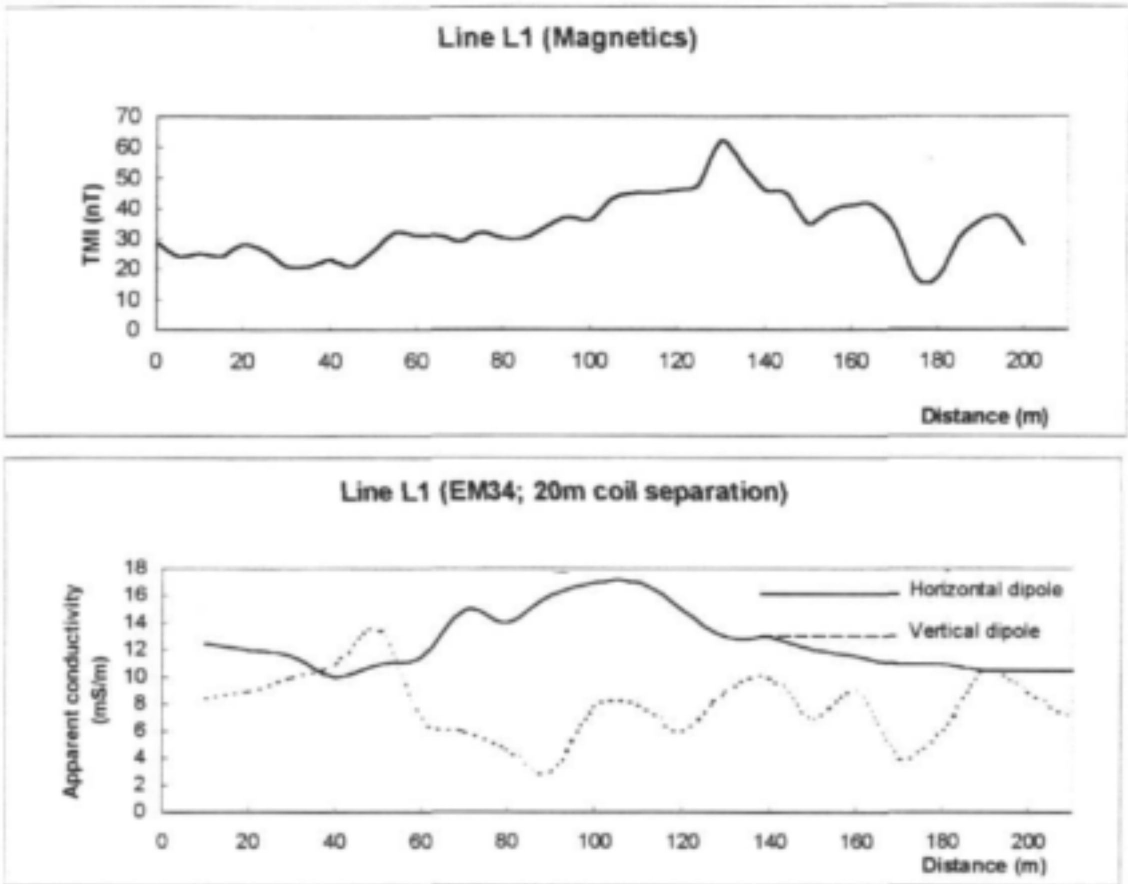

Figure 55a: Profiles for line L1

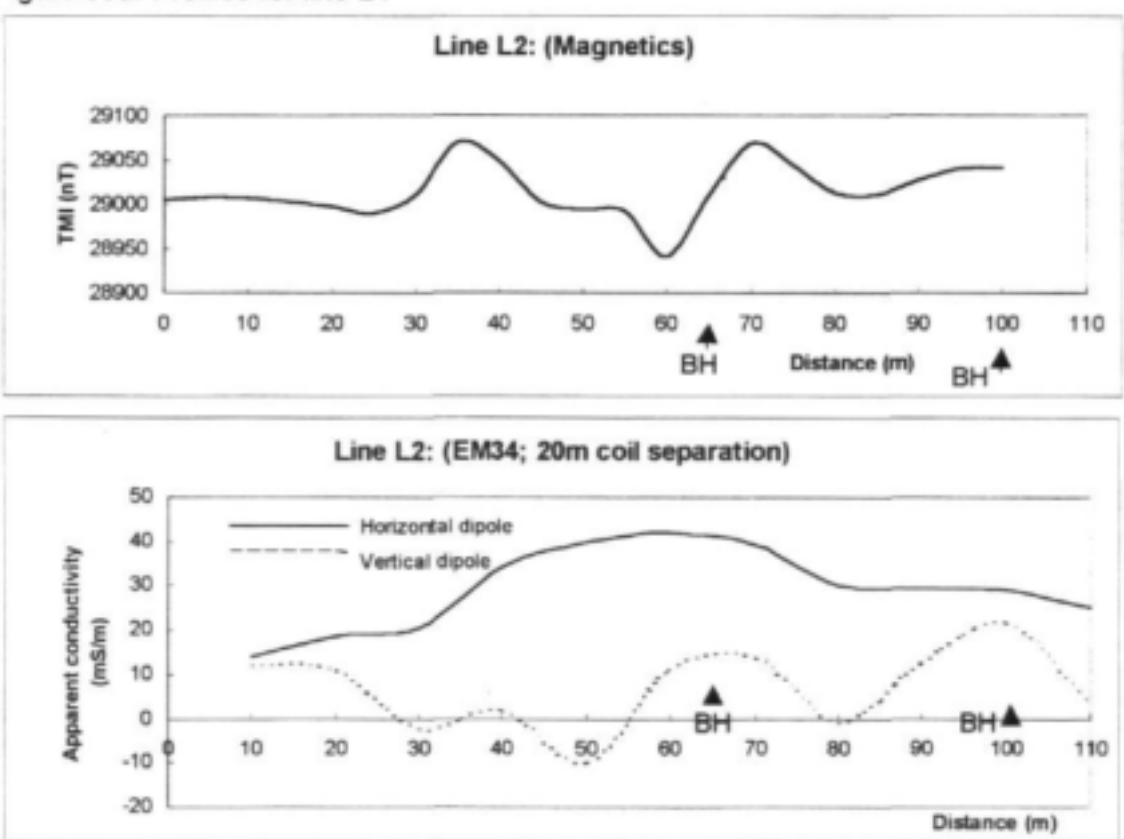

Figure 55b: Profiles for line L2

Site M:

Figure 56a: Location map with field profile and borehole position (Orthophoto series, 1983).

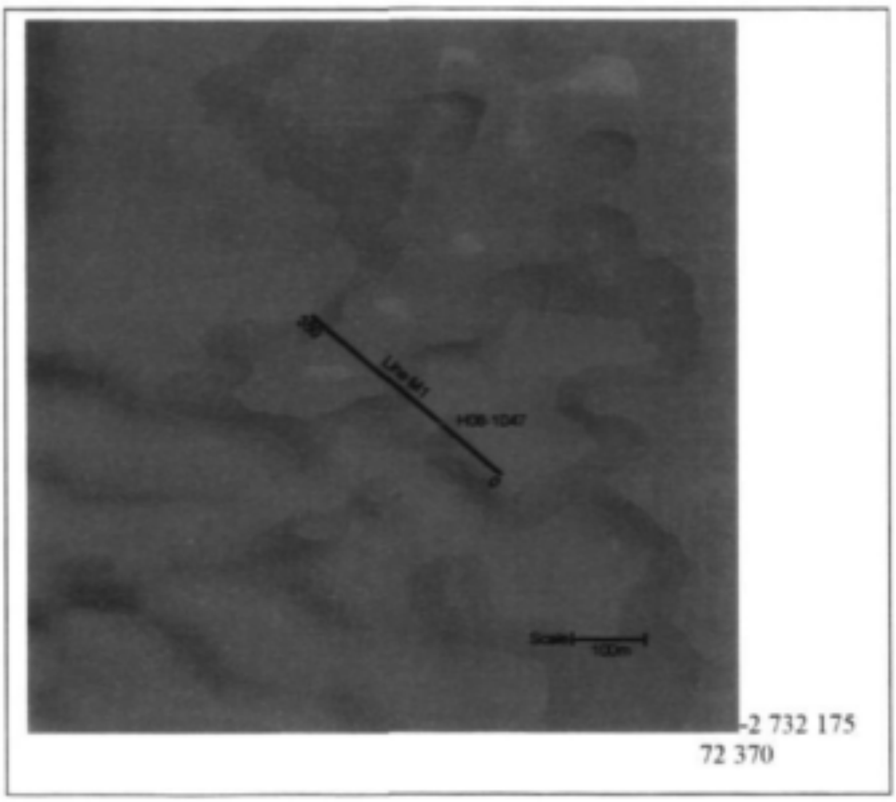

Figure 56b: Airborne magnetic data for the same area as shown above.

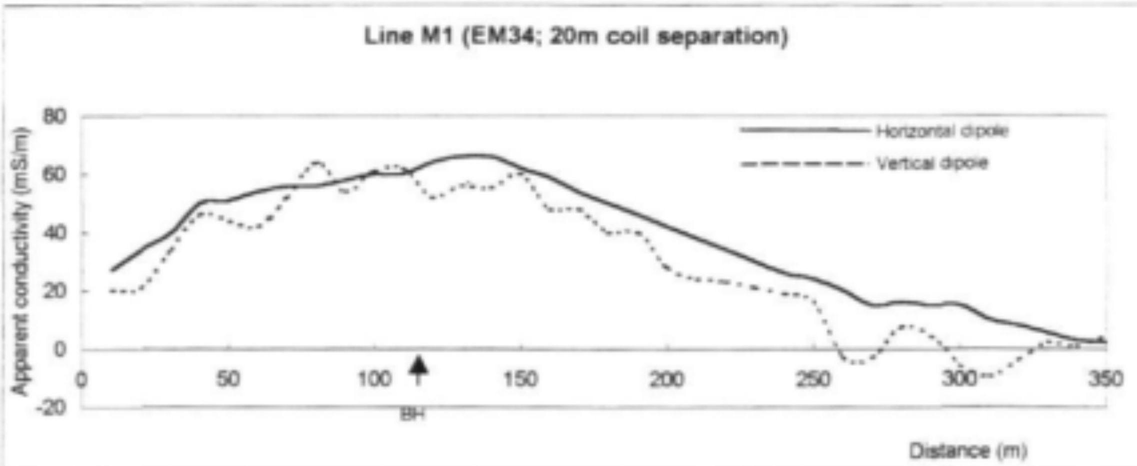

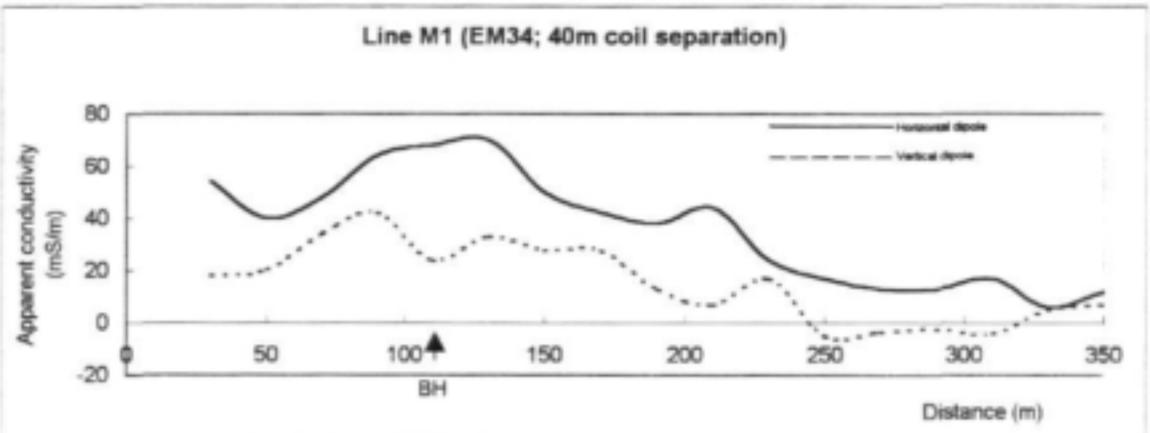

Figure 57: Profiles for line M1

Site N:

Figure 58a: Location map with field profile and borehole position (Orthophoto series, 1983).

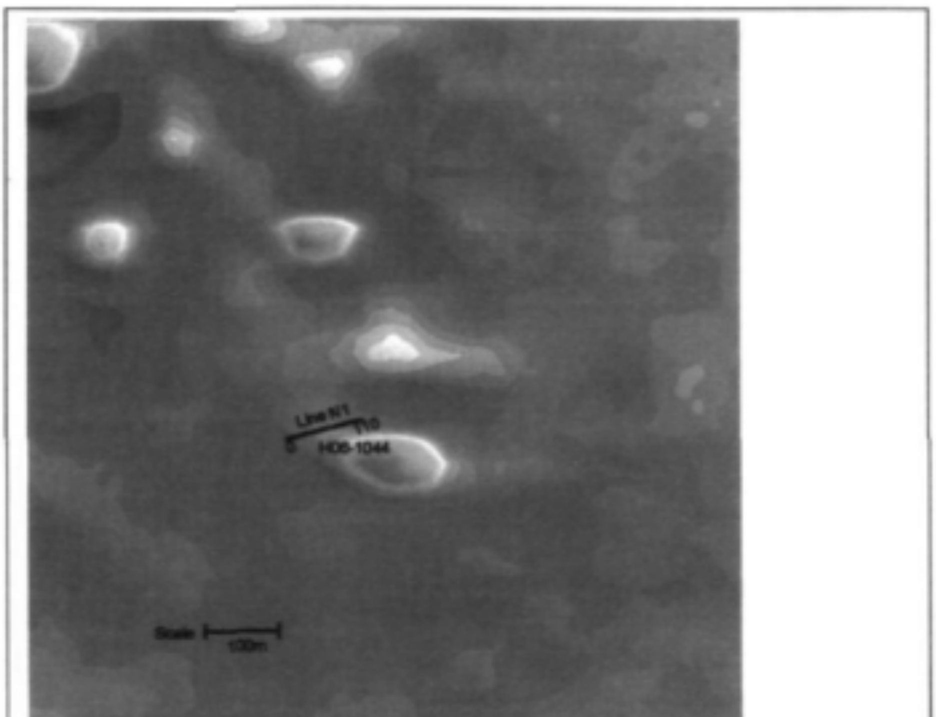

Figure 58b: Airborne magnetic data for the same area as shown above.

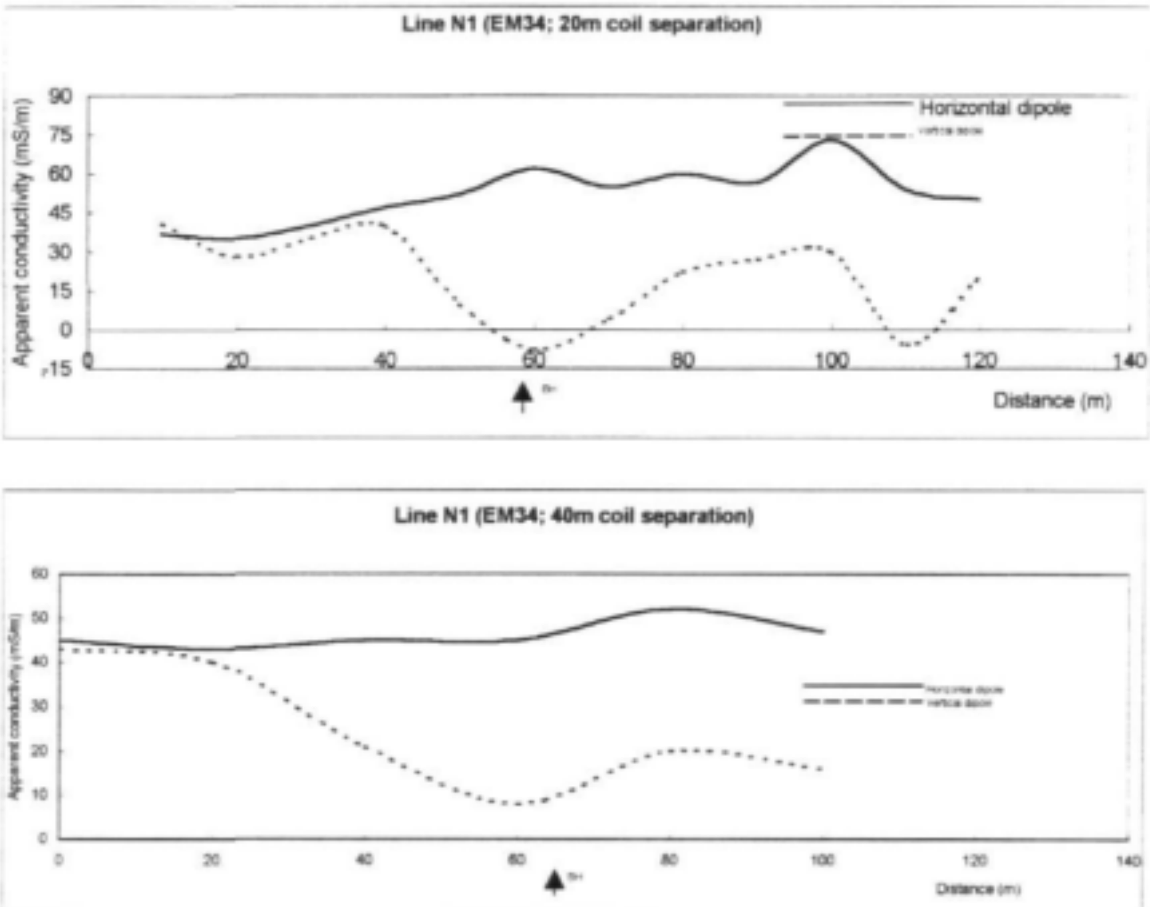

Figure 59: Profiles for line N1

CHAPTER 7

AIRBORNE SURVEY, TARGET IDENTIFICATION AND GROUND FOLLOW-UP, AREA 2

7.1 Airborne magnetic survey, Area 2.

Based on the analysis done of the airborne data of area 1, it was decided that an airborne magnetic survey of area 2 would be sufficient for target identification. This would also make the use of airborne geophysics cost effective for groundwater exploration.

An airborne magnetic survey was flown over area 2, using the microlight system developed by the Council for Geoscience. A line spacing of 100m and flight elevation of 50m were used. The airborne data with various filters applied, are shown in figures 60 to 62. The interpretation and selected sites for ground follow-up are shown in figure 63.

A total of 18 structures were identified as possible targets. Eleven of these were surveyed using a magnetometer and a MaxMin horizontal loop electromagnetic system. Ground profiles were usually 300m long. A station spacing of 5m was used for the magnetic survey, while a 20m station spacing and 100m coil spacing were used for the MaxMin survey, utilizing 444Hz and 1777Hz frequencies. Where no anomaly could be detected with the 300m line length, the line was extended up to a maximum total length of 600m. If an anomaly was still not detected it was interpreted that the magnetic anomaly was due to a dyke but that little or no weathering was associated with the dyke, and the site was abandoned. Sites where an anomaly with the MaxMin system was mapped, the line was repeated using the Geonics EM34 with a 20m coil spacing and a 10m station spacing.

The location maps, associated airborne data and ground profiles with borehole positions are shown in figures 64 -85.

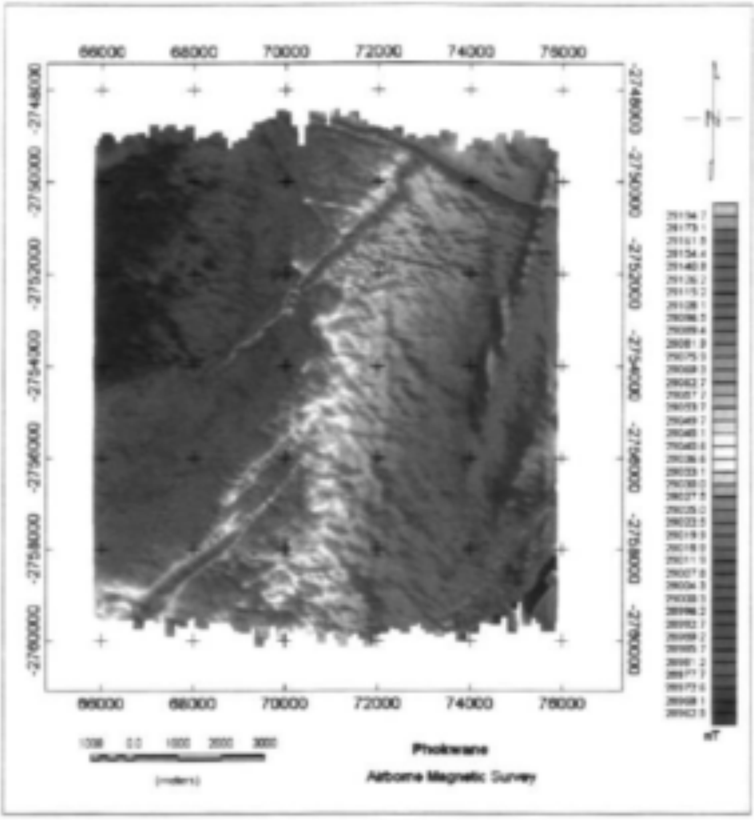

Figure 60: Total field airborne magnetic data, area 2

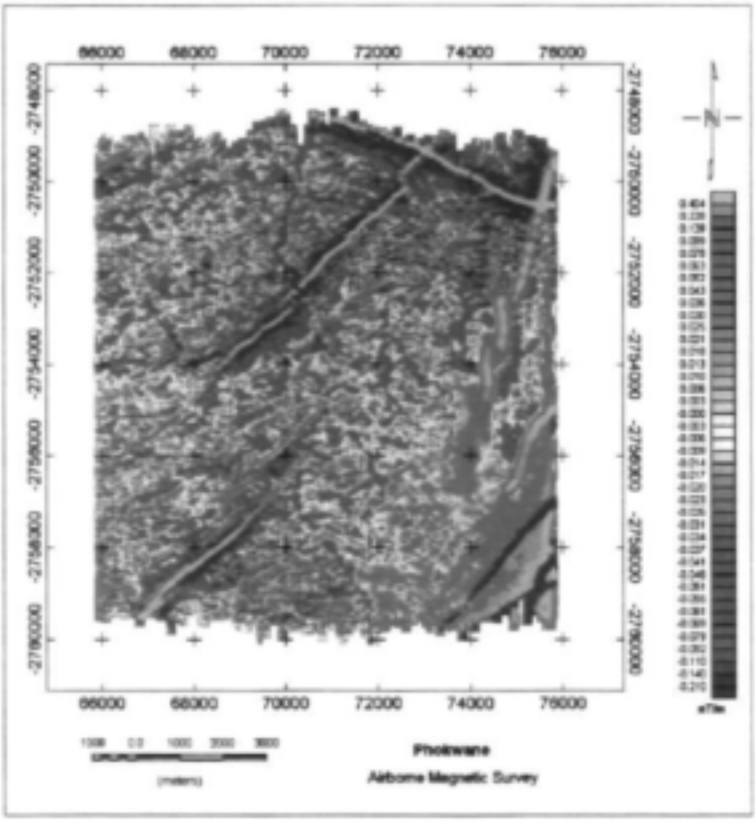

Figure 61: Vertical derivative of the airborne magnetic data, area 2.

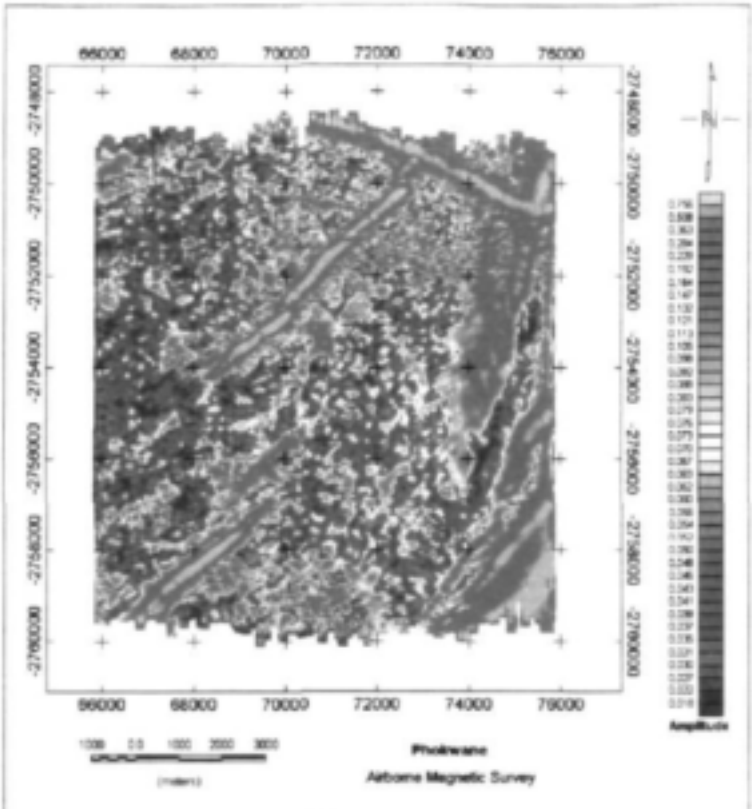

Figure 62: Analytical signal, Area 2.

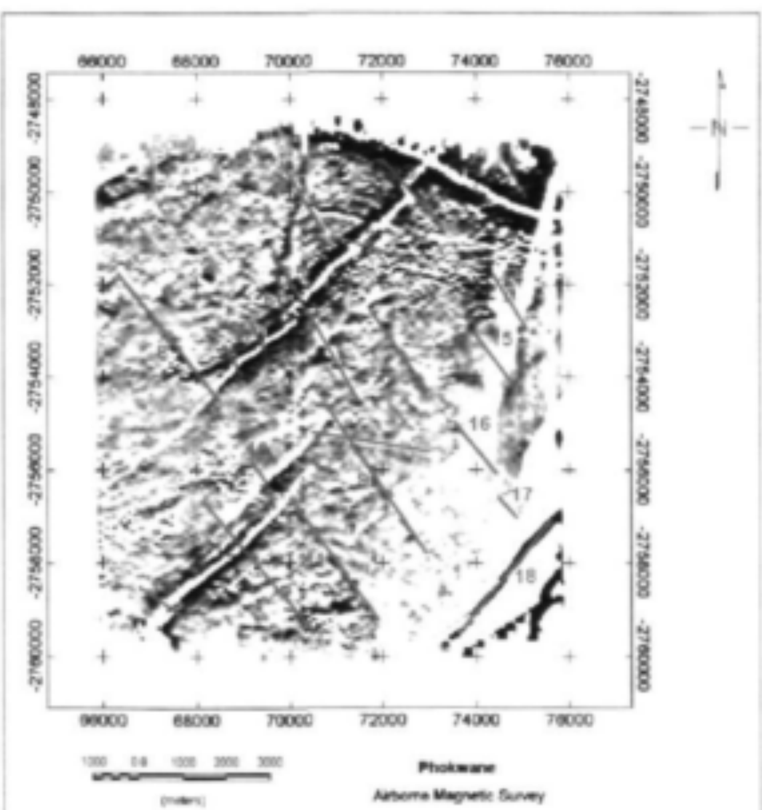

Figure 63: Magnetic data with selected targets for ground follow-up.

Site 1: This site was inaccessible by vehicle and consequently abandoned.

Site 2

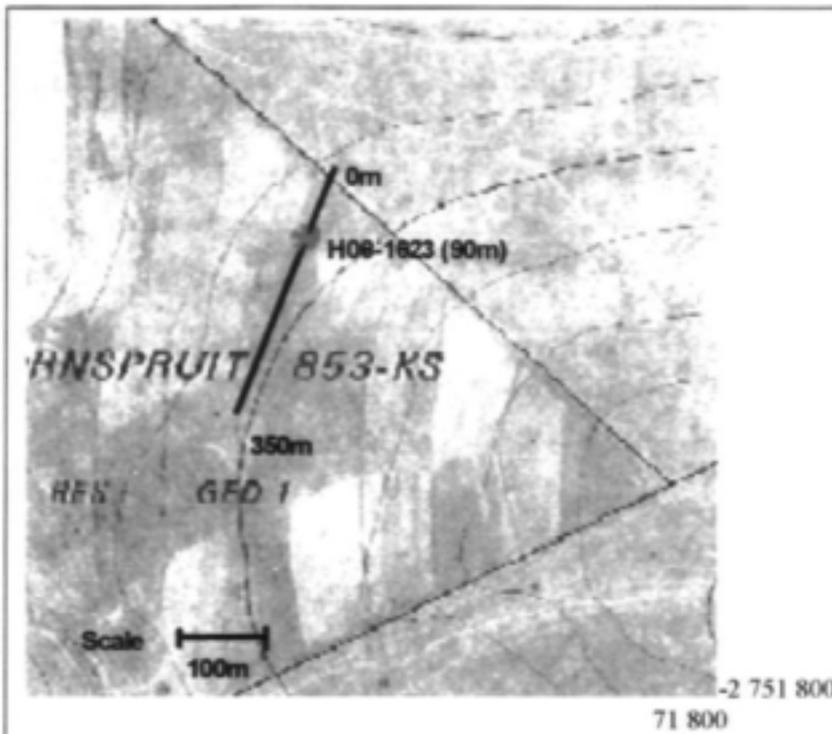

Figure 64a: Location map with field profiles and borehole position (Orthophoto series, 1983)

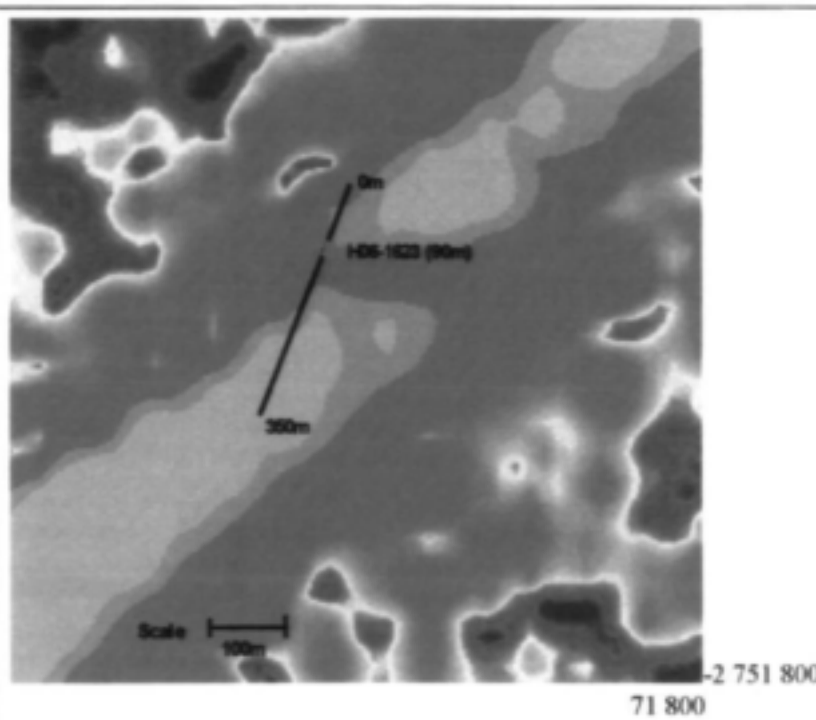

Figure 64b: Airborne magnetic data for the same area as shown above.

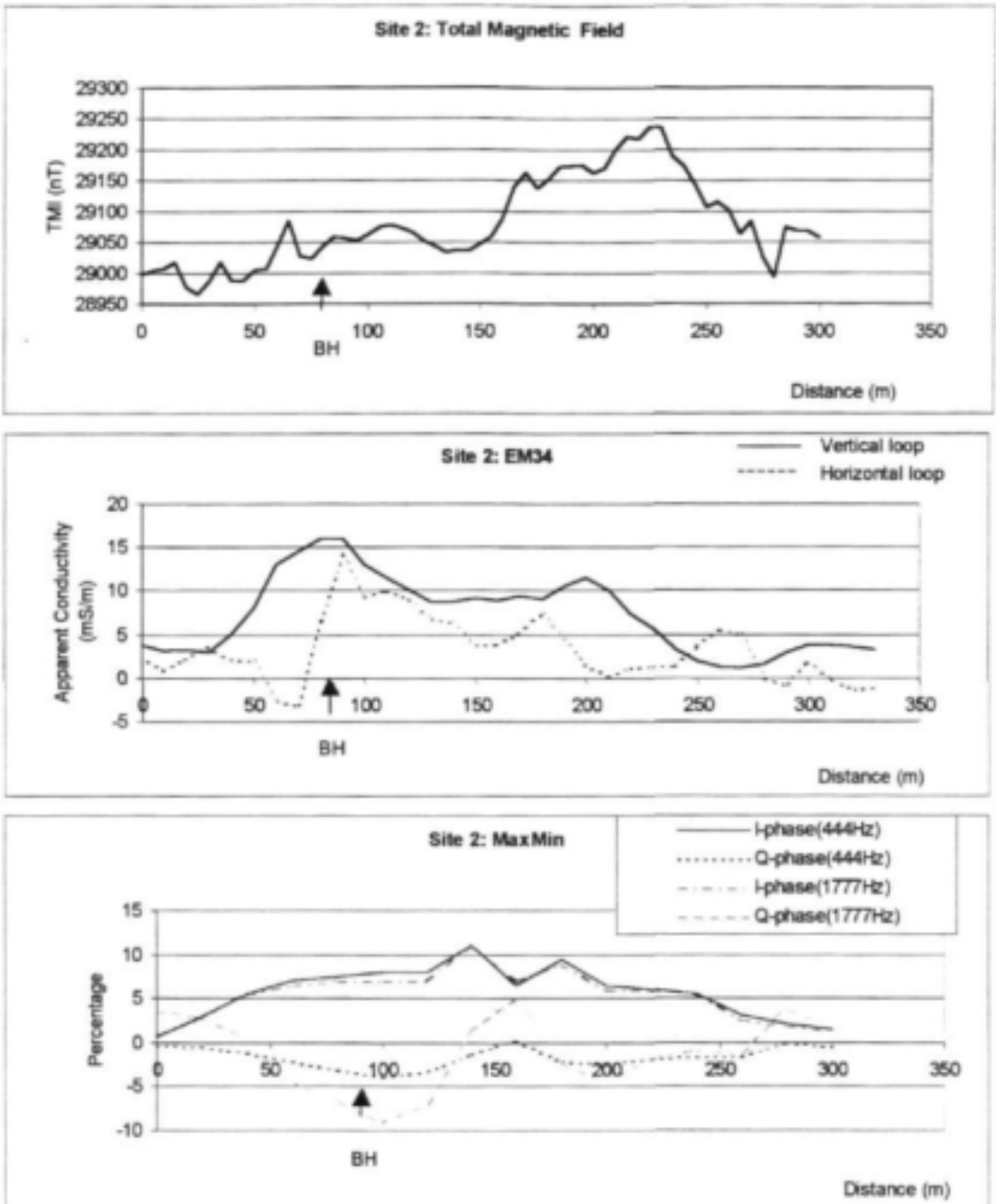

Figure 65: Profiles for Site 2

Site 3

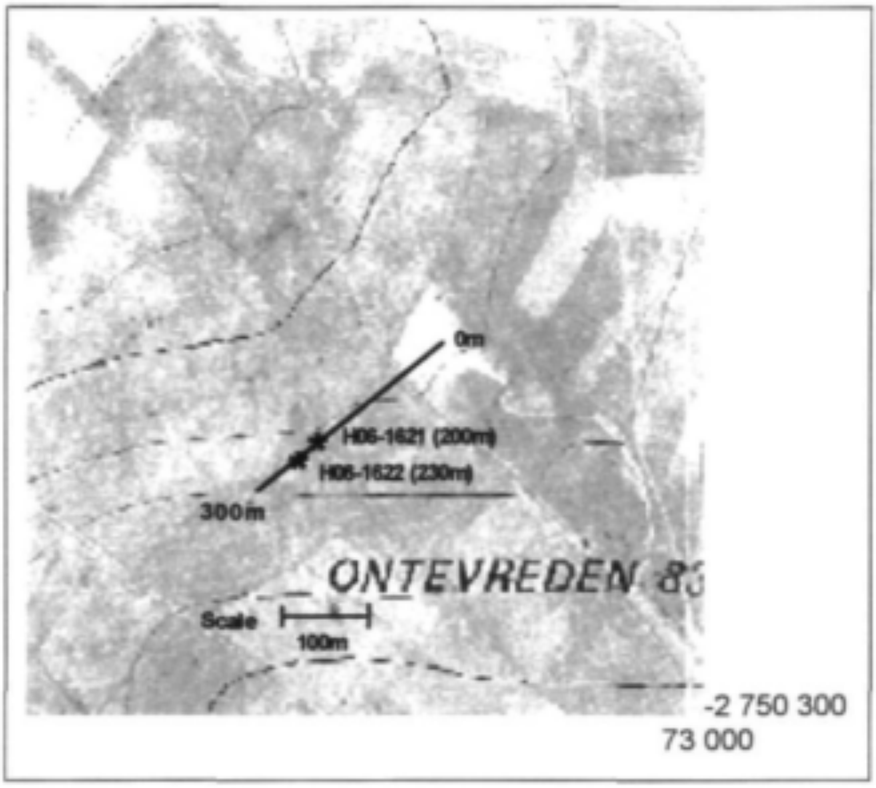

Figure 66a: Location map with field profiles and borehole positions. (Orthophoto series, 1983)

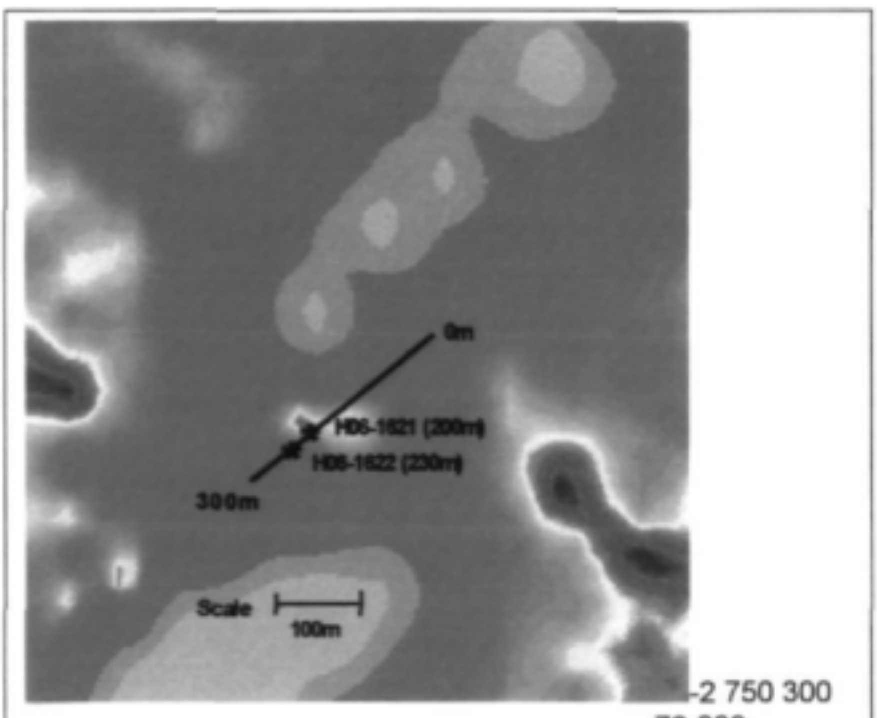

Figure 66b: Airborne magnetic data for the same area as shown above.

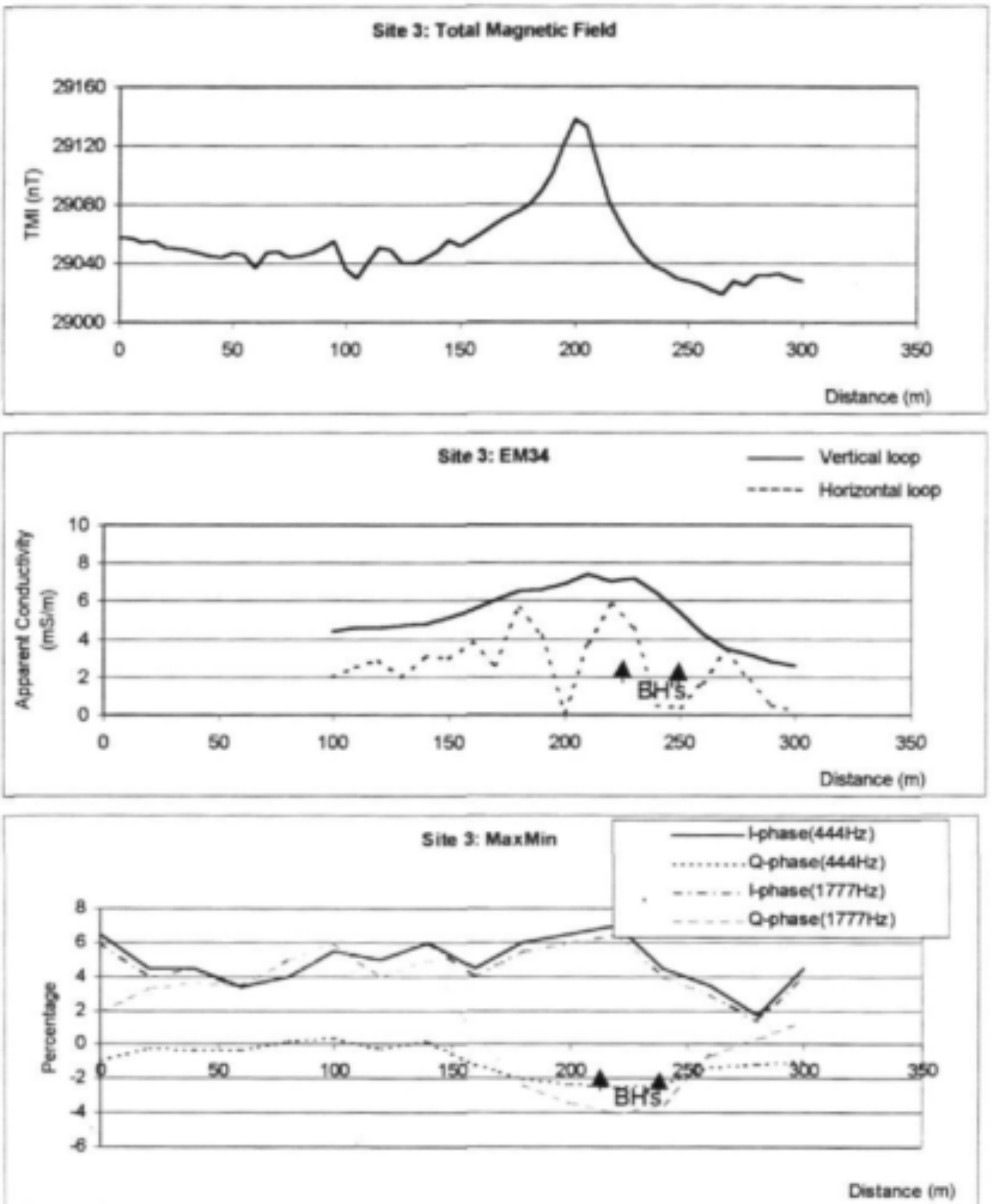

Figure 67: Profiles for site 3

Site 4

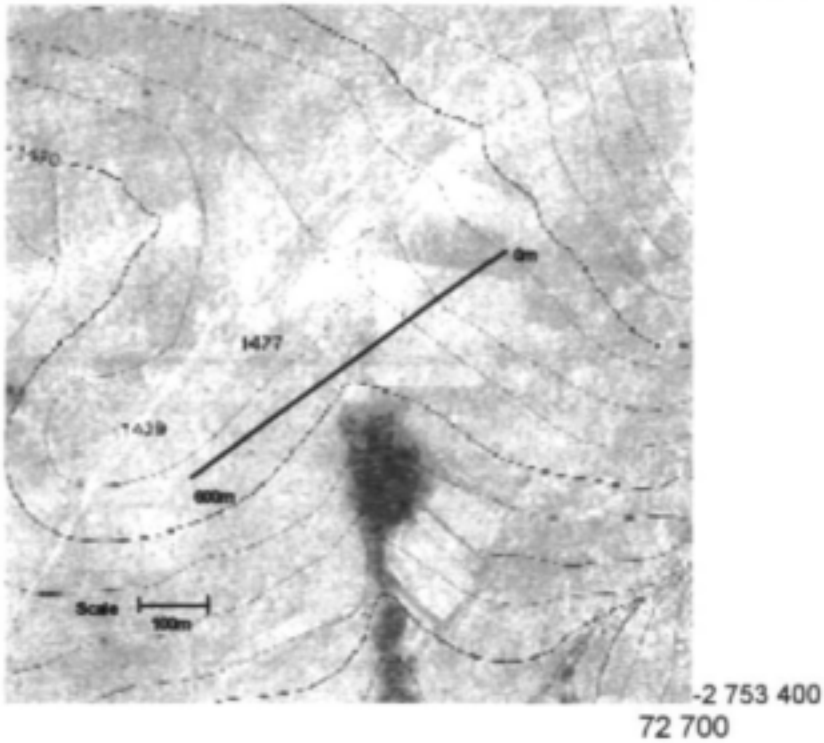

Figure 68a: Location map with field profiles.
(Orthophoto series, 1983)

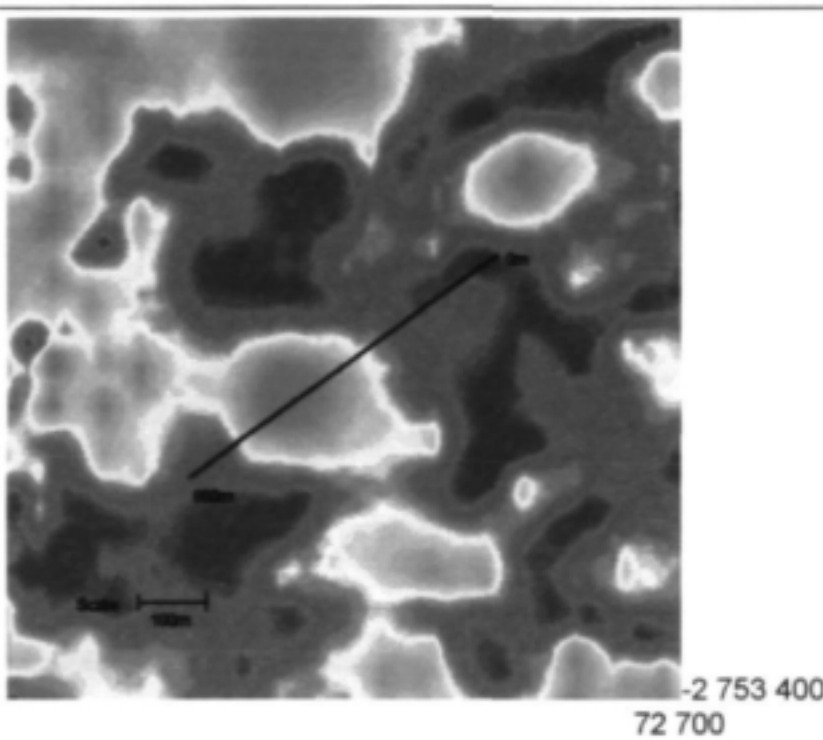

Figure 68b: Airborne magnetic data for the same area as shown above.

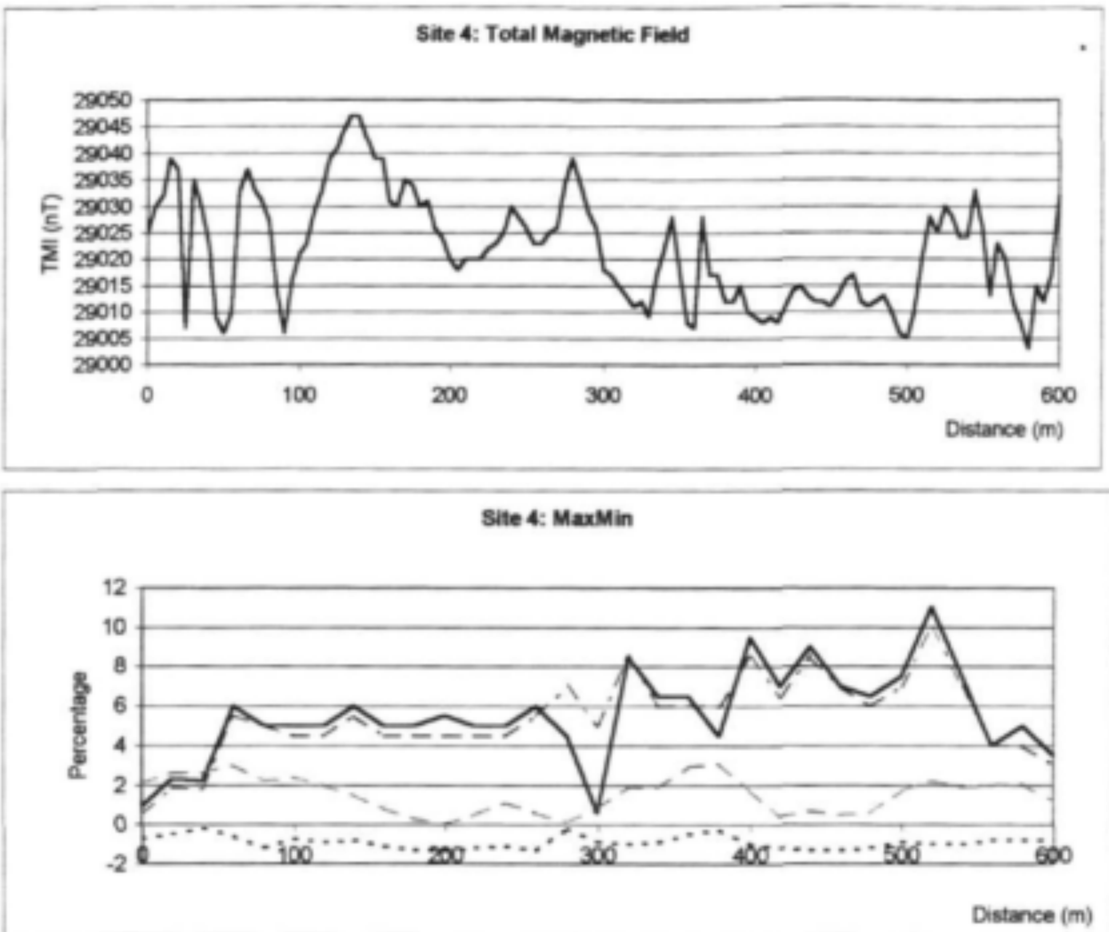

Figure 69: Profiles for site 4.

Site 5& 6

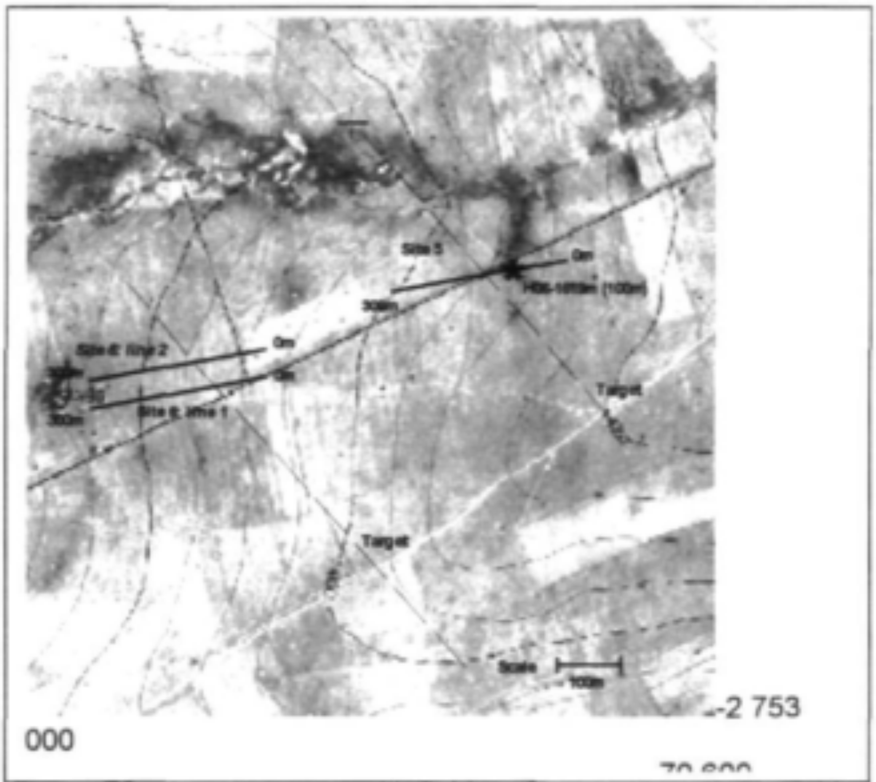

Figure 70a: Location map with field profiles and borehole position. (Orthophoto series, 1983)

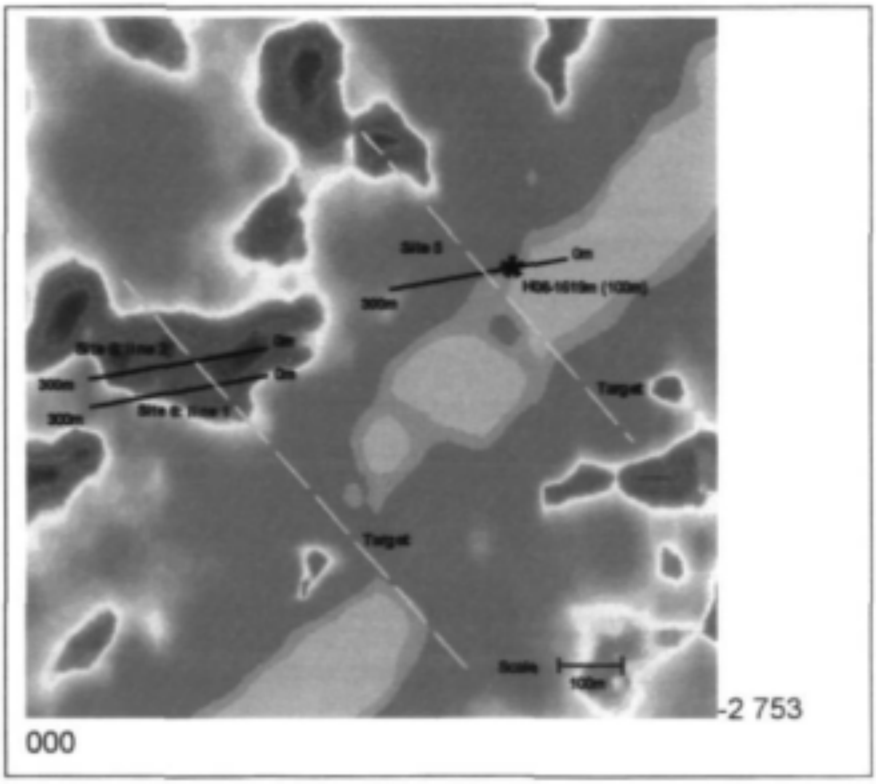

Figure 70b: Airborne magnetic data for the same area as shown above.

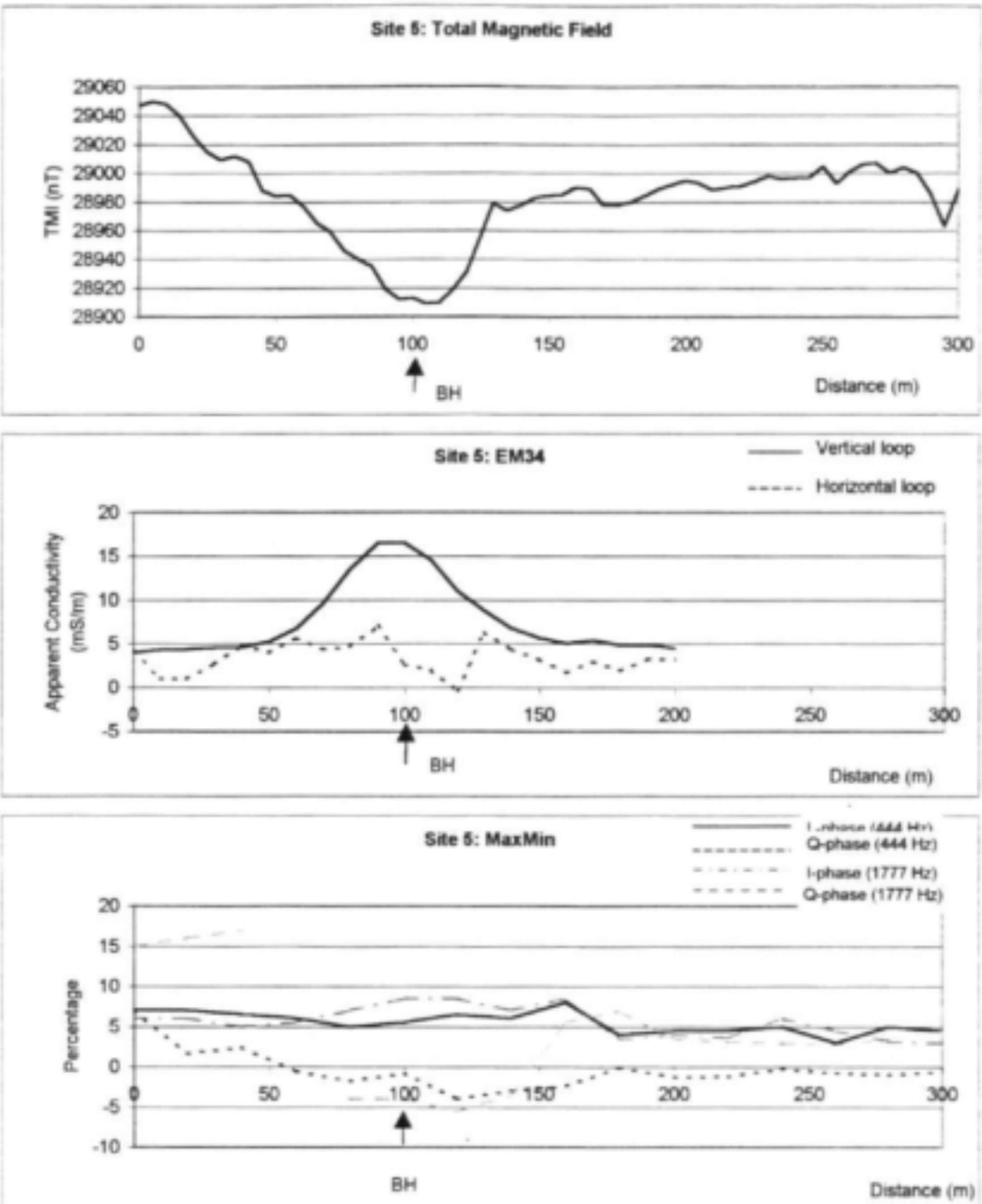

Figure 71: Profiles for site 5

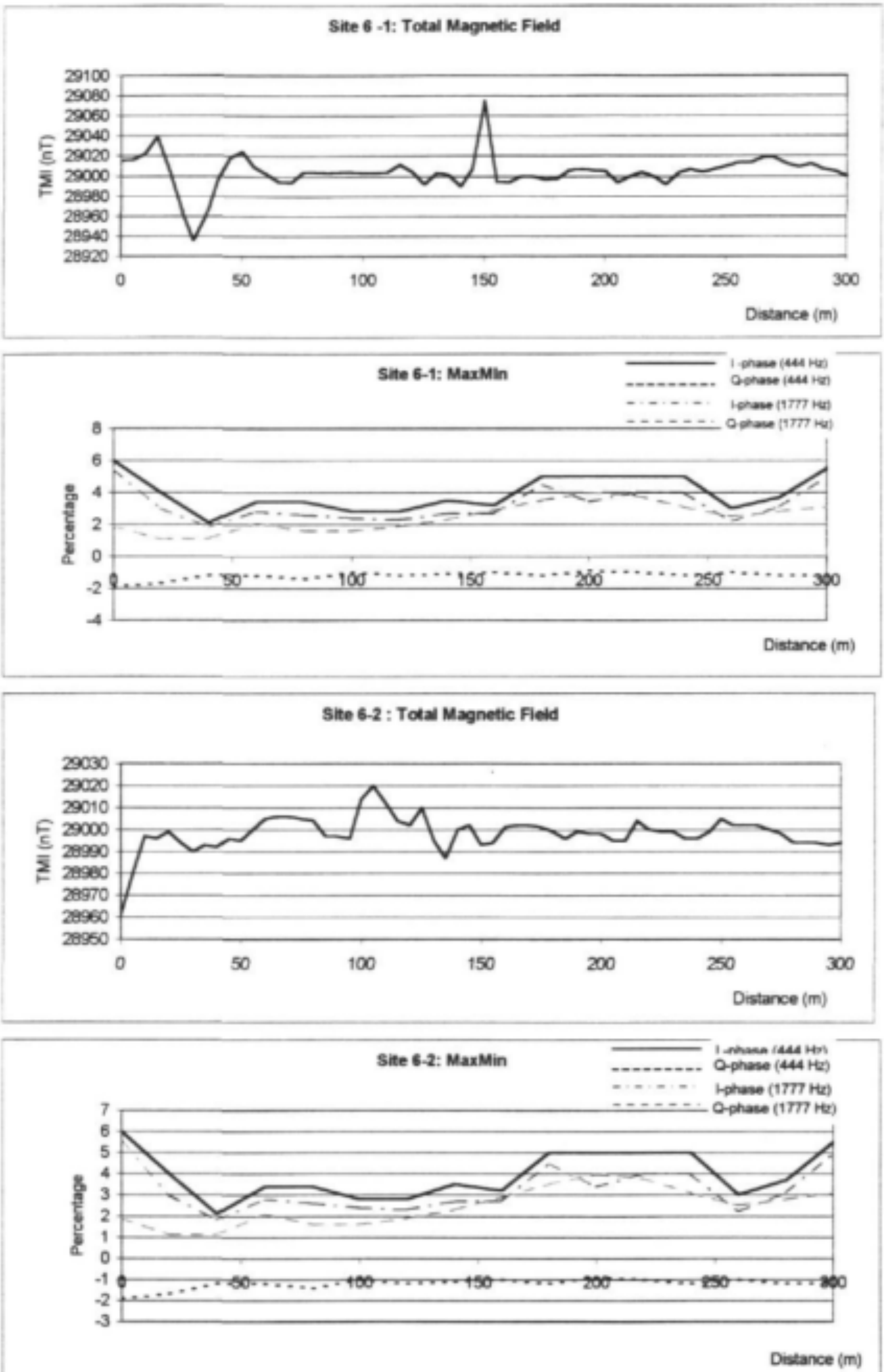

Figure 72: Profiles for site 6.

Site 7

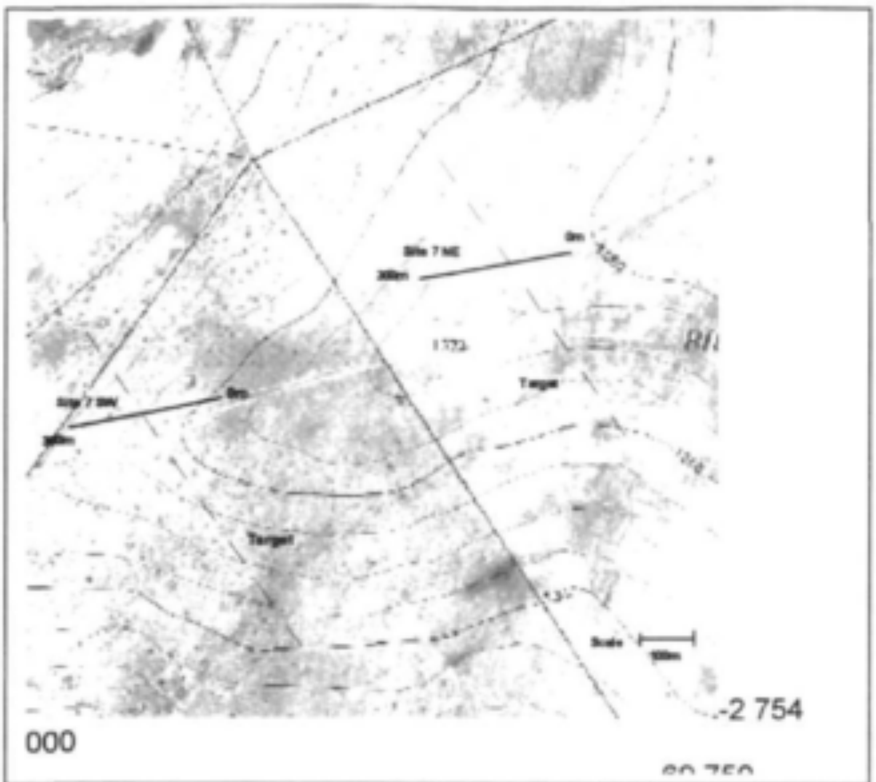

Figure 73a: Location map with field profiles.
(Orthophoto series, 1983)

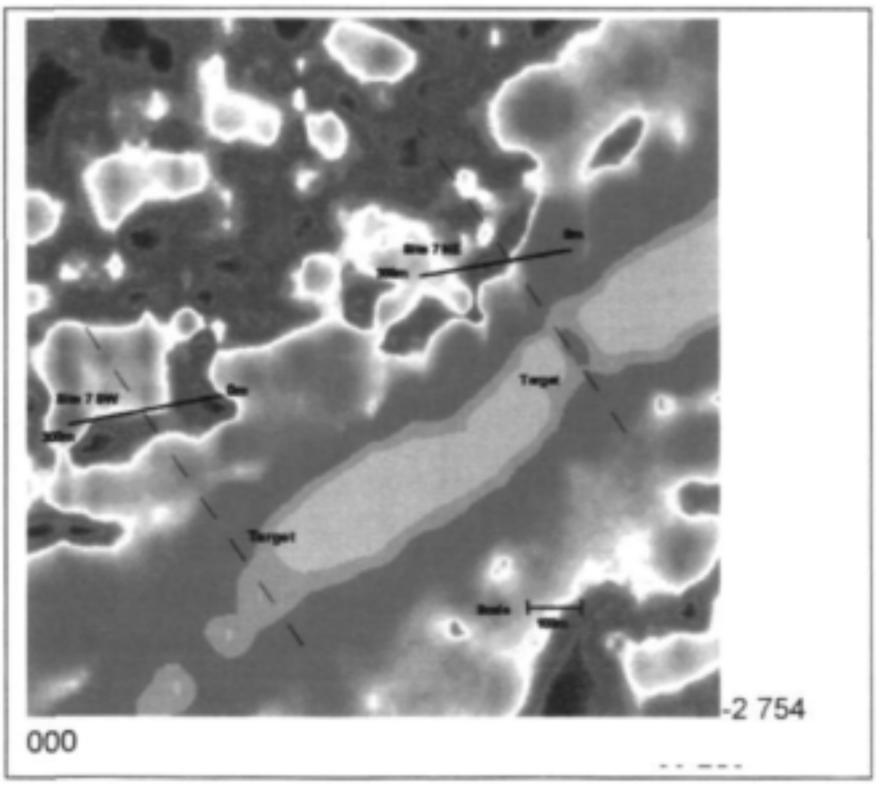

Figure 73b: Airborne magnetic data for the same area as shown above.

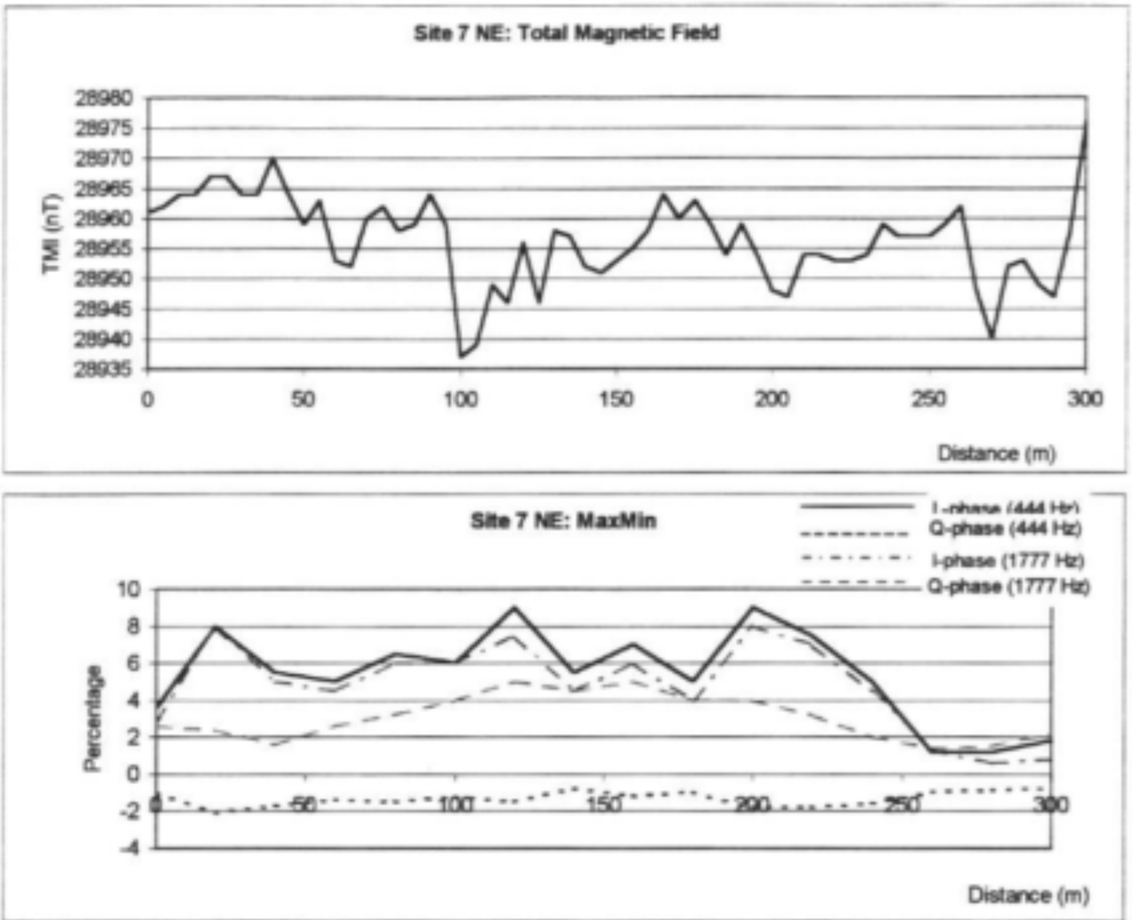

Figure 74: Profiles for site 7 North-East

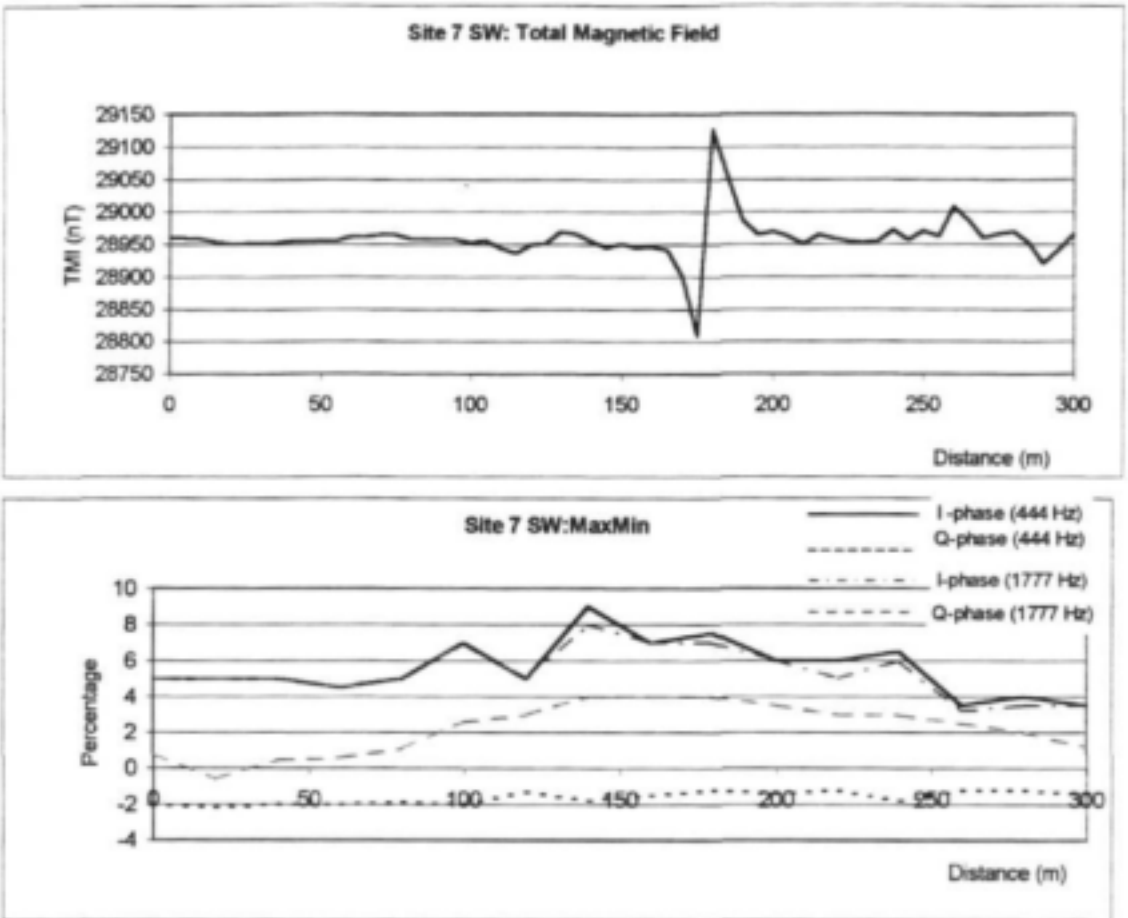

Figure 75: Profiles for site 7 South-West

Site 8

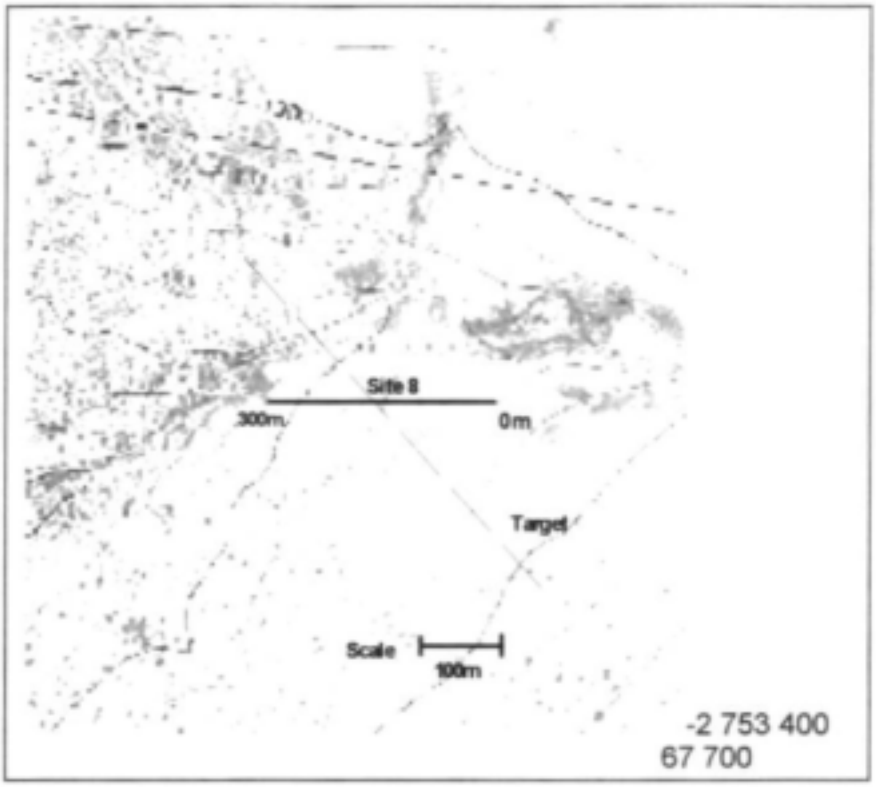

Figure 76a: Location map with field profiles.
(Orthophoto series, 1983)

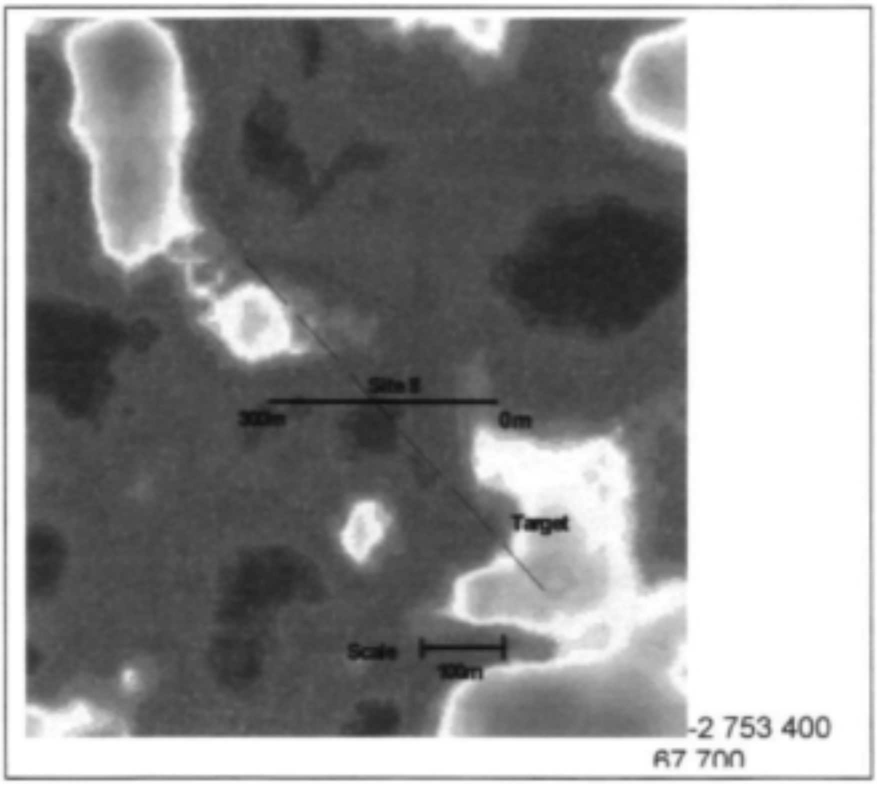

Figure 76b: Airborne magnetic data for the same area as shown above.

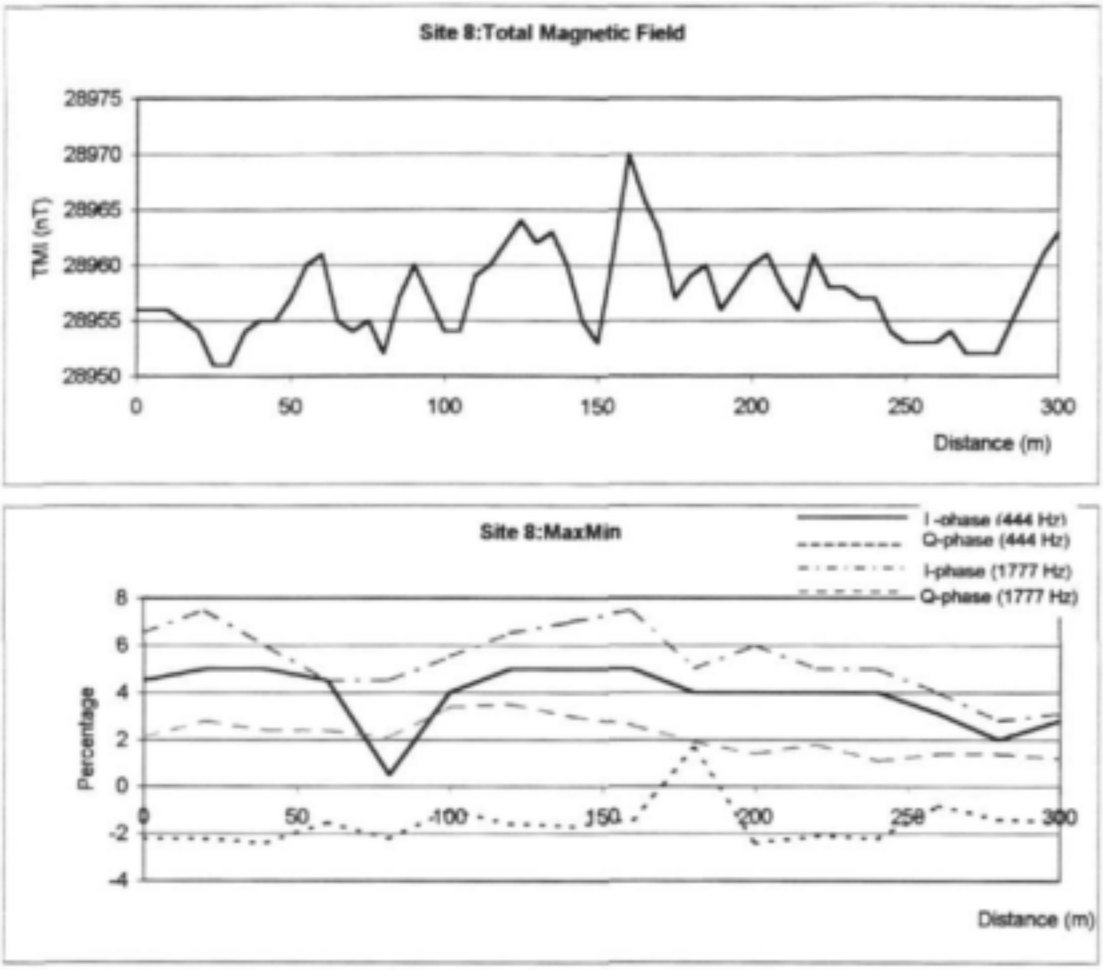

Figure 77: Profiles for site 8

Site 9

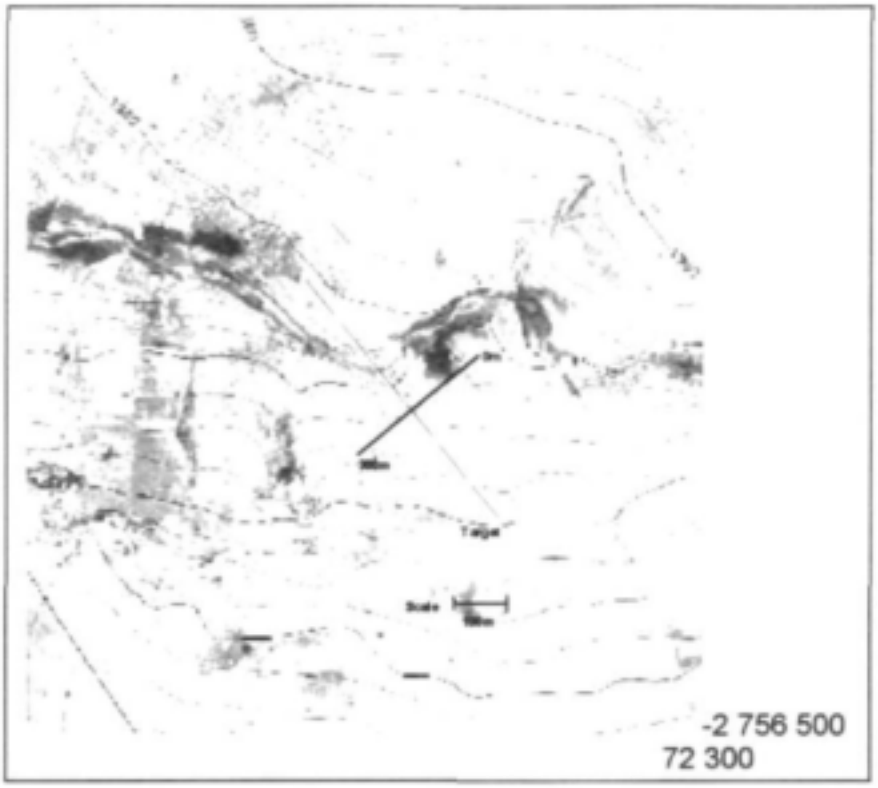

Figure 78a: Location map with field profiles. (Orthophoto series, 1983)

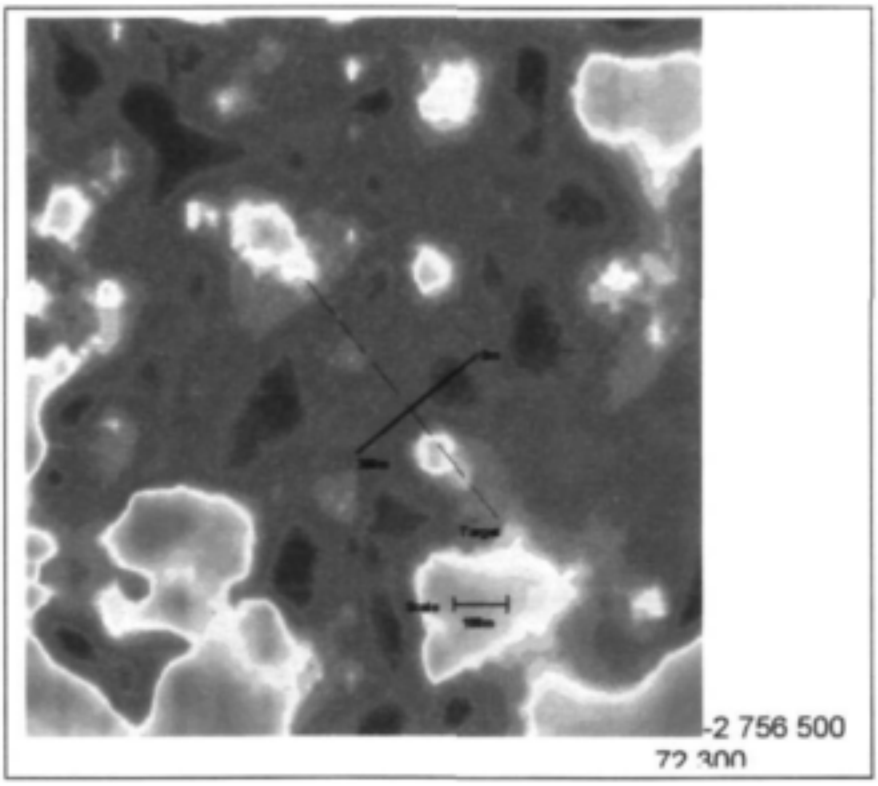

Figure 78b: Airborne magnetic data for the same area as shown above.

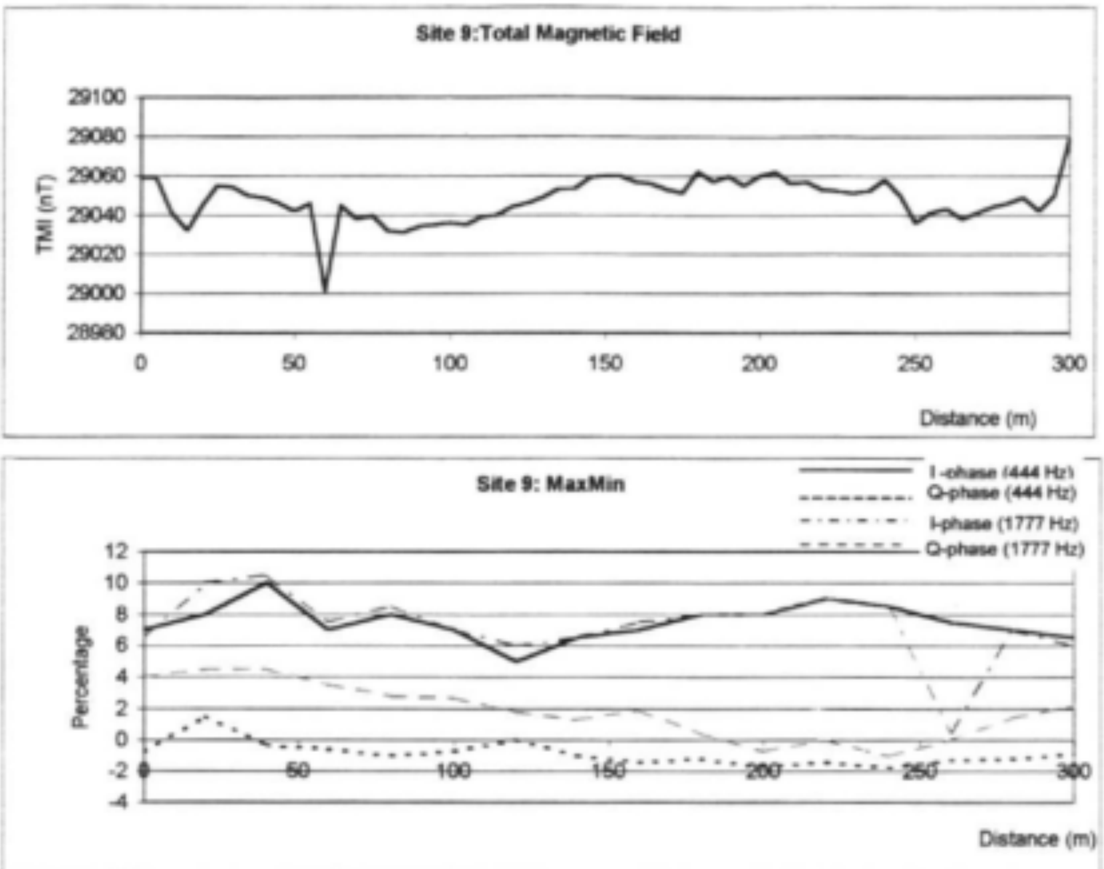

Figure 79: Profiles for site 9

Site 10: The site was inaccessible by vehicle and thus abandoned.

Site 11

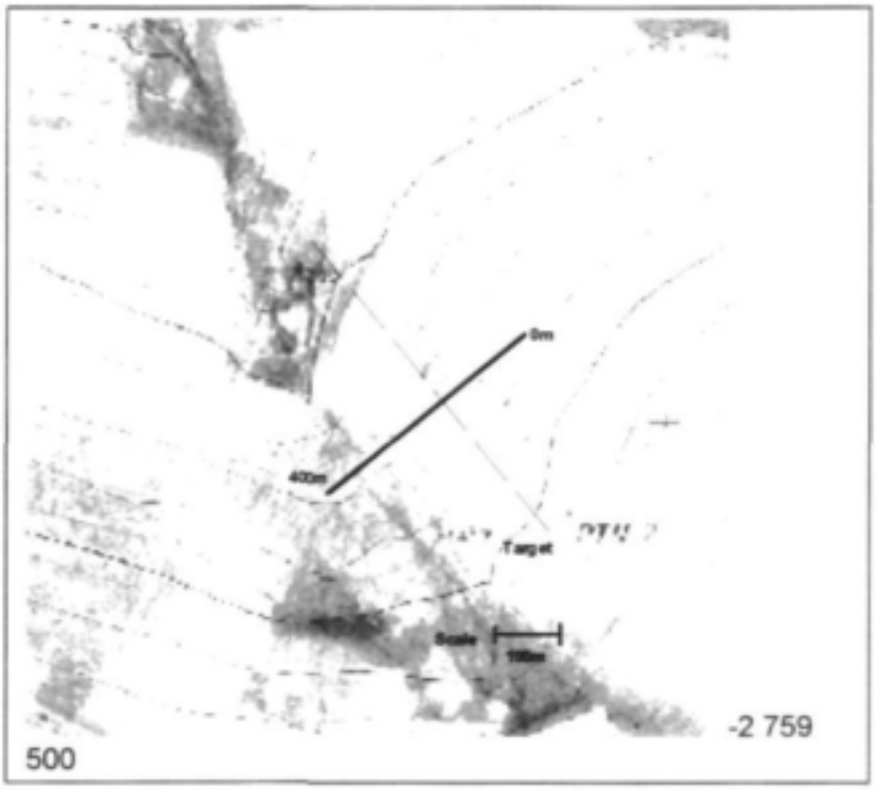

Figure 80a: Location map with field profiles.
(Orthophoto series, 1983)

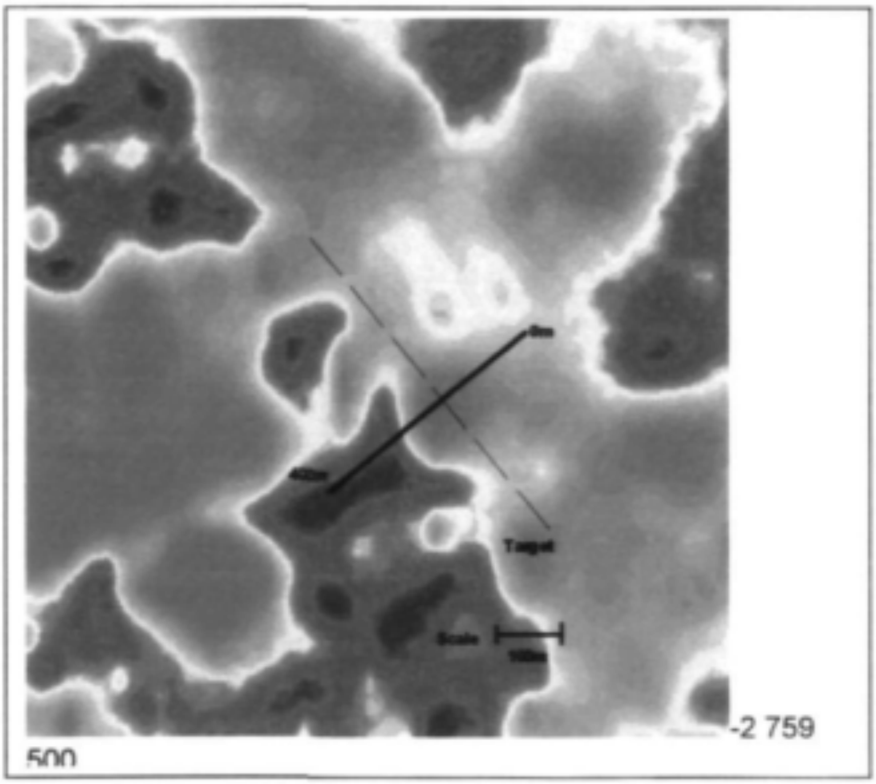

Figure 80b: Airborne magnetic data for the same area as shown above.

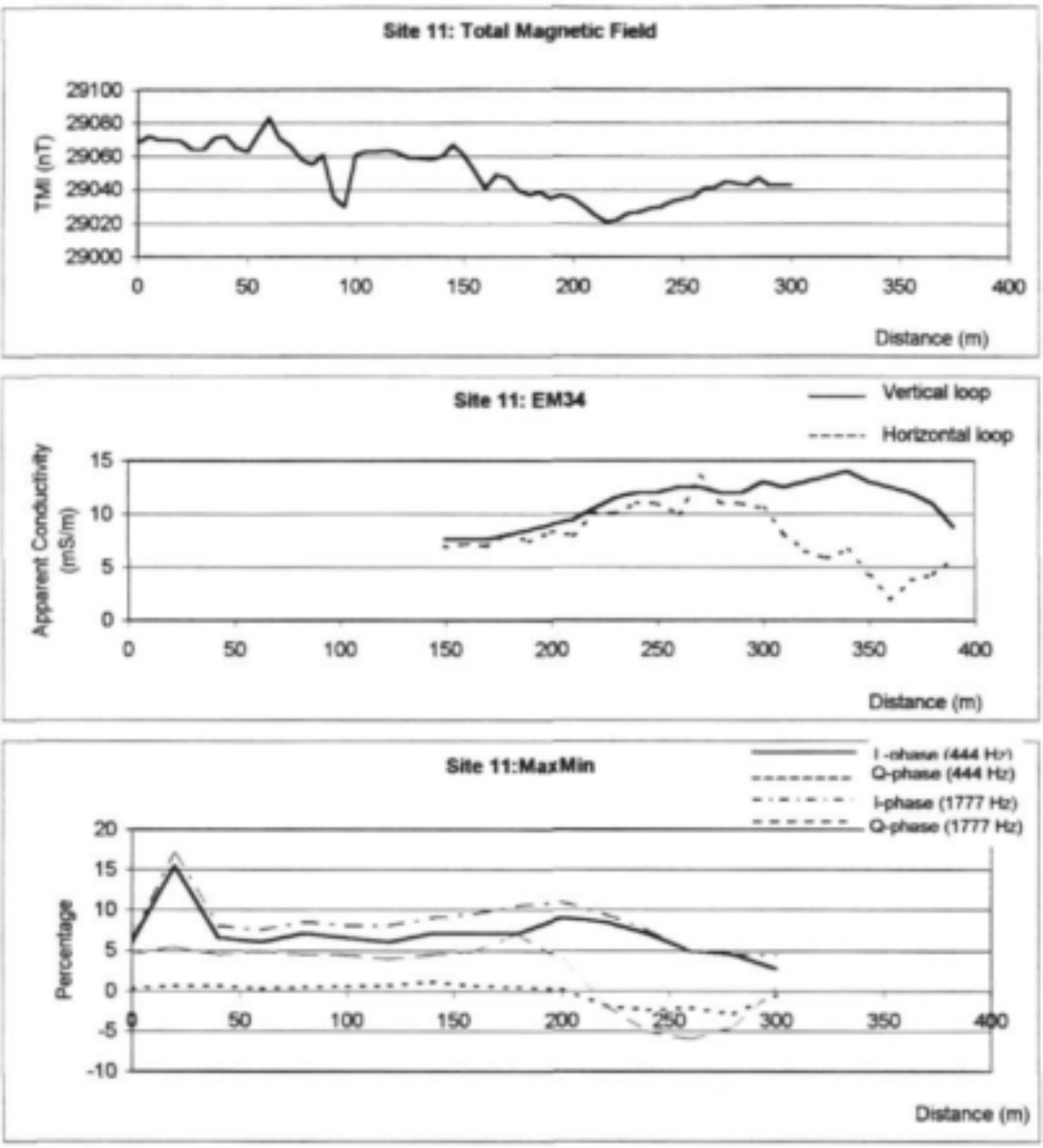

Figure 81: Profiles for site 11

Site 12

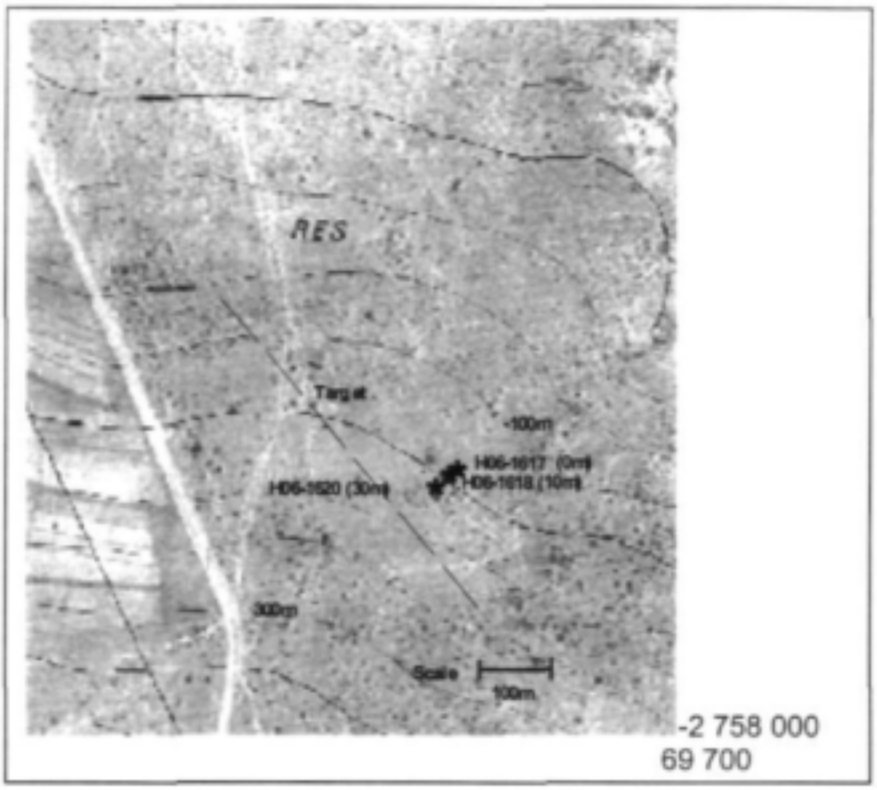

Figure 82a: Location map with field profiles and borehole positions. (Orthophoto series, 1983)

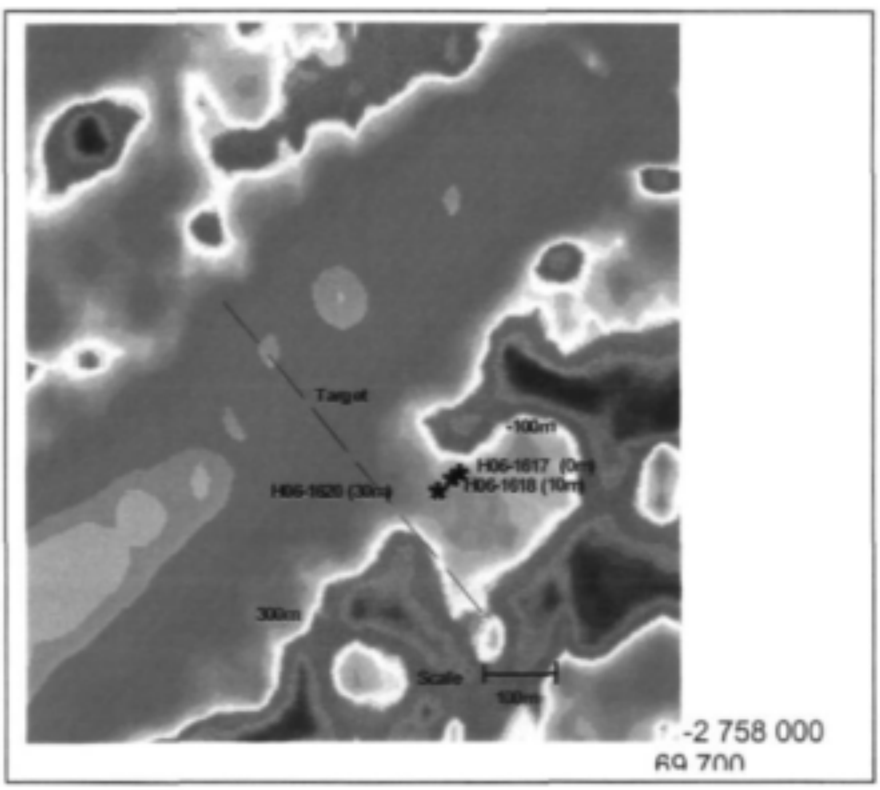

Figure 82b: Airborne magnetic data for the same area as shown above.

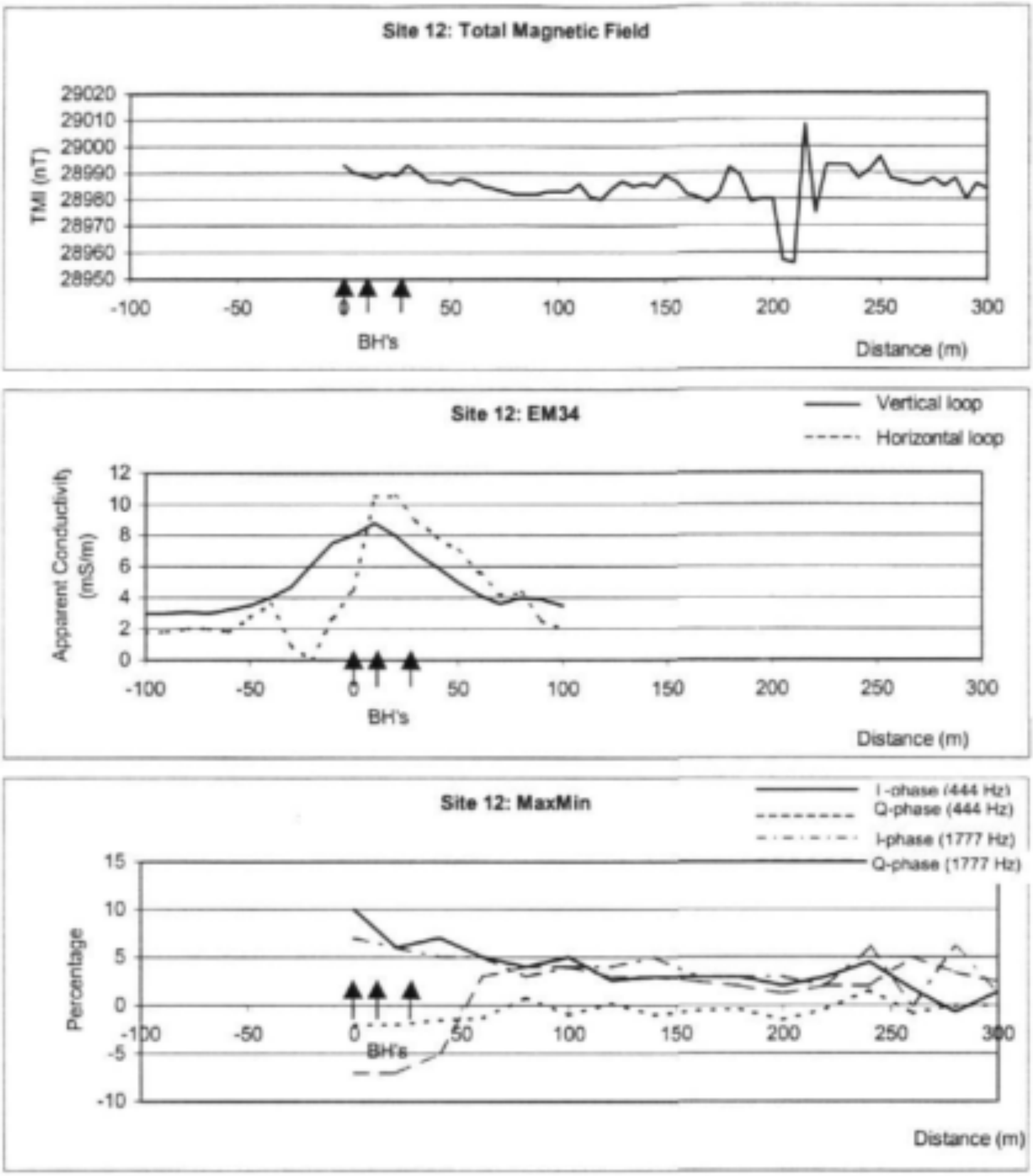

Figure 83: Profiles for site 12

Site 13

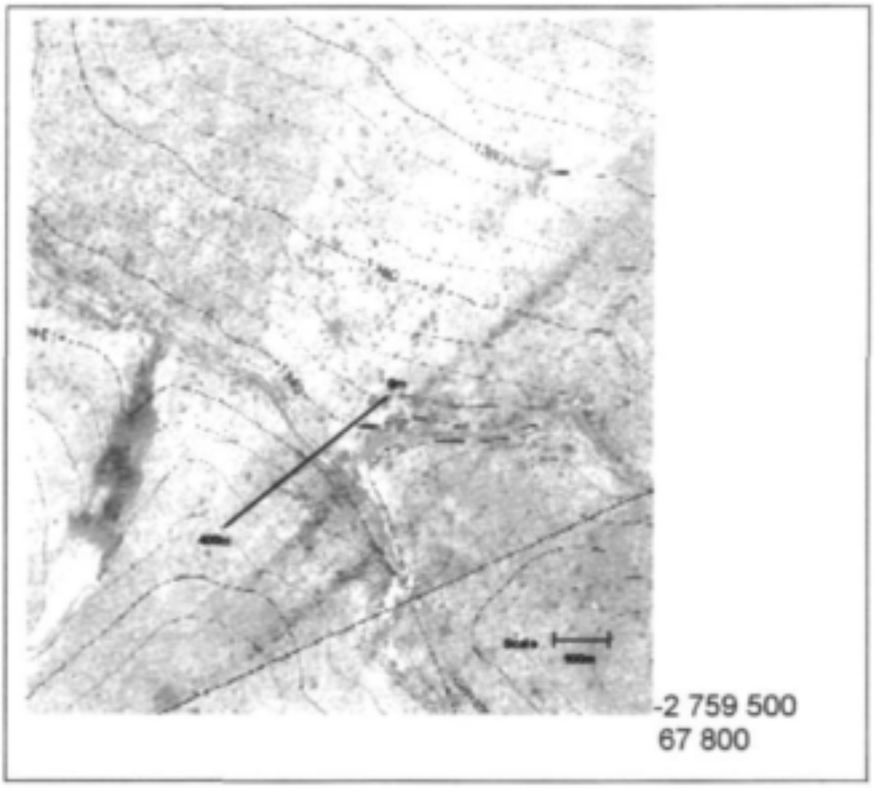

Figure 84a: Location map with field profiles.
(Orthophoto series, 1983)

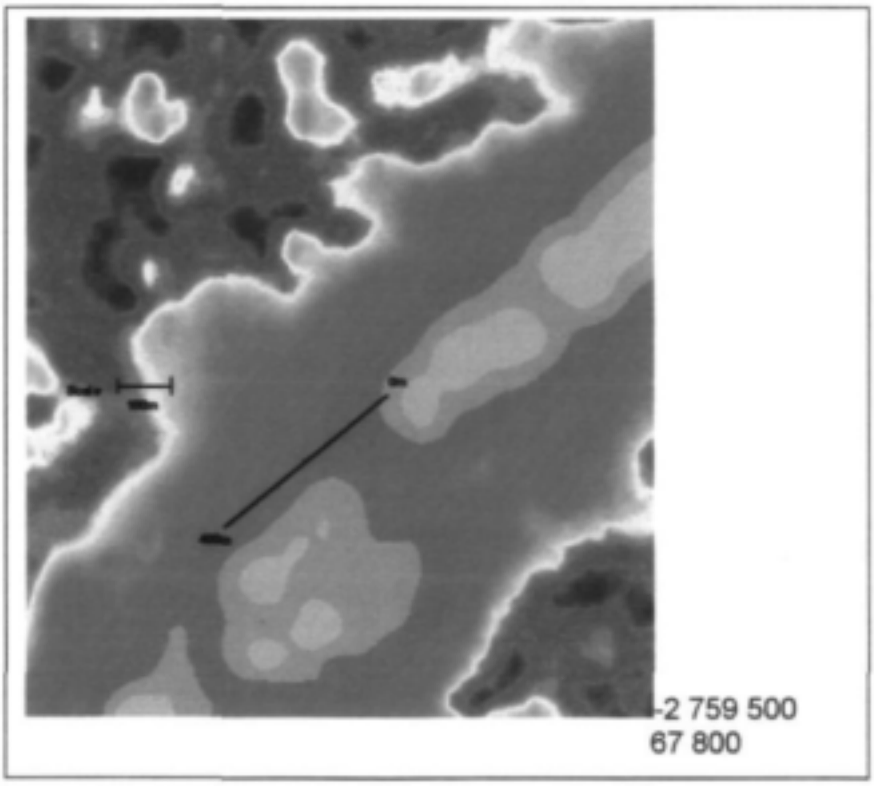

Figure 84b: Airborne magnetic data for the same area as shown above.

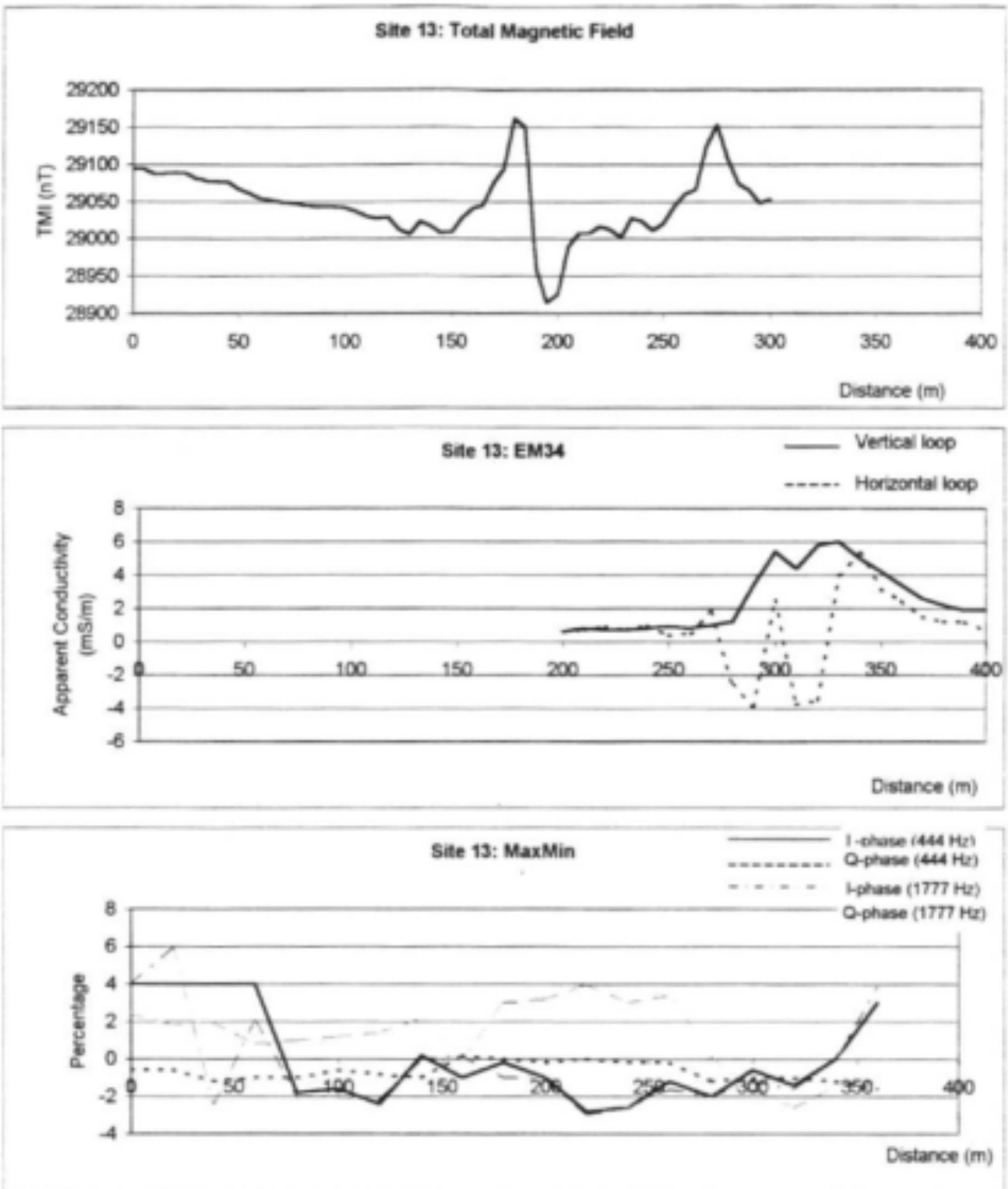

Figure 85: Profiles for site 13

CHAPTER 8

DRILLING RESULTS AND DISCUSSION

8.1 General

This chapter is a summary of the research done by Mr. S. Botha, submitted as a MSc thesis (Botha, 2000) and funded by the NRF. For a detailed discussion of his techniques and results the reader is referred to his thesis.

8.2 Drilling results, area 1

In order to evaluate the application of the airborne geophysical techniques, the holes that were sited based on the ground follow–up work, were drilled by the Department of Water Affairs and Forestry. The borehole numbers, coordinates, depths, air lift and depth of the deepest water strike are presented in Table 3. Holes that yielded an air lift of more than 0.1 l/s are rated as successful because they can be fitted with hand pumps.

The holes are grouped together as sites. Each site represents a certain structure or combination of structures. At sites F, H and G a number of holes were drilled close to one another on the same feature to serve as observation holes for pump testing and to compare the nature of fractured zones in granite to fractured zones in dolerite. The granite was more fractured than the dolerite dykes on the same fault with maximum weathering occurring at the contact. (Compare the yields of H06-1021 (dolerite), H06-1026 (granite) and H06-1038 (contact)).

At site I, H06-0904 was drilled to investigate the weathering associated with the dolerite/granite contact in the absence of a fault. Although the EM34 data show a small anomaly at this contact (Fig. 51), there are very limited signs of weathering and no water. This observation was confirmed at other sites where fault zones were drilled at a dolerite-granite contact – the fault zones yielding water but not the contacts.

Table 4: Summary of drilling results for area 1.

Site	*Borehole nr.*	*Lox*	*LOy*	*Depth(m)*	*Air Lift (l/s)*	*Deepest water strike (m)*
A	H06-0881	-2722535	68516	50	1	7
B	H06-0882	-2723302	67714	30	2	1.8
C	H06-0916	-2731093	68136	72	0.1	15
	H06-0917	-2731100	68143	72	0	*
					0.1	

E	W6128	-2731749	72925	138	**3**	
F	H06-1027	-2725669	74096	84	0.03	
	H06-1028	-2725630	74009	72	3.41	49
	H06-1029	-2725631	74010	88	1.9	35
	H06-1030	-2725621	74013	72	0.14	18
	H06-1031	-2725587	73920	72	1.8	54
					7.28	
G	H06-0918	-2726876	71595	90	2	26
	H06-0919	-2726877	71605	60	0.002	28
	H06-0920	-2726880	71625	72	0.001	28
					2.003	
H	H06-1054	-2727244	72041	150	3.37	
	H06-1053	-2727319	71895	150	3	
	H06-1021	-2727051	71870	72	0.3	23
	H06-1023	-2727059	71880	72	0.3	
	H06-1024	-2727048	71867	72	0.04	
	H06-1025	-2727057	71879	72	0.6	
	H06-1026	-2727062	71866	72	5	
	H06-1038	-2727201	71926	102	36	98
	H06-1039	-2727265	71928	114	5	80
	H06-0912	-2727255	71958	72	5	36
					55.24	
I	H06-0903	-2725179	71045	43	0.9	28
	H06-0904	-2724991	71055	43	0	*
					0.9	
J	H06-0901	-2726625	71524	49	0	*
	H06-0902	-2726568	71780	43	0.6	16
					0.6	
K	H06-1052	-2727521	71867	150	0	*
	H06-1050	-2727479	71499	150	0.2	
					0.2	
L	H06-1045	-2730734	72435	150	0	*
	H06-1046	-2730740	72412	150	3	20
					3	
M	H06-1047	-2731751	71960	150	**0.9**	
N	H06-1044	-2729380	72284	150	**0.3**	

An analysis of the drilling results of geophysically sited boreholes, based on the number of holes and the number of sites are given in table 5.

Table 5: Analysis of drilling results.

Dry holes	15%	Dry sites	7.6%
Successful holes	85%	Successful sites	92.3%
Holes yielding > 0.5 l/s	51%	Sites yielding > 0.5 l/s	77%
Holes yielding > 2 l/s	27%	Sites yielding > 2 l/s	46%
Average yield/hole	2.18l/s	Average yield/site	5.8 l/s (1.5 l/s excl. site H)

It should be noted that some of the boreholes were sited to investigate the dolerite/granite contact. Since these boreholes did intersect the contact, the geophysical interpretation was correct. The fact that these holes were dry should thus not be construed as a geophysical failure to find water, but as a scientific confirmation of the hypothesis that these contacts should not be groundwater targets in the investigation area.

8.3 Drilling results, area 2.

Due to accessibility and other factors, only 4 of the identified sites were drilled. In one of the 4 sites the interpreted structure was not intercepted. Due to time restrains it was however decided to discontinue the drilling program. The results of the drilling is given in table 6.

Table 6: Drilling results for area 2.

Site	Number	Latitude	Longitude	Depth	Water strike	Blow Yield	Geology (gr. – granite; dl. - dolerite)
2	H 06-1623	24.86625°	29.70525°	126 m	74 m	0.1 l/s	0-8m: fractured gr. 8-64m: solid gr. 64-120m: slightly fractured gr.
3	H 06-1621	24.85514°	29.71760°	126 m	Dry		0-19m: weathered gr. 19-126m: unweathered gr.
	H 06-1622	24.85536°	29.71725°	126 m	Dry		0-18m: weathered gr. 18-126m: unweathered gr.
5	H 06-1619	24.87584°	29.69529°	126 m	80 m	0.5 l/s	0-24m: weathered gr. 24-79m: unweathered gr. 79-126m: fractured dl. & gr.
12	H 06-1617	24.92430°	29.68677°	126 m	Dry		0-23m: weathered gr. 23-114m: unweathered gr. 114-126m: fractured gr.
	H 06-1618	24.92460°	29.68669°	126 m	Dry		0-24m: weathered gr. 24-74m: unweathered gr. 74-126m: fractured gr.
	H 06-1620	24.92442°	29.68656°	126 m	Dry		0-25m: weathered gr. 25-120m: unweathered gr. 120-126m: fractured gr.

8.4 Drilling conditions

In addition to the geophysically sited boreholes, a large number of boreholes were sited and drilled on extrapolation of outcrop mapped fracture sones. Pump test analysis were done on some of these as well as a number of the boreholes in table 3. The following interpretation of the results was done by Botha (Botha, 2000).

Most of the boreholes drilled, were drilled into hard rock granite covered with a thin layer of alluvium or colluvium and a thin weathered layer. Casing was installed at average depths of 12 to 18 metres. Major water strikes were recorded at an average depth of 69 metres with an average yield of 2.25 litres per second. Boreholes sited on major joint sets had striking depths of 100 metres and deeper.

Penetration rates in shear zones are much higher than those next to the shear zones where jointing is not as prominent. At surface it may seem as if the joints are in a compressive stress regime but at depth it seems as if the stress regime changes and the compressive stress lessens with the joints being more open. Due to the fact that this phenomena can not fully be identified with normal percussion drilling it was decided to drill a core borehole.

One core borehole was completed and preliminary results confirm that the jointing is vertical and little horizontal faulting could be identified. Shearing planes could be identified and secondary mineralisation could also be identified and this confirms the theory that the joints tend to be more open at depth. To speculate on the theory why the granites tend to be in a less compressive stress field in depth is not appropriate at this stage.

8.5 Pump test results

The boreholes were all evaluated according to the Rule of Thumb method, the Recovery method and the FC_Method (Botha, 2000). Generally the boreholes have a poor recovery and the calculations were done on extrapolated recovery periods (Table 7).

Table 7. Sustainable Yields

Regional Borehole number	PHYS	S.W.L. (m)	Pump depth (m)	Blow yield (l/s)	Production recommendation (l/s @ 24hrs)			
					Rule of thumb	Recovery	F.C-method	Average
H06 0881	1	7.5	45	4.1	1.58	1.13	1.38	1.36
H06 0882(A)	4	2.35	27	6	2.97	0.35	3.89	2.4
H06 0882(B)	4	1.69	32	3	1.65	-	2.35	1.85
H06 1043(A)	4	3.25	45	3	0.55	-	1.68	1.12
H06 1043(B)	4	3.58	68	3	-	-	0.3	0.3
H06 0907	5	2.43	56	1.8	0.4	0.31	0.65	0.45
H06 0910(A)	7	2.05	60	25	-	0.6	1.69	1.15
H06 0910(B)	7	3.63	86	25	-	0.9	1.95	1.43
H06 1028	10	5.48	64	3	0.64	0.66	0.28	0.53
H06 1496	11	2.43	96	3	0.39	0.39	0.32	0.37
H06 1038	14	10.28	93	36	2.4	1.1	1.11	1.54
H06 1448	19	22.6	58	3.6	1.4	1.25	0.51	1.05
H06 1049	20	3.2	64	12	1.11	-	1.25	1.18
H06 1054	21	0	80	6	3.81	3.82	2.49	3.37
H06 1420	22	11.68	46	3.6	1.21	1.21	1.33	1.25

The static water level is quite close to the surface except for borehole H06 1448. This borehole was drilled into a weathered aquifer and sited on a geophysical anomaly interpreted as a fault sone. All the tested boreholes had blow yields ranging from 1.8 to 36 l/s, and with little exception all the boreholes had a much lower constant discharge.

8.6 Aquifer types identified.

According to the pump test results, taking into account the blow yield, recommended yield and the geology, three major aquifer types could be identified:

1) Fractured aquifers associated with major structures.
2) Fracture aquifers associated with dykes.
3) Weathered aquifers resulting from weathering of major structures.

8.6.1 Fractured aquifers associated with major structures.

Boreholes H06-1043, -0907, -1054, and -1420 were drilled in this aquifer type. The aquifer is typically a major structure not associated with dykes. These boreholes had an average blow yield of 3.6 l/s and an average recommended yield of 1.5 l/s, almost 42% of the measured blow yield. Borehole H06-1054 is an artesian well with a yield of 0.5 l/s and have a recommended yield of 3.37 l/s, almost 56 % of the measured blow yield. Boreholes sited on structures which did not intersect any dolerite, generally had a better recovery than those boreholes which intersected doleritic material. Borehole H06-1420 could be fitted on a leaky aquifer or recharge boundary type model. A T-early value of 14.79 and a T-late value of 7.64 were calculated. A very low S-value of 10^{-5} were estimated.

8.6.2 Fractured aquifers associated with dyke material.

The boreholes situated on these aquifers are H06-1038, -0910 and -1049 associated with dykes and H06-1496 associated with the plate like dyke intrusion. These boreholes tend to have excellent blow yields especially those associated with the dykes, with an average blow yield of 24 l/s. The average recommended yield, however is 1.38 l/s, only 6% of the measured blow yield. The recovery period for these boreholes is poor, indicating a poor T-value. H06-1038 could be fitted on a barrier boundary or a typical fractures de-watered curve. It had a T-early of 9.80 and a T-late of 3.5, with an estimated S-value of 10^{-3}.

8.6.3 Weathered aquifers resulted from the weathering of major structures.

Boreholes associated with the weathering due to structural features include H06-0881, -0882, -1448 and -1028. Generally these boreholes had a fair recovery with good recommended yields. The four boreholes had an average blow yield of 4.18 l/s and an average recommended yield of 1.34 l/s. These boreholes therefore had an average recommended yield of 32% of the measured blow yield. The boreholes also had a fair recovery indicating a marginal S-value. H06-0882 could be fitted on an unconfined delayed yield or double porosity aquifer model. It had a T-early of 100.46 and a T-late of 28.80 with an estimate S-value of 10^{-4}.

8.7 Summary and conclusions.

- A regional approach to groundwater exploration is essential.

- A previously conceived pearl of wisdom applied to the Ga-Masemola area, that drilling deeper than 30m is a waste of effort due to the closure of fractures and faults, has been disproved. It is recommended that boreholes can be drilled to a depth of 130m.

- The granites are fairly uniform, but were exposed to various structural influences resulting in major shear zones.

- Structural events may be associated with the Wonderkop Fault, the Steelpoort Fault, Sekhukhune Fault and massive jointing in the granites.

- Five prominent shear zone orientations could be identified: A (40^0 - 50^0), B (80^0 - 90^0) , C (120^0 - 130^0), D (140^0 - 150^0) and E (170^0 - 180^0).

- Boreholes were tested and three aquifer types could be identified:

  Fractured aquifer associated with major structures.
  Fracture aquifer associated with dyke material.
  Weathered aquifer resulted from weathering of major structures.

- Recovery in the aquifers associated with dyke material is poor.

- The recovery of the weathered aquifers are fair and their chemical quality is also fair. These aquifers are however susceptible to organic pollution due to poor sanitation and poor land use.

CHAPTER 9

SUMMARY, CONCLUSIONS AND RECOMMENDATIONS

9.1 summary of geophysical results

The geophysical approach used in this project introduced two inovations relative to the traditional approach for groundwater exploration used on the Nebo granites. In the first instance the area was investigated on a regional scale rather than the very localized scale used in the past. In the second instance, airborne geophysical data was used as an aid in identifying and mapping structures of regional extent.

In the first test area airborne data included Magnetic, radiometric and electromagnetic values. Interpretation of these results indicated that airborne magnetic data should be sufficient to allow for the mapping of major structures. Downward continuation of this data significantly reduced the amount of ground follow-up that was needed to locate the target in the field.

The electromagnetic technique then proved to work exceptionally well in determining whether there were weathering associated with the target structure and in locating an optimum borehole position.

In the second test area the airborne data were limited to magnetic and radiometric information. Since only four targets, all with the same strike orientation, were drilled in this area, it is difficult to evaluate the geophysical results for this area, except that the interpreted structures were intersected in the drilled boreholes.

9.2 Conclusions and recommendations

Based on the results obtained in area 1, it is concluded that a regional approach to groundwater exploration is essential before any area can be classified as unsuitable for groundwater development. In a regional approach the use of airborne magnetic data has long been proven by the mineral industry to be a cost effective and essential aid in regional structural mapping. A line spacing of 100m for an airborne survey for groundwater development is recommended. It is not recommended that the airborne data alone should be used for borehole siting, but that interpreted structures should be pin pointed in the field, using ground geophysics.

Where faults and fracture sones are the primary targets, it is recommended that the electromagnetic technique be used. This technique is more sensitive to these kinds of targets, yields more information and is more cost effective than the traditional DC resistivity techniques.

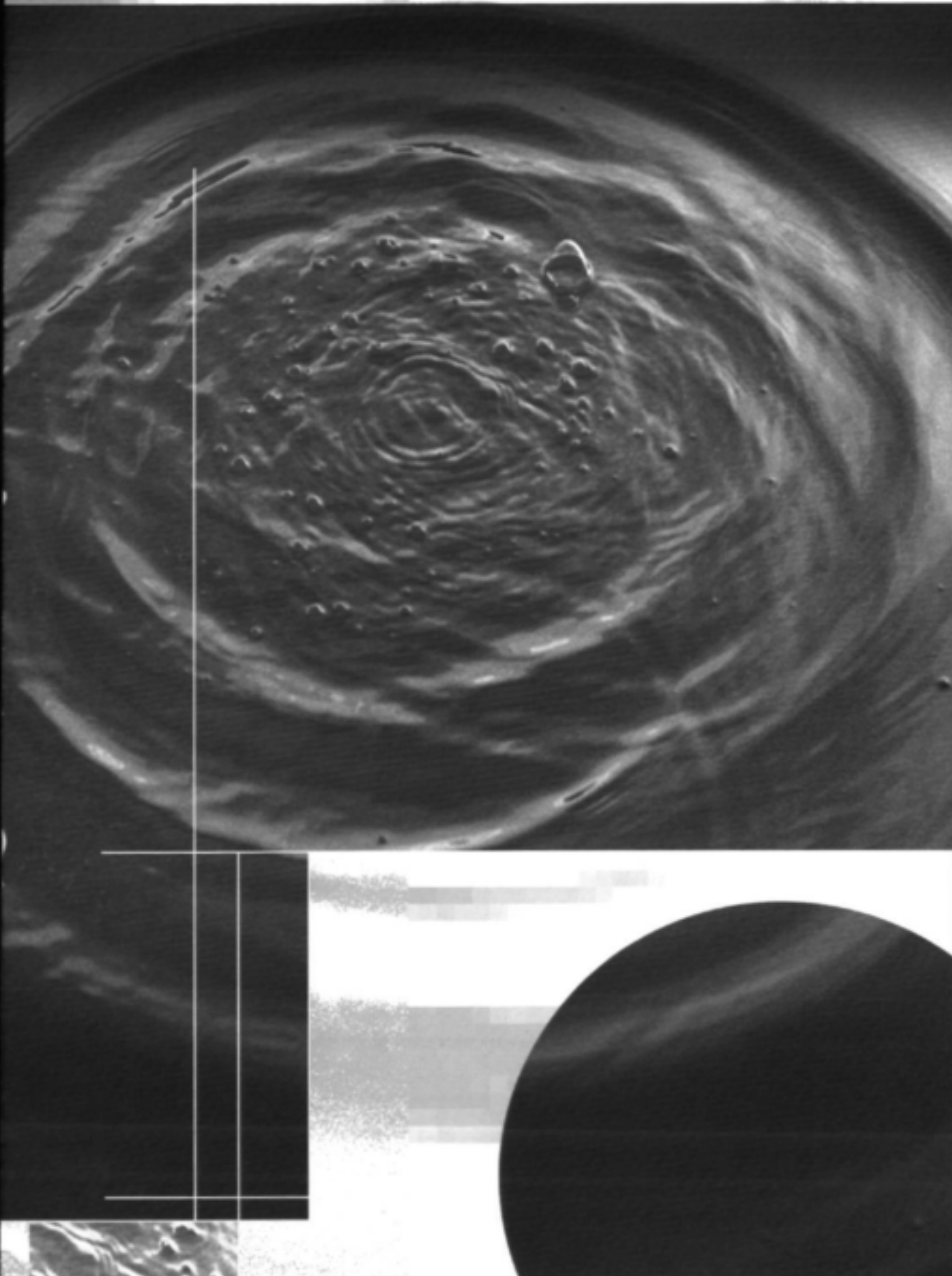

Water Research Commission

PO Box 824, Pretoria, 0001, South Africa

Tel: +27 12 330 0340, Fax: +27 12 331 2565

Web: http://www.wrc.org.za